Eur. Phys. J. C (2025) 85:153
https://doi.org/10.1140/epjc/s10052-024-13715-4

THE EUROPEAN PHYSICAL JOURNAL C

Regular Article - Experimental Physics

Search for a light charged Higgs boson in $t \to H^{\pm}b$ decays, with $H^{\pm} \to cs$, in pp collisions at $\sqrt{s} = 13$ TeV with the ATLAS detector

ATLAS Collaboration[⋆]

CERN, 1211 Geneva 23, Switzerland

Received: 16 July 2024 / Accepted: 17 December 2024

Abstract A search for a light charged Higgs boson produced in decays of the top quark, $t \to H^{\pm}b$ with $H^{\pm} \to cs$, is presented. This search targets the production of top-quark pairs $t\bar{t} \to WbH^{\pm}b$, with $W \to \ell\nu$ ($\ell = e, \mu$), resulting in a lepton-plus-jets final state characterised by an isolated electron or muon and at least four jets. The search exploits b-quark and c-quark identification techniques as well as multivariate methods to suppress the dominant $t\bar{t}$ background. The data analysed correspond to 140 fb^{-1} of pp collisions at $\sqrt{s} = 13$ TeV recorded with the ATLAS detector at the LHC between 2015 and 2018. Observed (expected) 95% confidence-level upper limits on the branching fraction $\mathscr{B}(t \to H^{\pm}b)$, assuming $\mathscr{B}(t \to Wb) + \mathscr{B}(t \to H^{\pm}(\to cs)b) = 1.0$, are set between 0.066% (0.077%) and 3.6% (2.3%) for a charged Higgs boson with a mass between 60 and 168 GeV.

Contents

1 Introduction . . . . . .
2 ATLAS detector . . . . . .
3 Data and simulated event samples . . . . . .
4 Object definition and event selection . . . . . .
5 Background modelling . . . . . .
6 Analysis strategy . . . . . .
6.1 $t\bar{t}$-system reconstruction . . . . . .
6.2 Multivariate signal extraction . . . . . .
7 Systematic uncertainties . . . . . .
8 Statistical interpretation . . . . . .
9 Results . . . . . .
10 Conclusions . . . . . .
References . . . . . .

1 Introduction

The discovery of the Higgs boson at the Large Hadron Collider (LHC) in 2012 was a great achievement of the ATLAS and CMS Collaborations [1,2], and has led to numerous measurements to determine its properties [3,4]. One of the main goals of these studies is to establish if the discovered Higgs boson is the single fundamental scalar particle of the Standard Model (SM) or rather the first observed particle of an extended scalar sector.

Extensions to the scalar sector are motivated by the solutions they provide to several open questions in particle physics. An extended scalar sector can modify the electroweak phase transition and facilitate baryogenesis [5], enhance vacuum stability, provide a dark-matter candidate [6,7] or yield a solution to the strong CP problem [8]. Many physics models beyond the SM (BSM) require an extended scalar sector. For example, in the minimal supersymmetric extension of the SM the existence of two Higgs doublets is required [9]. In models with a Type-II seesaw mechanism, Higgs triplets [10–14] are required.

Two-Higgs-doublet models (2HDMs) [15,16] are popular and simple extensions of the scalar sector and predict the existence of two charged Higgs bosons, H^+ and H^-, and two neutral Higgs bosons in addition to the discovered neutral one. The various 2HDMs are categorised into types defined by the Yukawa couplings of the fermions to the Higgs doublets. The production mechanisms and decay modes of charged Higgs bosons depend on the Yukawa couplings and other model parameters, especially the ratio of the two Higgs-doublet vacuum expectation values ($\tan\beta$) and the charged Higgs boson's mass ($m_{H^{\pm}}$). Many phenomenology studies advocate searching for a light charged Higgs bosons (below the top-quark mass) in the decays to a charm quark and a strange quark, $H^{\pm} \to cs$,[1] to a charm quark and a bot-

⋆ e-mail: atlas.publications@cern.ch

[1] Unless explicitly stated otherwise, charge conjugation is implied in this paper; the notation cs is used in place of $c\bar{s}/\bar{c}s$.

Published online: 06 February 2025

tom quark, $H^\pm \to cb$, and to a τ-lepton and a τ-neutrino, $H^\pm \to \tau\nu_\tau$ [6,15]. The branching fraction for $H^\pm \to cb$ is typically smaller than for $H^\pm \to cs$, due to the different values of the CKM matrix elements, $V_{cs} \gg V_{cb}$. In the Type-I 2HDM, only the $\tau\nu_\tau$ and cs decay modes are relevant. In Type-II and Type-X (or "lepton-specific") models the cs channel is dominant for values of $\tan\beta < 1$. In Type-Y (or "flipped") models the cs and cb channels are important for $\tan\beta > 5$ [6]. For a 2HDM model where one doublet couples mainly to the third generation, while the other doublet couples mainly to the first and second generations, the cs and cb channels are dominant [17]. This is also the case for leptophobic multiple-Higgs-doublet models [6].

Searches for $H^\pm \to cs$ in top-quark decays have been performed by the ATLAS and CMS Collaborations, based on 4.7 fb^{-1} and 35.9 fb^{-1} of proton–proton (pp) collision data collected at centre-of-mass energies of $\sqrt{s} = 7$ TeV and $\sqrt{s} = 13$ TeV, respectively. The search performed by the ATLAS Collaboration obtained 95% confidence level (CL) observed (expected) upper limits on the branching fraction $\mathscr{B}(t \to H^\pm b)$ ranging from 1.2% (1.5%) to 5.1% (8%), assuming $\mathscr{B}(H^\pm \to cs) = 1.0$, for $m_{H^\pm}$ between 90 and 150 GeV [18]. The search performed by the CMS Collaboration obtained 95% CL observed (expected) upper limits on $\mathscr{B}(t \to H^\pm b)$ ranging from 0.25% (0.29%) to 1.68% (2.39%), assuming $\mathscr{B}(H^\pm \to cs) = 1.0$, for $m_{H^\pm}$ between 80 and 160 GeV [19]. Related searches for $H^\pm \to cb$ in top-quark decays were performed by the ATLAS and CMS Collaborations using 139 fb^{-1} and 19.7 fb^{-1} of pp collision data collected at $\sqrt{s} = 13$ TeV [20] and 8 TeV [21], respectively. The most stringent observed limits on $\mathscr{B}(t \to H^\pm b) \times \mathscr{B}(H^\pm \to cb)$ are set by ATLAS and range from 0.15 to 0.42% for $m_{H^\pm}$ between 60 GeV and 160 GeV. In that analysis a moderate excess of signal events is observed in the vicinity of 130 GeV, with a global significance of 2.5σ. Searches for $H^\pm \to \tau\nu$ in 36.1 fb^{-1} of pp collision data recorded with the ATLAS and CMS detectors at $\sqrt{s} = 13$ TeV were carried out over a wide mass range, from 90 to 2000 GeV [22] or from 80 to 3000 GeV [23] respectively, covering the masses of light and heavy charged Higgs bosons. The ATLAS (CMS) Collaboration set observed upper limits on the branching fraction $\mathscr{B}(t \to H^\pm b) \times \mathscr{B}(H^\pm \to \tau\nu)$ ranging from 0.25 to 0.031% (0.36–0.079%) in the mass range between 90 GeV (80 GeV) and 160 GeV. In the absence of other new physics, measurements of the process $b \to s\gamma$ exclude in Type-II and Type-Y models a charged Higgs boson with mass below 580 GeV independent of $\tan\beta$ [24].

This analysis searches for a charged Higgs boson with a mass below the top-quark mass. In this regime the main production mode for charged Higgs bosons is via $t\bar{t}$ events, with the charged Higgs boson emerging from rare top-quark decays: $t \to H^\pm b$. This analysis focuses on the $t\bar{t} \to WbH^\pm b$ process, with $W \to \ell\nu$ ($\ell = e, \mu$) and $H^\pm \to cs$, resulting in a lepton-plus-jets final state (see Fig. 1). Only events with an electron or muon, including those produced via leptonically decaying τ-leptons, denoted by τ_{lep}, are considered.

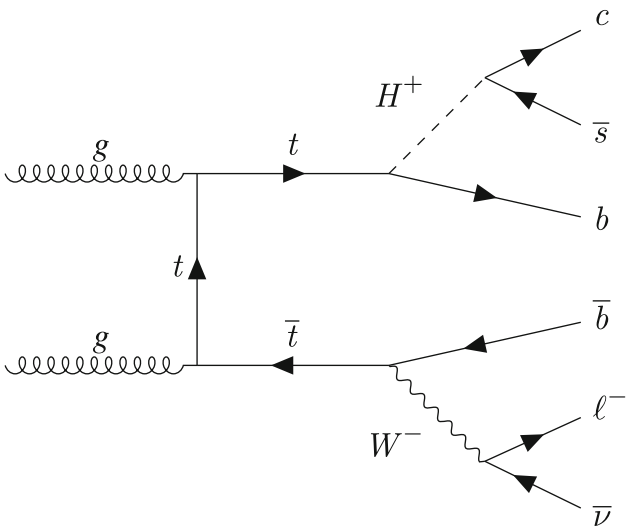

Fig. 1 Illustrative Feynman diagram of the signal process

This paper is based on 140 fb^{-1} of pp collision data at $\sqrt{s} = 13$ TeV. In contrast to previous $H^\pm \to cs$ searches, multivariate analysis techniques are deployed here to search for a potential signal in the data. This approach exploits both the kinematic properties of signal events, including the $H^\pm$ candidate mass, and their flavour composition, which differs from that of the mostly SM $t\bar{t}$ background events. The kinematics of the top-quark decays are derived by reconstructing the $t\bar{t}$ event topology. Flavour-tagging algorithms are utilised to tag jets as b-jets, c-jets or light-flavour jets. A dedicated flavour-tagging scheme which facilitates simultaneous tagging of b-jets and c-jets is adopted.

2 ATLAS detector

The ATLAS detector [25] at the LHC covers nearly the entire solid angle around the collision point.[2] It consists of an inner tracking detector surrounded by a thin superconducting solenoid, electromagnetic (ECAL) and hadronic calorime-

[2] ATLAS uses a right-handed coordinate system with its origin at the nominal interaction point (IP) in the centre of the detector and the z-axis along the beam pipe. The x-axis points from the IP to the centre of the LHC ring, and the y-axis points upwards. Polar coordinates (r, ϕ) are used in the transverse plane, ϕ being the azimuthal angle around the z-axis. The pseudorapidity is defined in terms of the polar angle θ as $\eta = -\ln\tan(\theta/2)$ and is equal to the rapidity $y = (1/2)\ln\left[(E + p_z)/(E - p_z)\right]$ in the relativistic limit. Angular distance is measured in units of $\Delta R \equiv \sqrt{(\Delta y)^2 + (\Delta\phi)^2}$.

ters, and a muon spectrometer (MS) incorporating three large superconducting air-core toroidal magnets.

The inner-detector system (ID) is immersed in a 2 T axial magnetic field and provides charged-particle tracking in the range $|\eta| < 2.5$. The high-granularity silicon pixel detector covers the vertex region and typically provides four measurements per track, the first hit generally being in the insertable B-layer (IBL) installed before Run 2 [26,27]. It is followed by the SemiConductor Tracker (SCT), which usually provides eight measurements per track. These silicon detectors are complemented by the transition radiation tracker (TRT), which enables radially extended track reconstruction up to $|\eta| = 2.0$. The TRT also provides electron identification information based on the fraction of hits (typically 30 in total) above a higher energy-deposit threshold corresponding to transition radiation.

The calorimeter system covers the pseudorapidity range $|\eta| < 4.9$. Within the region $|\eta| < 3.2$, electromagnetic calorimetry is provided by barrel and endcap high-granularity lead/liquid-argon (LAr) calorimeters, with an additional thin LAr presampler covering $|\eta| < 1.8$ to correct for energy loss in material upstream of the calorimeters. Hadronic calorimetry is provided by the steel/scintillator-tile calorimeter, segmented into three barrel structures within $|\eta| < 1.7$, and two copper/LAr hadronic endcap calorimeters. The solid angle coverage is completed with forward copper/LAr and tungsten/LAr calorimeter modules optimised for electromagnetic and hadronic energy measurements respectively.

The MS comprises separate trigger and high-precision tracking chambers measuring the deflection of muons in a magnetic field generated by the superconducting air-core toroidal magnets. The field integral of the toroids ranges between 2.0 and 6.0 T m across most of the spectrometer. Three layers of precision chambers, each consisting of layers of monitored drift tubes, cover the region $|\eta| < 2.7$, complemented by cathode-strip chambers in the forward region, where the background is highest. The muon trigger system covers the range $|\eta| < 2.4$ with resistive-plate chambers in the barrel, and thin-gap chambers in the endcap regions.

The luminosity is measured mainly by the LUCID-2 [28] detector that records Cherenkov light produced in the quartz windows of photomultipliers located close to the beam pipe.

Events are selected by the first-level trigger system implemented in custom hardware, followed by selections made by algorithms implemented in software in the high-level trigger [29]. The first-level trigger accepts events from the 40 MHz bunch crossings at a rate below 100 kHz, which the high-level trigger further reduces in order to record complete events to disk at about 1 kHz.

A software suite [30] is used in data simulation, in the reconstruction and analysis of real and simulated data, in detector operations, and in the trigger and data acquisition systems of the experiment.

3 Data and simulated event samples

This search is based on data collected from pp collisions at the ATLAS experiment during LHC Run 2 at a centre-of-mass energy of $\sqrt{s} = 13$ TeV. After applying quality requirements, the dataset corresponds to an integrated luminosity of $140.1 \pm 1.2\,\text{fb}^{-1}$ [28,31]. Signal and background processes, except multijet processes, were simulated using Monte Carlo (MC) event generators.

The main background in this search is SM $t\bar{t}$ production. The production of $t\bar{t}$ and single-top-quark events in the tW-, s- and t-channels was modelled with the POWHEG BOX v2 [32–35] generator at next-to-leading order (NLO), using the five-flavour scheme (four-flavour scheme for single-top-quark t-channel events) with the NNPDF [3.0nlo] [36] parton distribution function (PDF) set and the h_{damp} parameter[3] set to $1.5\,m_{\text{top}}$ [37]. The events were interfaced to PYTHIA 8.230 [38] to model the parton shower (PS), hadronisation, and underlying event. For all samples in this search, PYTHIA 8 used the NNPDF2.3LO set of PDFs [39], and its parameter values were set to those of the A14 tune [40]. The decays of bottom and charm hadrons were performed by EVTGEN 1.6.0 [41]. To assess the uncertainty in the matching of NLO matrix elements (ME) to the PS, the nominal samples were compared with samples of $t\bar{t}$ and single-top-quark events generated with MADGRAPH5_AMC@NLO 2.6.0 and 2.6.2 [42] respectively, using the NNPDF3.0NLO set of PDFs, and interfaced with PYTHIA 8.230. The impact of using a different PS and hadronisation model was evaluated by comparing the nominal samples with alternative samples produced with the POWHEG BOX v2 generator using the NNPDF3.0NLO PDF set and interfaced with HERWIG [43,44]. HERWIG 7.13 and HERWIG 7.16 were used for $t\bar{t}$ and single-top-quark events, respectively, and both used the HERWIG 7.1 default set of tuned parameters [44,45] and the MMHT2014LO PDF set [46]. The $t\bar{t}$–tW interference was handled using the diagram removal scheme [47]. The uncertainty associated with this choice is estimated by comparing the nominal sample with an alternative sample generated using the diagram subtraction scheme [37,47]. The $t\bar{t}$ production cross-section is calculated at next-to-next-to-leading-order and next-to-next-to-leading-logarithm (NNLO+NNLL) accuracy [48]. The cross-sections for the three single-top-quark production

[3] The h_{damp} parameter is a resummation damping factor and one of the parameters that controls the matching of POWHEG matrix elements to the parton shower and thus effectively regulates the high-p_{T} radiation against which the $t\bar{t}$ system recoils.

channels are calculated at NLO [49–51]. Simulated $t\bar{t}$ events are categorised according to the flavour of additional jets in the event, using the procedure described in Ref. [52]. Events with at least one additional b-flavour or c-flavour jet are labelled as $t\bar{t}$ +HF (where HF stands for "heavy-flavour"). The remaining events are labelled as $t\bar{t}$ +LF (where LF stands for "light-flavour"). This category is split into $t\bar{t}(ud)$ and $t\bar{t}(cs)$ subcategories according to the decay of the W bosons. If at least one W boson decays as $W \to cs$ the event falls into the $t\bar{t}(cs)$ category, otherwise it falls into the $t\bar{t}(ud)$ category. This categorisation is motivated by the fact that the final state is identical for $t\bar{t}(cs)$ and signal events.

The rare top-quark processes considered in this analysis are $t\bar{t}H$, $t\bar{t}W$, $t\bar{t}Z$, $t\bar{t}t\bar{t}$, $t\bar{t}t$, $tHjb$, tWH, tWZ and tZq. The $t\bar{t}H$ events were modelled with the same generators and versions as the exclusive $t\bar{t}$ events. The $t\bar{t}W$, $t\bar{t}Z$, tWZ and $t\bar{t}t\bar{t}$ processes were modelled using MadGraph5_aMC@NLO 2.3.3, the $t\bar{t}t$ process using MadGraph5_aMC@NLO 2.2.2, and the $tHjb$ and tWH processes using MadGraph5_aMC@NLO 2.6.2, in all cases at NLO with the NNPDF3.0nlo PDF (NNPDF3.1nlo for the $t\bar{t}t\bar{t}$ process). The $t\bar{t}t$ and tZq processes were modelled with MadGraph 2.2.2 at LO with the NNPDF2.3nlo PDF. The events were then interfaced with Pythia 8.186–8.235 and the decays of bottom and charm hadrons were simulated using the EvtGen 1.2.0–1.6.0 program. The $t\bar{t}H$, $t\bar{t}W$ and $t\bar{t}Z$ samples were normalised using cross-sections calculated at NLO QCD and NLO EW accuracy using MadGraph5_aMC@NLO as reported in Ref. [53].

The production of a W or Z/γ^* boson in association with jets ($V+$ jets) and of dibosons (VV) was modelled with the Sherpa 2.2.11 [54] and Sherpa 2.2.1 generators, respectively, for both the ME and PS. The only exception is the $VV \to \ell\nu\nu\nu$ process, which was modelled with Sherpa 2.2.2. The NLO ME for up to two partons (one parton) and leading-order ME for up to five (three) partons were calculated with the Comix [55] and OpenLoops [56–58] libraries for V+jets (VV) events. They were matched with the Sherpa PS [59] using the MEPS@NLO prescription [60–63] and the set of tuned parameters developed by the Sherpa authors. The NNPDF3.0nnlo set of PDFs was used.

Signal events were modelled by first generating top-quark pairs, similar to the SM $t\bar{t}$ background, using the Powheg Box v2 generator at NLO with the NNPDF3.0nlo PDF set and the h_{damp} parameter set to $1.5\,m_{\text{top}}$. The decays $t \to H^{\pm}b$ and $t \to W^{\pm}b$ were modelled by MadSpin [64] using the Type-II 2HDM [15,65] for BSM decays. Subsequent decays of the $H^{\pm}$ and $W^{\pm}$ bosons, as well as the showering of the final-state hadrons, were modelled by Pythia 8.307. The $W^{\pm}$ were forced to decay leptonically, with all three lepton flavours allowed. The $H^{\pm}$ were forced to decay into a cs-quark pair. The decays of bottom and charm hadrons were performed by EvtGen 1.7.0. Signal samples were generated with zero decay width for twelve charged-Higgs-boson mass points: eleven in steps of 10 GeV from 60 GeV to 160 GeV, and one at 168 GeV. The signal samples are denoted by $H^{\pm}_x$, where x is the mass of the charged Higgs boson in GeV. If the mass difference between the $H^{\pm}$ and W bosons is smaller than one of their total widths, the interference term might be of the order of a few percent of the $H^{\pm}$ contribution. The size and the sign of the interference term depend on the model [66]. For larger mass differences, the interference term can be omitted with high accuracy. The interference term is neglected in this analysis for all mass points. Production of charged Higgs bosons via single-top-quark processes is neglected in this analysis because such events usually do not contain a prompt lepton and are therefore suppressed by the event selection (cf. Sect. 4), and also because the production cross-section is much smaller than for $t\bar{t}$ processes.

The effect of multiple interactions in the same and neighbouring bunch crossings (pile-up) was modelled by overlaying the simulated hard-scattering event with inelastic pp events generated with Pythia 8.186 [67] using the NNPDF2.3lo PDF set and the A3 set of tuned parameters [68]. Events in the nominal background samples were passed through the full ATLAS detector simulation [69] based on Geant4 [70]. Signal, $t\bar{t}t\bar{t}$, tH and alternative samples were passed through a fast simulation in which the response of the calorimeter is parameterised [71]. Both simulation methods were found to provide a similar level of modelling accuracy for the physics objects used in the analysis. A full list of samples used in this search is summarised in Table 1.

4 Object definition and event selection

Tracks are required to have transverse momentum (p_{T}) greater than 500 MeV, $|\eta| < 2.5$, and at least seven hits in the pixel and SCT detectors. A maximum of one (two) of the expected hits may be missing from the pixel (SCT) detector, and no more than one hit may be shared with other tracks [72]. Events are required to have at least one primary vertex reconstructed from two or more associated tracks [73]. If multiple vertices are found, the one with the highest scalar sum of the p_{T}^2 of associated tracks is selected as the primary vertex.

Electrons are reconstructed from topological energy clusters in the ECAL that are matched to tracks in the ID [74]. Electrons are required to have $p_{\text{T}} > 10$ GeV and $|\eta| < 2.47$, excluding the barrel–endcap transition region $1.37 < |\eta| < 1.52$. They must pass track-quality requirements followed by a loose likelihood-based selection that requires the shower profile to be compatible with that of the electro-

Table 1 Generators used to simulate the signal and background processes. The symbol q is used for u, d, c, s quarks. For the signal processes the subscript "x" is a placeholder for the mass of the charged Higgs boson in GeV. For the "Other top" and VV processes, only the range of used generator versions is quoted. The exact generator version used for each process is described in Sect. 3

Name	Process	ME generator	PS and hadronisation
Signal			
$H_x^{\pm}$	$t\bar{t} \to H^{\pm}(\to cs)W^{\mp}(\to \ell\nu_\ell)b\bar{b}$	POWHEG BOX v2	MADSPIN + PYTHIA 8.307 + EVTGEN 1.7.0
Top-quark			
$t\bar{t}(ud)$	$t\bar{t} \to W^{\pm}(\to \ell\nu_\ell)W^{\mp}(\to ud)b\bar{b}$	POWHEG BOX v2	PYTHIA 8.230 + EVTGEN 1.6.0
$t\bar{t}(cs)$	$t\bar{t} \to W^{\pm}(\to \ell\nu_\ell)W^{\mp}(\to cs)b\bar{b}$		
$t\bar{t}$ +HF	$t\bar{t} \to W^{\pm}(\to \ell\nu_\ell)W^{\mp}(\to q\bar{q})b\bar{b} + \geq 1c/b$		
$t\bar{t}$(allHad)	$t\bar{t} \to W^{\pm}(\to q\bar{q})W^{\mp}(\to q\bar{q})$		
tW	tW		
Single top	single t-quark s- & t-channel		
$t\bar{t}H$	$t\bar{t}H$		
Other top	$t\bar{t}W, t\bar{t}Z, t\bar{t}t\bar{t}, tHjb, tWH, tWZ,$	MADGRAPH5_AMC@NLO 2.3.3–2.6.2	PYTHIA 8.186–8.230 + EVTGEN 1.2.0–1.6.0
	$t\bar{t}t, tZq$	MADGRAPH 2.2.2–2.3.3	
Weak-boson			
W+ jets	W+ jets	SHERPA 2.2.11	SHERPA 2.2.11
Z + jets	Z + jets		
VV	WW, WZ, ZZ	SHERPA 2.2.1–2.2.2	SHERPA 2.2.1– 2.2.2

magnetic shower. Electrons are required to have transverse (d_0) and longitudinal (z_0) impact parameters, measured relative to the beam-line and primary vertex respectively, satisfying $|d_0|/\sigma(d_0) < 5$ and $|z_0 \sin\theta| < 0.5$ mm. Isolation requirements are applied via a boosted decision tree (BDT) which was trained on track-isolation, cluster-isolation, and secondary-vertex information, referred to as "non-prompt-lepton BDT" [75,76]. The electron energy scale and resolution calibrations are obtained from $Z \to ee$ events and applied to data and simulations, respectively [74].

Muon candidates are reconstructed by matching MS tracks to ID tracks. In the absence of full tracks in the MS, muons can be reconstructed from ID tracks extrapolated to the MS which match at least three loosely aligned MS hits. The information from the ID and the MS, and the energy loss in the calorimeters, are then used in a combined track fit [77]. Muons have to satisfy $p_{\mathrm{T}} > 10$ GeV and $|\eta| < 2.5$, and pass quality requirements based on the number of hits used to reconstruct the tracks. Muons are also required to satisfy $|d_0|/\sigma(d_0) < 3$ and $|z_0 \sin\theta| < 0.5$ mm. Lastly, isolation requirements are also made based on the non-prompt-lepton BDT.

Jets are reconstructed with the anti-k_t jet clustering algorithm [78,79] with a radius parameter $R = 0.4$. The clustering is applied to noise-suppressed positive-energy topological energy clusters [80,81] and charged-particle tracks, processed using a particle-flow algorithm [82]. Jet energies are corrected for contributions from pile-up, calibrated using energy- and η-dependent correction factors determined from comparisons between particle-level objects and reconstructed physics objects in simulated events, and then corrections are applied to account for effects due to the initiating-parton type and hadron composition [83]. In data, a residual in situ correction is applied in order to correct for differences relative to simulation. Jets in the analysis are required to have $p_{\mathrm{T}} > 25$ GeV and $|\eta| < 2.5$. Jets with $p_{\mathrm{T}} < 60$ GeV and $|\eta| < 2.4$ also have to pass a jet-vertex-tagger [84] requirement to reduce the number of selected jets which originate from pile-up.

Jets containing b- or c-hadrons are identified with the DL1r tagger [85], which is a multivariate classification algorithm based on a deep neural network using information about the impact parameters of tracks, the jet kinematics, and displaced vertices. The b- and c-tagging scores are based on log-likelihood ratios of the neural-network output scores. To assign jets to top quarks or to $H^{\pm}$ boson candidates, one needs to identify b- and c-quark-initiated jets simultaneously and distinguish them from the light-flavour jets. Correction factors are applied to the simulated events to compensate for differences between data and simulation in the b- and c-tagging efficiencies or misidentification rates for b-jets, c-jets and light-flavour jets [86–88]. This search uses a pseudo-continuous flavour-tagging (PCFT) calibration with five exclusive calibrated bins. Jets passing a fixed b-tagging working point (WP) defined by b-jet efficiencies, measured

in $t\bar{t}$ events, of 70% and 60% have PCFT scores of 3 and 4, respectively. These two b-tagging WPs have background tagging efficiencies for c-jets (light-jets) of 7.9% (0.18%) and 2.7% (0.05%), respectively [89]. Other jets (b-veto) receive a PCFT score of 1 or 2 if they pass a fixed c-tagging score defined by a c-jet efficiency of 45% or 24%, respectively. These two c-tagging WPs have background tagging efficiencies for b-jets (light-jets) of 16.3% (7.4%) and 4.8% (0.9%), respectively [89]. Jets passing none of the b- and c-tagging WPs (untagged) are assigned a PCFT score of 0. Any jet passing the loosest calibrated $b(c)$-tagging WP is referred to as a $b(c)$-tagged jet.

The missing transverse momentum ($\mathbf{p}_{\mathrm{T}}^{\mathrm{miss}}$) is defined as the negative vector sum of the transverse momenta of all reconstructed and calibrated leptons and jets, and all tracks matched to the primary vertex but not to other reconstructed objects in the event [90]. The absolute value of $\mathbf{p}_{\mathrm{T}}^{\mathrm{miss}}$ is denoted by $E_{\mathrm{T}}^{\mathrm{miss}}$.

An overlap-removal procedure is applied to resolve ambiguities where multiple physical objects are reconstructed from the same detector signature. The angular distance ΔR is used to measure the overlap of two reconstructed objects. The following procedure is applied in order:

1. any calorimeter-tagged muon [77] sharing a track with an electron is removed;
2. any electron sharing a track with a muon is removed;
3. any jet within $\Delta R = 0.2$ of an electron is removed;
4. any electron within $\Delta R = 0.4$ of a jet is removed;
5. any jet with less than 3 tracks that is within $\Delta R = 0.2$ of a muon is removed;
6. any jet with less than 3 tracks that has a muon ID track ghost-associated [78,91] with it is removed;
7. any muon within $\Delta R = 0.4$ of a jet is removed.

Events were recorded with a single-electron or single-muon trigger with a threshold requirement imposed on the lepton p_{T}. For the data-taking periods 2015 and 2016–2018, the lowest electron p_{T} threshold was 24 GeV or 26 GeV respectively, and similarly the lowest muon-p_{T} threshold was 20 GeV or 26 GeV. The trigger includes lepton identification and isolation requirements based on ID or ECAL measurements [92–94]. Furthermore, events are required to have exactly one offline reconstructed lepton with $p_{\mathrm{T}} >$ 27 GeV that meets the "medium" identification and isolation criteria [74,77]. Events with an additional lepton with $p_{\mathrm{T}} > 10$ GeV that satisfies the medium identification criteria are vetoed to reduce dileptonic $t\bar{t}$ and Z + jets backgrounds. The offline reconstructed lepton is required to be geometrically matched ($\Delta R < 0.1$) to the online reconstructed lepton which fired the trigger. At least four jets with $p_{\mathrm{T}} > 25$ GeV have to be present, and at least one is required to be b-tagged. Finally, events in the signal region are required to have exactly one "tight" identified and isolated lepton and at least two b-tagged jets [74,77]. The $t\bar{t}$ background contribution in the signal region is about 92%.

5 Background modelling

The main background in this search is $t\bar{t}$ production in association with jets. As in many other analyses targeting a kinematic phase space similar to the signal region of this search, differences between MC-based background predictions and data are observed in multiple kinematic quantities [20,95]. This disagreement can be attributed to missing higher-order QCD and electroweak corrections in $t\bar{t}$ MC simulation leading to harder top-quark p_{T} spectra in simulation than in data [96]. A data-driven correction is derived to improve the modelling of the $t\bar{t}$ background and signal, particularly of p_{T}-dependent variables.

The correction is derived as a function of S_{T}. The S_{T} variable is defined as the sum of the scalar transverse momenta of all calibrated objects in the event, i.e. jets, leptons and $E_{\mathrm{T}}^{\mathrm{miss}}$, and is therefore related to the transverse momenta of individual top quarks. The corrections are derived in bins of the number of jets in the event ($N_{\mathrm{jets}} = 4, 5, 6, 7, 8, \geq 9$), as this quantity also shows discrepancies between MC events and data and is correlated with S_{T}. The correction is derived in the signal region, since the $t\bar{t}$ contribution is around 92% in that region, and is applied to signal events as well as $t\bar{t}$ events because the mismodelling is expected to affect the signal MC prediction in the same way. It was checked that the S_{T} distribution in bins of N_{jets} is similar for $t\bar{t}$ and signal events. A possible signal contribution in data will therefore not change the correction weights and the correction will not bias the signal extraction.

The $t\bar{t}$ correction weights are defined as the ratio of data templates (with non-$t\bar{t}$ backgrounds subtracted) to MC $t\bar{t}$ templates. In order to mitigate the effects of statistical fluctuations in the data and simulation samples, a linear + exponential function is fitted to the derived $t\bar{t}$ correction weights. The fit is performed separately for even and odd event numbers to avoid overfitting. The weights from the fit to even-numbered events are applied to odd-numbered events and vice versa.

Figure 2 shows the S_{T} and lepton-p_{T} distributions after applying the $t\bar{t}$ correction. The red dashed line represents the total background prediction before applying the correction. Agreement between the data and MC prediction clearly improves for S_{T} and other related distributions, especially at high values. The S_{T} and lepton-p_{T} distributions of the alternative $t\bar{t}$ MC samples differ significantly from those of the nominal $t\bar{t}$ sample. Hence, alternative $t\bar{t}$ correction weights are derived and applied to these events.

Multijet (MJ) processes can contribute to the background when jets are misidentified as leptons or when real non-

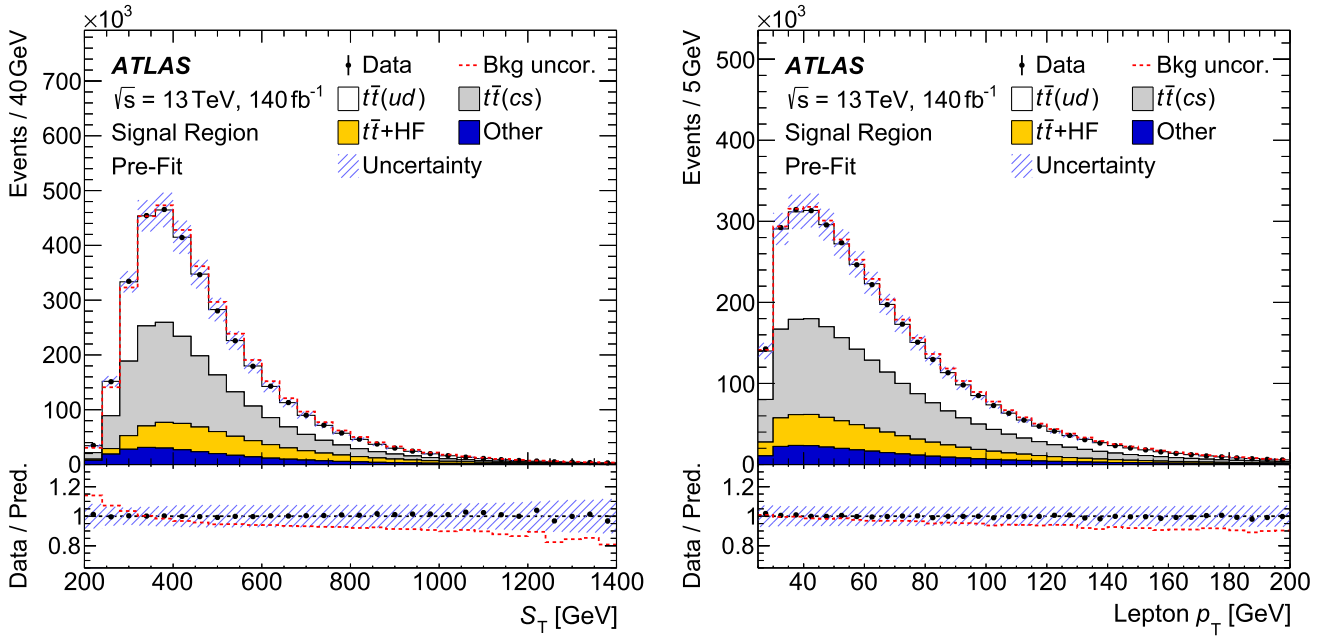

(a) (b)

Fig. 2 Distribution of **a** S_{T} and **b** lepton p_{T} after applying the $t\bar{t}$ correction. The processes $t\bar{t}$(allHad), tW, Single top, $t\bar{t}H$, Other top, W+ jets, Z + jets, and VV listed in Table 1 are combined with the multijet background in the "Other" category. The uncertainty band represents the combined statistical and systematic uncertainty of the prediction. The red dashed line represents the total background prediction before applying the correction

prompt leptons are produced in the decays of heavy-flavour hadrons. A data-driven method commonly called the ABCD method (see e.g. Ref. [97]) is used to estimate the MJ background in the signal region. The lepton isolation requirement and the number of b-tagged jets are used to define the four ABCD regions. The shape of the MJ background is estimated from a region with a looser lepton-isolation requirement. The normalisation is derived from events with exactly one b-tagged jet. The ABCD method is applied separately to electron and muon events. The size of the total MJ background in the signal region is about 0.3% of the total estimated background.[4]

6 Analysis strategy

The presence of a potential signal in data is quantified first by reconstructing the $t\bar{t}$ event topology, and then extracting the signal using a BDT. The $t\bar{t}$-system is reconstructed by using calibrated physics objects, i.e. leptons, $\mathbf{p}_{\mathrm{T}}^{\mathrm{miss}}$ and jets, as proxies for the lepton, neutrino and quarks from the top-quark decays. Kinematic properties of the reconstructed $t\bar{t}$-system are then used to train a BDT to classify events as signal or background.

6.1 $t\bar{t}$-system reconstruction

The $t\bar{t}$-system consists of a semileptonically decaying top quark (t_{lep}) and a hadronically decaying top quark (t_{had}). The t_{lep} decays into a b-quark (b_{lep}) and a W boson, which decays into a lepton and neutrino. The t_{had} decays into a b-quark (b_{had}) and a $H^{\pm}$ or W boson, which decays into c- and s-quarks or other quarks (j_1, j_2), respectively.

The lepton from the W-boson decay is unambiguously identified as the single reconstructed lepton. The momentum of the neutrino from the W-boson decay is reconstructed using $\mathbf{p}_{\mathrm{T}}^{\mathrm{miss}}$ and a W-boson mass constraint. The neutrino pseudorapidity, η_ν, is calculated by setting the invariant mass of the lepton and neutrino equal to the W-boson mass, $m_W = 80.379$ GeV [98]:

$$\eta_\nu = \eta_\ell \pm \operatorname{arccosh}\left(\frac{m_W^2}{2p_{\mathrm{T}}^{\nu}p_{\mathrm{T}}^{\ell}} + \cos\left(\phi_\nu - \phi_\ell\right)\right).$$

This equation generally has two solutions and the one that is chosen depends on the jet labelling, described below. If the

[4] The MJ background is considered when deriving the $t\bar{t}$ correction. The $t\bar{t}$ correction weights are also applied in the MJ-enriched regions. The reciprocal dependence of the MJ background estimate and the $t\bar{t}$ correction is considered when deriving the correction weights. The impact on the correction weights is minor due to the overall small MJ contribution.

argument of arccosh is exactly one, there is only one solution ($\eta_\nu = \eta_\ell$). Due to reconstruction inefficiencies or additional neutrinos in the event, e.g. from the decay of τ_{lep}, it may also happen that the argument of arccosh is smaller than one, for which arccosh is not defined. In this case the argument of arccosh is set to one. This means $\eta_\nu = \eta_\ell$, in which case the invariant mass of the lepton and the neutrino exceeds m_W. The latter case occurs for about 35% of the simulated $t\bar{t}$ events.

The labelling of the jets as b_{lep}, b_{had}, j_1 and j_2 suffers from a combinatorics problem, which the analysis tries to resolve by comparing the top-quark candidate's mass with the predicted top-quark mass. Because the mass resolution differs between semileptonically and hadronically decaying top quarks, the approach adopted uses probability density functions of the reconstructed top-quark masses (PDF_t). These are built from $t\bar{t}$ MC events, using reconstructed jets matched to the generator-level ("truth") quarks. Since there is only one lepton candidate, no matching is applied for it. For the neutrino, if there are two solutions for η_ν, the one closest to the true value of η_ν is selected. The "truth" quarks are geometrically matched to the closest reconstructed jet within $\Delta R = 0.4$. The b- and c-quarks are only matched if the reconstructed jet has a respective "truth" hadron ($p_{\text{T}} > 5$ GeV) associated with it. Other quark types are only matched to the reconstructed jet if no heavy-flavour hadron is associated with it. If multiple "truth" quarks are matched to the same reconstructed jet, ambiguities are resolved by minimising the sum of the (four) ΔR values between the "truth" quarks and any reconstructed jet within $\Delta R = 0.4$ of the "truth" quarks. In roughly 53% of the events, at least one "truth" quark cannot be matched to a reconstructed jet. Such cases are typically associated with "truth" quarks produced outside the detector acceptance. Such events are not considered in the PDF_t. In order to get a smooth prediction over the full top-quark mass range, Crystal Ball + Cauchy and Crystal Ball + Gaussian functions [99–101] are fitted to the t_{lep}-mass and t_{had}-mass PDF_t, respectively. The PDF_t are shown with the corresponding fits in Fig. 3.

The derived top-quark mass PDF_t are then used to label jets in an event. All possible permutations of b_{lep}, b_{had}, j_1, j_2 labellings and η_ν solutions are built simultaneously. The permutation with the largest product of the t_{lep}-mass and t_{had}-mass PDF_t, i.e. $\text{PDF}_{t_{\text{lep}}}(m^{\text{cand}}_{t_{\text{lep}}}) \times \text{PDF}_{t_{\text{had}}}(m^{\text{cand}}_{t_{\text{had}}})$, is chosen, and the jets are labelled accordingly. The highest PDF_t product value is denoted by $P_{t\bar{t}}$, and $P_{t\bar{t}}$ divided by the sum of PDF_t product values for all considered permutations is denoted by $\overline{P}_{t\bar{t}}$.

However, a few physics-motivated requirements are applied to limit the number of jet permutations. A maximum of six jets are considered when building the permutations. The b-jets are always considered, whereas the highest-p_{T} non-b-jets are considered first. The jets labelled as b_{lep}-jets or b_{had}-jets have to be b-tagged and their PCFT scores are required to be greater than or equal to the PCFT scores of j_1 and j_2. It is also required that the p_{T} of j_1 is greater than the p_{T} of j_2. This requirement removes redundant permutations, since interchanging j_1 and j_2 yields identical values for the top-quark and charged-Higgs-boson candidate masses. Finally, if multiple jets among b_{had}, j_1, j_2 are b-tagged and the b-tagged jets have the same PCFT score, multiple permutations will yield the same top-quark candidate mass. In these rare cases the b-tagged jet with the larger p_{T} is labelled as the b_{had}-jet. In 64% of the events entering the PDF_t, all four jets are labelled correctly. The performance for signal events is comparable.

6.2 Multivariate signal extraction

The multivariate signal extraction exploits differences between the characteristics of the charged Higgs boson and the W boson. These are the boson mass, spin and decay properties. These differences are seen in many variables related to flavour-tagging and the kinematics of the top-quark decay products. The discriminating variables are combined into a single discriminant through the use of BDTs.

The BDT classifies events as signal-like or background-like. Background-like events receive BDT scores close to 0, whereas signal-like events receive BDT scores close to 1. Separate BDTs are trained for each signal mass-point hypothesis with 5-fold cross-training and using the gradient boosting technique [102]. All simulated background samples listed in Sect. 3 are used in the BDT training. Events included in the training have to pass the event selection described in Sect. 4. Training and application are carried out within the *XGBoost* [103] framework.

Any variable describing the properties of top quarks and their decay products is considered as an input to the BDT training. The final set of BDT input variables is obtained by recursively removing variables with relatively small power to separate the signal from the background, and low importance in the BDT training, until a statistically significant loss in performance is observed. The performance is quantified by the area under the receiver-operating-characteristic curve. This optimisation is performed with the 130 GeV signal sample. The signal and $t\bar{t}$ background kinematics are very similar for the signal mass points close to the W-boson mass but differ greatly for signal mass points closer to the top-quark mass; the intermediate 130 GeV mass point covers both cases.

The final BDT uses the 26 input variables which are listed in Table 2. The variables can be sorted into three categories: top-quark kinematic variables, event variables, and flavour-tagging variables. The first category contains variables related to the kinematics of the top quarks and their decay products. These variables are mainly sensitive to the mass difference between the $H^\pm$ and W bosons. If the mass

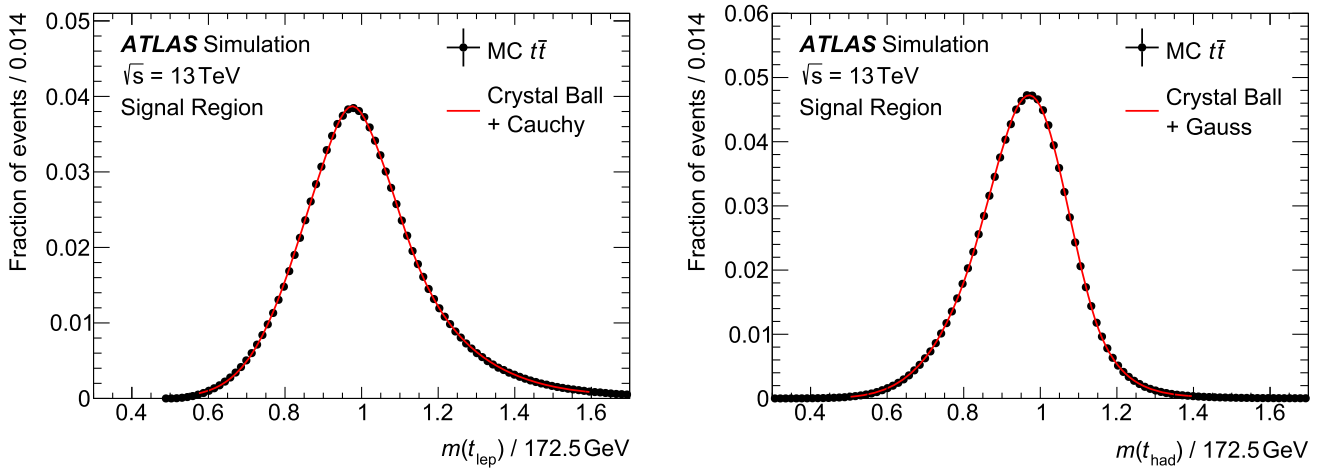

Fig. 3 Probability density functions of the reconstructed mass for **a** semileptonically and **b** hadronically decaying top quarks

Table 2 Final list of BDT input variables used in the training

Variable type	Variable name	Definition
Top-quark kinematic variables		
t_{had}	j_1 p_{T}	p_{T} of j_1-labelled jet
	j_2 p_{T}	p_{T} of j_2-labelled jet
	b_{had} p_{T}	p_{T} of b_{had}-jet
	$b_{\text{had}}^{t_{\text{had}}-\text{rest}}$ p	Momentum of b_{had}-jet in t_{had} rest frame
	dijet mass	Invariant mass of j_1+j_2 jets
	(j_1+b_{had}) mass	Invariant mass of j_1+b_{had} jets
	(j_2+b_{had}) mass	Invariant mass of j_2+b_{had} jets
	$\cos\theta$	Boson spin sensitive variable
t_{lep}	b_{lep} p_{T}	p_{T} of b_{lep}-jet
	Lepton p_{T}	p_{T} of reconstructed lepton
	W mass	Invariant mass of reconstructed W boson
	t_{lep} mass	Invariant mass of reconstructed t_{lep}
	t_{lep} p_{T}	p_{T} of reconstructed t_{lep}
$t\bar{t}$-system	$\Delta R(b_{\text{lep}},b_{\text{had}})$	ΔR between the b_{lep}-jet and b_{had}-jet
	$t\bar{t}$ mass	Invariant mass of t_{had}+t_{lep}
Event variables		
Event level	N_{jets}	Number of jets in the event
	S_{T}	Scalar p_{T} sum of all calibrated objects
	$\overline{P}_{t\bar{t}}$	Normalised probability of correct jet labelling
Flavour-tagging variables		
Flavour-tagging score	j_1 PCFT	PCFT score of j_1
	j_2 PCFT	PCFT score of j_2
	b_{had} PCFT	PCFT score of b_{had}-jet
	b_{lep} PCFT	PCFT score of b_{lep}-jet
Number of tags	$N_{c\text{-tagLo}}$	Number of jets passing loose c-tag WP (b-veto)
	$N_{c\text{-tagTi}}$	Number of jets passing tight c-tag WP (b-veto)
	$N_{b\text{-tag70}}$	Number of jets passing 70% b-tag WP
	$N_{b\text{-tag60}}$	Number of jets passing 60% b-tag WP

difference is comparable to or larger than the dijet mass resolution [83], the kinematic variables exhibit larger separation power than variables in the other categories. The most important variables (in order of decreasing area under the receiver-operating-characteristic curve) are the invariant mass of j_1 and j_2 and the transverse momentum of the b_{had}-jet, followed by the invariant mass of j_1 and b_{had}-jet, the invariant mass of j_2 and b_{had}-jet, and the transverse momenta of j_1 and j_2. Variables related to the $t\bar{t}$-system, the t_{lep}-quark and the decay products provide separation power between signal and non-$t\bar{t}$ backgrounds. In addition, they can carry information about possible wrong jet labelling and add information via correlation with other input variables.

The $\cos\theta$ variable is the only variable that is sensitive to the spin of the boson from the t_{had} decay and therefore shows separation power for any $H^{\pm}$ boson mass. The angle θ is defined as the angle between the b_{had}-jet and the up-type-quark-initiated jet from the hadronically decaying boson ($H^{\pm}$ or W) in the boson's rest frame. The up-type-quark-initiated jet is identified with the help of the PCFT scores of j_1 and j_2. The c-tagged jets are prioritised over b-tagged jets, which in turn are prioritised over untagged jets. If the PCFT scores of j_1 and j_2 are identical, j_1 is assigned to be the jet from the up-type quark. The $\cos\theta$ distribution is flat for spin-0 particles, like the $H^{\pm}$ boson. For spin-1 particles, like the W boson, the distribution is more complex because polarisation effects play a role, and there are fewer events close to -1 and 1. However, it is difficult to identify the quark flavours in the decay of the boson. In addition, the $\cos\theta$ distribution is heavily affected by jet resolution effects because three jets are used in the calculation.

The second category of variables involves event variables. The $\overline{P}_{t\bar{t}}$ variable facilitates the identification of wrongly labelled jets and can also reject non-$t\bar{t}$ background. The N_{jets} and S_{T} variables are correlated with most top-quark kinematic variables. For example, an event with small b_{had}-jet p_{T} and large S_{T} suggests a signal event with a high-mass charged Higgs boson.

The third category contains flavour-tagging variables, which are the PCFT scores of the four labelled jets and the number of jets passing a given PCFT working point. Of special interest are the PCFT scores of j_1 and j_2, as they are sensitive to the different decay characteristics of the charged Higgs boson. While all signal events involve a c-quark in the boson decay, only about 50% of the $t\bar{t}$ background events share the same characteristic. Other flavour-tagging variables are useful in rejecting non-$t\bar{t}$ background and add information via correlations with other variables. The distributions of selected BDT input variables of different types and with large separation power are shown in Fig. 4.

The optimisation of the BDT input variables was performed with a baseline set of hyperparameters – including tree depth and learning rate – determined by a lightweight BDT hyperparameter scan. For the final training, the optimal configuration of the BDT hyperparameters is determined for each signal mass point separately with the help of the *hyperopt* [104] tool. The *hyperopt* tool performs a Bayesian optimisation using Tree-structured Parzen Estimators to obtain the optimal parameter set from a given parameter range. It is more efficient than grid or random searches because it uses previous training steps to learn where the optimum is going to be. To avoid any bias between the hyperparameter optimisation dataset and the final test dataset, the scan was carried out using nested cross-training. For each of the 5-folds the scan is performed using 4-fold cross-training on the other four folds. For the final training the BDTs are retrained using all four folds as training data. The BDT-score distributions after training with the $H^{\pm}_{80}$, $H^{\pm}_{110}$, $H^{\pm}_{130}$ and $H^{\pm}_{150}$ signal samples are shown in Fig. 5.

7 Systematic uncertainties

This section discusses systematic uncertainties the analysis is sensitive to, including those affecting the detector response, theoretical uncertainties, and modelling of signal and background processes that affect the normalisation and shapes of the simulated signal and background distributions. The individual systematic uncertainties are considered to be uncorrelated, while correlations for a given systematic uncertainty are maintained across signal and background processes.

The uncertainty in the combined 2015–2018 integrated luminosity is 0.83% [31], obtained using the LUCID-2 detector [28] for the primary luminosity measurements, complemented by measurements using the inner detector and calorimeters. This uncertainty is assigned to all physics processes whose normalisations are taken from simulation. An uncertainty in the correction of the pile-up distribution [105] in simulation to that in data is taken into account as well.

Uncertainties in the calibration of physics objects affect all simulated samples. Uncertainties associated with the trigger, reconstruction, identification and isolation efficiency calibration [74,77], as well as the impact of the energy (momentum) scale and resolution uncertainties [74,106] on the selection efficiency are considered for electrons (muons). Jet energy scale (JES) [107] and resolution (JER) [108] uncertainties and the uncertainty in the efficiency of matching jets to the primary vertex [84] are taken into account. The energy scale and resolution uncertainties for leptons and jets are propagated to the $E_{\text{T}}^{\text{miss}}$. In addition, the uncertainty in the $E_{\text{T}}^{\text{miss}}$ from tracks matched to the primary vertex but not to other reconstructed objects [90] is considered. Corrections to simulations to match the flavour-tagging and mistagging efficiencies in data are taken into account in bins of the jet p_{T} [86–88].

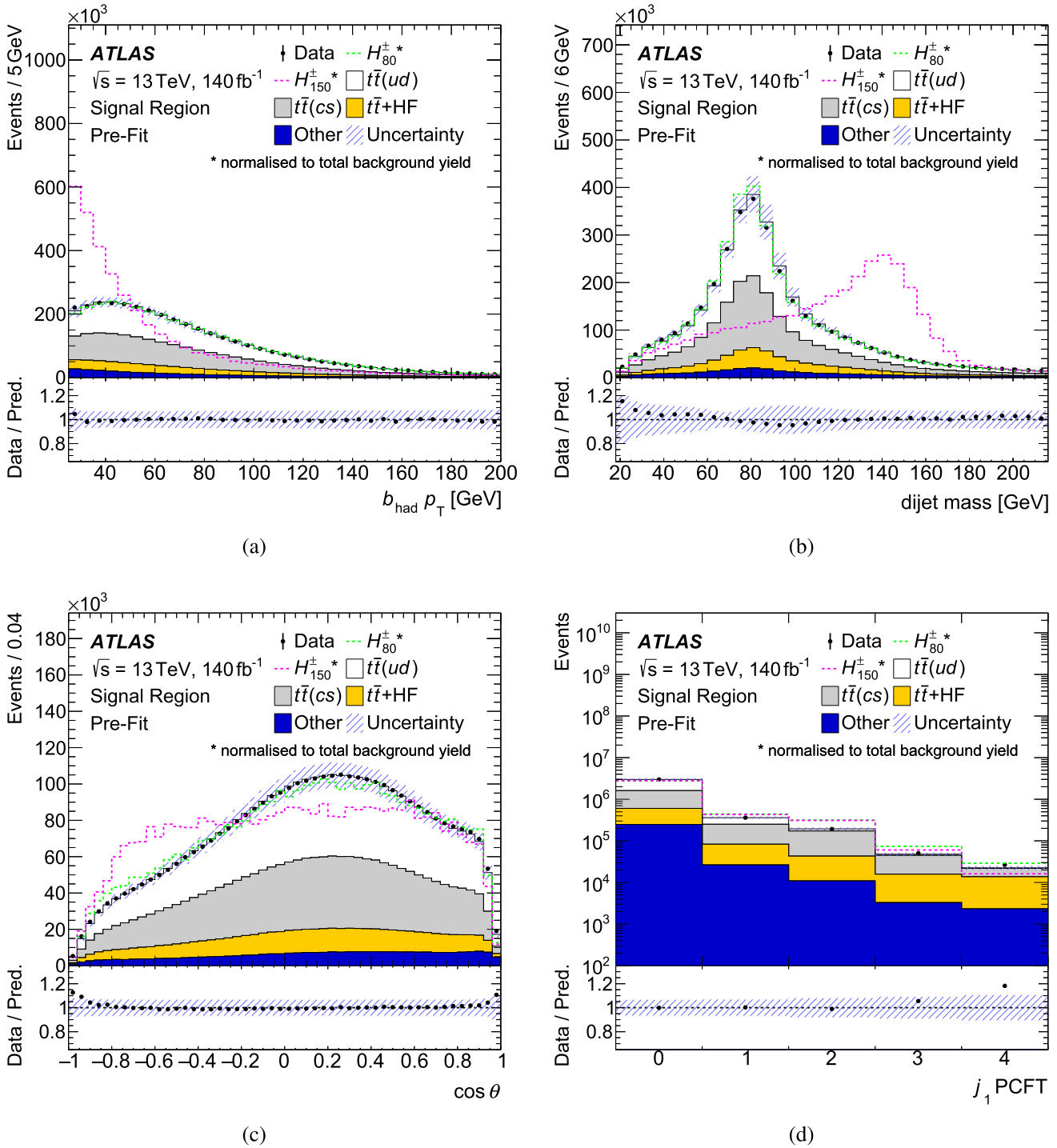

Fig. 4 Distributions of selected BDT input variables. The variables are defined in Table 2. The processes $t\bar{t}$(allHad), tW, Single top, $t\bar{t}H$, Other top, W+ jets, Z + jets, VV listed in Table 1 are combined with the multijet background in the "Other" category. The uncertainty band represents the combined statistical and systematic uncertainty of the prediction. Overlaid are the shapes for the $H^{\pm}_{80}$ and $H^{\pm}_{150}$ signal samples normalised to the total background prediction

Uncertainties in the modelling of different processes are assumed to be uncorrelated. Modelling uncertainties for processes making a small contribution to the total background yield ($t\bar{t}$(allHad), $t\bar{t}H$ and Other top samples) are neglected. Some modelling uncertainties are estimated in the same way for all processes. These are the uncertainties due to miss-

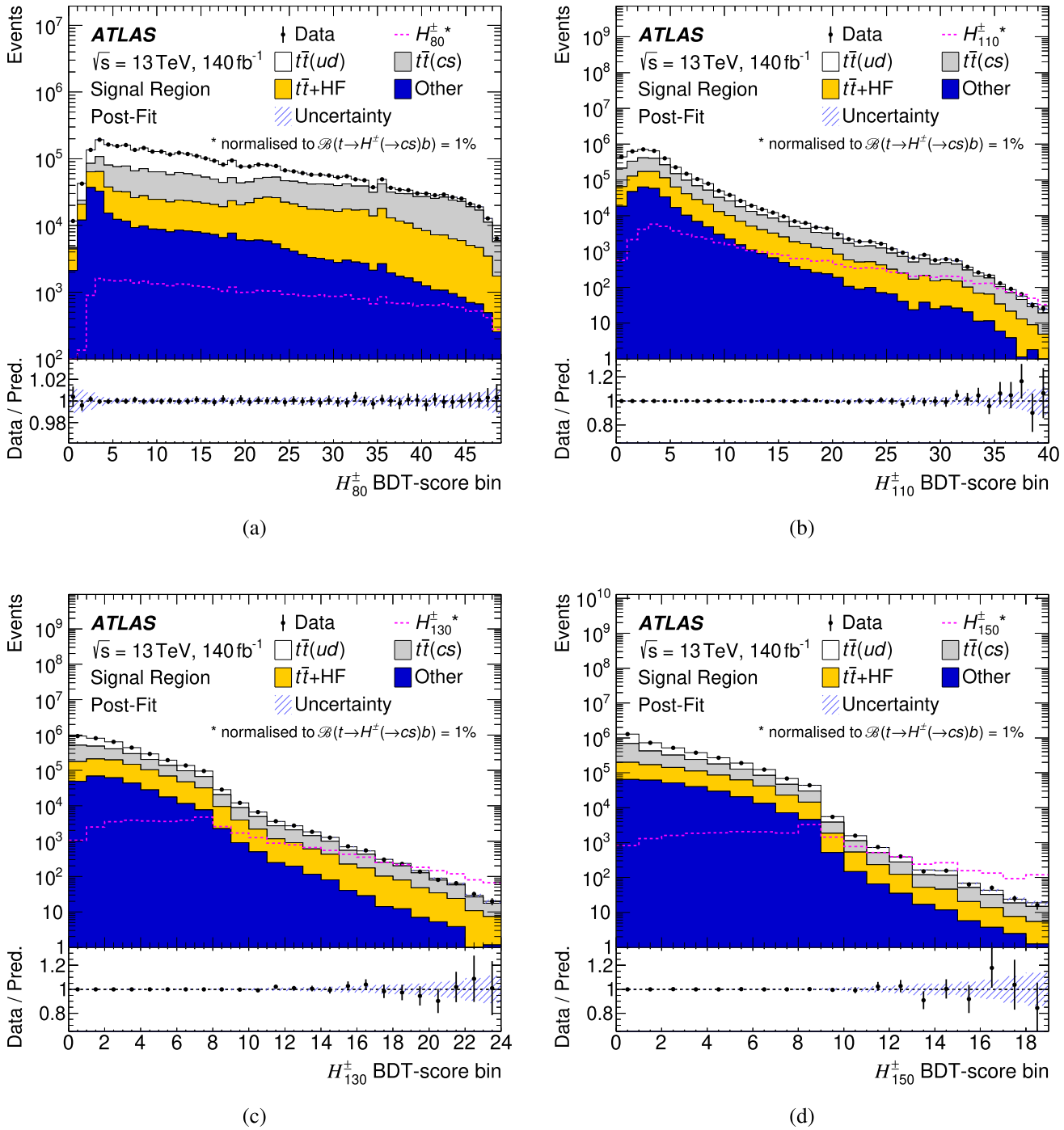

Fig. 5 BDT-score distributions for the training with the **a** 80 GeV, **b** 110 GeV, **c** 130 GeV and **d** 150 GeV signal mass hypotheses after performing background-only binned-likelihood fits to the distributions as described in Sect. 8. The processes $t\bar{t}$(allHad), tW, Single top, $t\bar{t}H$, Other top, W+ jets, Z + jets, VV listed in Table 1 are combined with the multijet background in the "Other" category. The background yields are normalised to their best-fit values. The uncertainty band represents the combined statistical and systematic uncertainty of the prediction. Overlaid is the signal shape normalised to $\mathcal{B}(t \to H^{\pm}(\to cs)b) = 1\%$. The binning procedure for the BDT score is defined in Sect. 8

ing higher orders in the perturbative expansion of the partonic cross-section, which are estimated by varying the renormalisation (μ_r) and factorisation (μ_f) scales by a factor of two. The uncertainties associated with the choice of PDF are evaluated by using dedicated PDF error eigensets. The PDF uncertainties are combined by calculating their standard

deviation with respect to the nominal set or by summing the differences in quadrature for Hessian sets. The uncertainty related to the choice of strong coupling constant value α_s is evaluated by comparing predictions using PDF sets obtained with two alternative α_s values. The uncertainties in the production cross-sections are included as normalisation uncertainties [109–112] for all processes whose normalisations are taken from simulation.

For top-quark processes the uncertainties associated with the choice of generator for ME and PS simulation are assessed by comparing the nominal sample with alternative samples generated with aMC@NLO instead of Powheg Box and with Herwig 7 instead of Pythia, respectively. The uncertainty due to the choice of h_{damp} parameter value is determined by comparison with an alternative sample generated with $h_{\text{damp}} = 3\,m_{\text{top}}$ instead of $1.5\,m_{\text{top}}$. The alternative samples are described in detail in Sect. 3. The interference between $tW(b)$ and $t\bar{t}$ processes [47] is handled using the diagram removal scheme, which removes diagrams with intermediate top quarks. The uncertainty associated with this procedure is evaluated with the help of an alternative tW sample where a subtraction term is added to the matrix element to cancel out the resonant top-quark pole contribution.

For top-quark and signal processes the uncertainties in the amounts of initial- and final-state QCD radiation (ISR and FSR) are estimated by varying the corresponding parameter (Var3c) of the A14 PS tune and by varying the FSR scale ($\mu_{\text{r}}^{\text{FSR}}$) by a factor of two, respectively. The systematic uncertainty introduced by the $t\bar{t}$ correction, described in Sect. 5, is estimated by performing an eigenvalue decomposition of the fitted parameters and varying the eigenvalues separately by one standard deviation. Uncertainties related to the $t\bar{t}$ ME, PS, h_{damp} parameter and FSR show, among the considered systematic uncertainties, the largest shape differences in the high BDT-score regions and are therefore the dominant uncertainties in this search.

For weak-boson processes, electroweak corrections at next-to-leading order are estimated using the electroweak virtual approximation. The electroweak and QCD components are combined using an exponentiated prescription [113,114]. CKKW and QSF are two parameters of Sherpa that define the scale for merging/matching jets from the ME with the PS, and the scale used for resummation of soft gluon emissions, respectively. Their impact on the BDT input observables is measured at generator-level with the help of alternative samples in which the nominal values are varied. The observed differences are covered by a 17% normalisation uncertainty. The effect of NNLO correction factors on the cross-section of single-boson processes is 5%. This is added as a normalisation uncertainty to all weak-boson processes.

To evaluate the systematic uncertainty of the multijet background estimate, an alternative estimate is made in which, instead of the lepton isolation criterion, a looser lepton identification is used to define the ABCD regions. In addition, a conservative 50% normalisation uncertainty is added to account for statistical uncertainties of the transfer factor and MC uncertainties in regions B, C and D.

The uncertainty in the expected event count in each bin, due to the finite MC sample sizes, is accounted for by one Gaussian-constrained parameter per bin, which represents the total uncertainty of the MC event content in that bin [115].

8 Statistical interpretation

The presence of a charged Higgs boson signal in data is quantified with the help of binned maximum-likelihood fits to the BDT-score distributions. The statistical model is implemented using the Histfactory format [116]. Minimisation of the likelihood function is performed in the pyhf framework [117].

The parameter of interest is the branching fraction of the process $t \to H^{\pm}b$ ($\mathscr{B}_{H^{\pm}}$), which is constrained to $\mathscr{B}_{H^{\pm}} \in [0, 0.1]$,[5] while assuming $\mathscr{B}(t \to Wb) + \mathscr{B}(t \to H^{\pm}(\to cs)b) = 1.0$. The $t\bar{t}$ cross-section scaling factor ($\mu_{t\bar{t}}$) and the fraction of $t\bar{t}$ +HF events among $t\bar{t}$ background events (f_{HF}) are unconstrained parameters in the fit, with nominal values of 1.0 and 0.1364, respectively. These parameters relate the signal and background yields before the fit (pre-fit) and after the fit (post-fit) as follows:[6]

$$\begin{aligned} N_{H^{\pm}}(\text{post-fit}) &= \mu_{t\bar{t}} \times 2(1-\mathscr{B}_{H^{\pm}})\,\mathscr{B}_{H^{\pm}} \\ &\quad \times N_{H^{\pm}}(\text{pre-fit}), \\ N_{t\bar{t}\,+\text{LF}}(\text{post-fit}) &= \mu_{t\bar{t}} \times (1-f_{\text{HF}}) \times (1-\mathscr{B}_{H^{\pm}})^2 \\ &\quad \times N_{t\bar{t}\,+\text{LF}}(\text{pre-fit}), \\ N_{t\bar{t}\,+\text{HF}}(\text{post-fit}) &= \mu_{t\bar{t}} \times f_{\text{HF}} \times (1-\mathscr{B}_{H^{\pm}})^2 \\ &\quad \times N_{t\bar{t}\,+\text{HF}}(\text{pre-fit}). \end{aligned}$$

The systematic uncertainties described in Sect. 7 are implemented as Gaussian-constrained nuisance parameters (NPs) in the fit. Systematic uncertainties with just one component are symmetrised by mirroring the nominal template. All two-point systematic uncertainties and some reweighting systematic uncertainties with large statistical fluctuations are smoothed. Uncertainties with a negligible impact on the uncertainty of $\mathscr{B}_{H^{\pm}}$ are removed from the likelihood fit to improve numerical performance.

The discovery significance of a signal in data is calculated in a likelihood ratio test where the background-only hypoth-

[5] The upper bound on $\mathscr{B}_{H^{\pm}}$ is justified by measurements setting lower bounds on $\mathscr{B}(t \to Wb)$ [118].

[6] The event yields before the fit are set to the total expected $t\bar{t}$ yield, so that $N_{H^{\pm}}(\text{pre-fit}) = N_{t\bar{t}\,+\text{LF}}(\text{pre-fit}) = N_{t\bar{t}\,+\text{HF}}(\text{pre-fit})$. For the nominal values of $\mu_{t\bar{t}}$ and f_{HF}, and $\mathscr{B}_{H^{\pm}} = 0$, one recovers the SM expectation.

esis is compared with the signal-plus-background hypothesis [119]. The asymptotic approximation is used to estimate the probability distribution of the test statistic [120]. Upper limits on $\mathscr{B}_{H^\pm}$ are set by determining the $\mathscr{B}_{H^\pm}$ value which can be rejected in 95% of the cases, i.e. at 95% confidence level (CL), with respect to the best-fit signal-plus-background hypothesis. The modified frequentist technique (CL_s) [121] is used to avoid excluding signal models where the analysis has little sensitivity. The median upper limit, referred to as the expected upper limit, and its 1σ and 2σ expected variations are derived from a background-only Asimov dataset [120].

The BDT-score templates are binned in such a way that the number of bins is minimised, while maximising the expected sensitivity and ensuring the stability of the fit and the validity of the asymptotic approximation. This is achieved by starting from templates with 10,000 equal-width bins and iteratively merging bins from right to left – starting from the most discriminating bins – until a bin in question fulfils all conditions. Each bin is required to contain at least 20 expected background events, and the signal and background MC statistical uncertainties have to be less than 20% and 10%, respectively. Each bin has to pass a given $S/\sqrt{B}$ threshold defined by the $S/\sqrt{B}$ ratio[7] in the first merged bin. In order to retain shape information in the low discriminating BDT-score region, a maximum of 1000 bins may be merged into a single bin. Additionally, the $S/\sqrt{B}$ threshold may be adjusted for BDT scores with very high or very low separation power such that each template has at least 19 and no more than 49 bins.

9 Results

The binned maximum-likelihood fit described in Sect. 8 is performed per signal mass-point hypothesis on the respective BDT-score distribution. Table 3 shows the data and background yields after the background-only fit of the BDT-score distribution trained with the 130 GeV signal mass point.

The fitted $\mu_{t\bar{t}}$ values agree within their uncertainties with the SM prediction of 1.0 for all mass points. The f_{HF} parameter is measured to be 0.19 ± 0.02 for the $H^\pm_{80}$ fit, which is the most precise fit. The measured values of f_{HF} in other fits agree with this value within their uncertainties. This is a larger heavy-flavour fraction than predicted by simulations, but agrees with many other ATLAS analyses [20,122–126]. The fitted $\mathscr{B}_{H^\pm}$ values are equal to, or compatible with, zero for most signal mass hypotheses. The largest signal significance observed in data is for the 110 GeV mass point, with a local p-value of 5% (1.5σ).

[7] S is the signal and B the total background prediction in the respective bin.

Table 3 Data and background yields after the background-only fit of the BDT-score distribution for the 130 GeV signal mass BDT training. For comparison, the expected signal yield for $\mathscr{B}_{H^\pm} = 1\%$ is added. The sample names are defined in Table 1

Name	Post-fit yields
$t\bar{t}(ud)$	1,400,000 ± 76,000
$t\bar{t}(cs)$	1,200,000 ± 92,000
$t\bar{t}$ +HF	710,000 ± 150,000
tW	100,000 ± 23,000
Single top	68,000 ± 28,000
W+ jets	70,000 ± 29,000
Z + jets & VV	21,000 ± 9500
Other top & $t\bar{t}$(allHad) & $t\bar{t}H$	17,000 ± 450
Multijet (MJ)	12,000 ± 6800
Total background	3,600,000 ± 11,000
Data	3,600,000
$H^\pm_{130}$ ($\mathscr{B}_{H^\pm} = 1\%$)	38,000

The impact of systematic uncertainties on the $\mathscr{B}_{H^\pm}$ measurement's accuracy is estimated by fixing the NP under consideration to its post-fit value, performing the fit and comparing the uncertainty of the fitted $\mathscr{B}_{H^\pm}$ with the one from the nominal fit. The results of these fits when fixing a group of systematic uncertainties are summarised in Table 4. For the 80 GeV signal hypothesis the kinematics are very similar for the signal and $t\bar{t}$ processes. Therefore, the flavour-tagging uncertainties have the largest impact on $\mathscr{B}_{H^\pm}$. For other signal hypotheses the $t\bar{t}$ modelling NPs, especially those for the ME, PS, FSR and h_{damp} uncertainties, have the largest impact on the $\mathscr{B}_{H^\pm}$ uncertainty. MC statistical uncertainties naturally become more important with finer BDT-score binning. Less impactful but still important are jet, single-top-quark and weak-boson modelling uncertainties. Least impactful are luminosity, pile-up, lepton and $E_{\text{T}}^{\text{miss}}$-related uncertainties.

Figure 6 shows the expected limits on $\mathscr{B}_{H^\pm}$ with their 1σ and 2σ uncertainty bands. The expected limits are least stringent for the 80 GeV mass point, at about 2.3%, as this signal mass point is closest to the W-boson mass. For this mass point, the flavour-tagging information is the most powerful discriminant between signal and background. Moving away from the W-boson mass the top-quark kinematics start to differ more and the limits improve. The most stringent limits are expected for the 150 GeV mass point, at about 0.077%. Close to the top-quark mass threshold the limits weaken again as the acceptance decreases. The small acceptance is caused by the low average momentum of the b_{had}-quark so that the resulting jets often fail the kinematic requirements. The solid line in Fig. 6 represents the observed limits. The observed limits vary between 0.066 to 3.6%. Expected and observed limits agree within uncertainties.

Table 4 Breakdown of the relative contributions to the uncertainty in the extracted $\mathscr{B}_{H^\pm}$ in the likelihood fit to data. The contributions are obtained by fixing the relevant NPs to their post-fit values in the likelihood fit. The square root of the difference of the squares of the nominal uncertainty and obtained uncertainty is divided by the nominal uncertainty to obtain the relative impact. The sum in quadrature of the individual components differs from the total uncertainty due to correlations between uncertainties in the different groups. The uncertainty from data statistical uncertainties is determined from fits with all NPs fixed to their post-fit values. The total uncertainty in $\mathscr{B}_{H^\pm}$ for the fits with $H^\pm_{80}$ and $H^\pm_{150}$ is 1.2% and 0.04%, respectively

$H^\pm_{80}$		$H^\pm_{150}$	
Category	Relative contribution	Category	Relative contribution
Data statistical	6%	Data statistical	38%
Systematic	99.8%	Systematic	93%
Flavour-tagging	64%	$t\bar{t}$ modelling	72%
MC statistical	64%	MC statistical	35%
$t\bar{t}$ modelling	50%	Weak-boson and MJ modelling	27%
$\mu_{t\bar{t}}$ and f_{LF}	21%	Single-top-quark modelling	25%
Jet	19%	$\mu_{t\bar{t}}$ and f_{LF}	24%
Single-top-quark modelling	16%	Jet	23%
Luminosity and pile-up	15%	Flavour-tagging	20%
Weak-boson and MJ modelling	12%	Lepton and $E_{\mathrm{T}}^{\mathrm{miss}}$	8%
Signal modelling	8%	Luminosity and pile-up	7%
Lepton and $E_{\mathrm{T}}^{\mathrm{miss}}$	7%	Signal modelling	5%

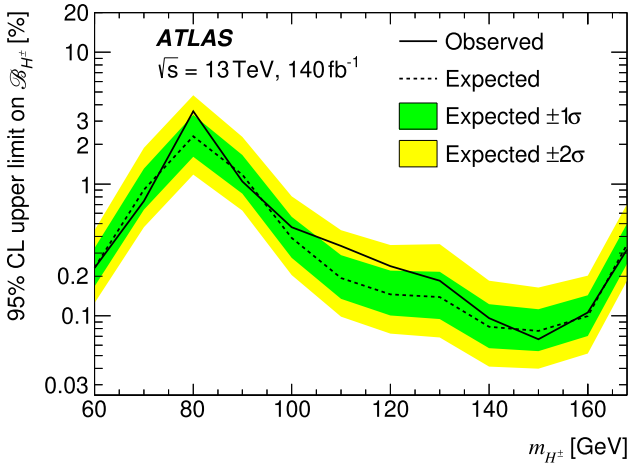

Fig. 6 Observed (solid line) and expected (dotted line) upper limits on $\mathscr{B}_{H^\pm}$ for charged Higgs boson with masses between 60 and 168 GeV, assuming $\mathscr{B}(t \to Wb) + \mathscr{B}(t \to H^\pm(\to cs)b) = 1.0$. The $\pm 1\sigma$ and $\pm 2\sigma$ variations around the expected upper limit are indicated by the green and yellow bands, respectively

10 Conclusions

A search for a light charged Higgs boson produced in decays of the top quark, $t \to H^\pm b$, with $H^\pm \to cs$ is performed in the $H^\pm$ mass range from 60 to 168 GeV. The data analysed corresponds to 140 fb^{-1} of pp collisions at $\sqrt{s} = 13$ TeV recorded with the ATLAS detector at the LHC between 2015 and 2018. This analysis focuses on the lepton-plus-jets final state, characterised by an isolated electron or muon and at least four jets. The search exploits b-quark and c-quark identification techniques as well as multivariate methods to suppress the dominant $t\bar{t}$ background. No significant signal excess is found in data. Observed and expected 95% CL upper limits on the branching fraction $\mathscr{B}(t \to H^\pm b)$, assuming $\mathscr{B}(t \to Wb) + \mathscr{B}(t \to H^\pm(\to cs)b) = 1.0$, are found to range from 0.066 to 3.6% and 0.077 to 2.3%, respectively, depending on the mass of the charged Higgs boson. These are the first direct limits on $\mathscr{B}(t \to H^\pm b)$ in the $H^\pm \to cs$ channel for charged Higgs bosons with masses of 60 GeV, 70 GeV and 168 GeV, and currently the most stringent limits for masses between 120 GeV and 160 GeV.

Acknowledgements We thank CERN for the very successful operation of the LHC and its injectors, as well as the support staff at CERN and at our institutions worldwide without whom ATLAS could not be operated efficiently. The crucial computing support from all WLCG partners is acknowledged gratefully, in particular from CERN, the ATLAS Tier-1 facilities at TRIUMF/SFU (Canada), NDGF (Denmark, Norway, Sweden), CC-IN2P3 (France), KIT/GridKA (Germany), INFN-CNAF (Italy), NL-T1 (Netherlands), PIC (Spain), RAL (UK) and BNL (USA), the Tier-2 facilities worldwide and large non-WLCG resource providers. Major contributors of computing resources are listed in Ref. [127]. We gratefully acknowledge the support of ANPCyT, Argentina; YerPhI, Armenia; ARC, Australia; BMWFW and FWF, Austria; ANAS, Azerbaijan; CNPq and FAPESP, Brazil; NSERC, NRC and CFI, Canada; CERN; ANID, Chile; CAS, MOST and NSFC, China; Minciencias, Colombia; MEYS CR, Czech Republic; DNRF and DNSRC, Denmark; IN2P3-CNRS and CEA-DRF/IRFU, France; SRNSFG, Georgia; BMBF, HGF and MPG, Germany; GSRI, Greece; RGC and Hong Kong SAR, China; ISF and Benoziyo Center, Israel; INFN, Italy; MEXT and JSPS, Japan; CNRST, Morocco; NWO, Netherlands; RCN, Norway; MNiSW, Poland; FCT, Portugal; MNE/IFA, Romania; MSTDI, Serbia; MSSR, Slovakia; ARIS and MVZI, Slove-

nia; DSI/NRF, South Africa; MICIU/AEI, Spain; SRC and Wallenberg Foundation, Sweden; SERI, SNSF and Cantons of Bern and Geneva, Switzerland; NSTC, Taipei; TENMAK, Türkiye; STFC/UKRI, United Kingdom; DOE and NSF, United States of America. Individual groups and members have received support from BCKDF, CANARIE, CRC and DRAC, Canada; CERN-CZ, FORTE and PRIMUS, Czech Republic; COST, ERC, ERDF, Horizon 2020, ICSC-NextGenerationEU and Marie Skłodowska-Curie Actions, European Union; Investissements d'Avenir Labex, Investissements d'Avenir Idex and ANR, France; DFG and AvH Foundation, Germany; Herakleitos, Thales and Aristeia programmes co-financed by EU-ESF and the Greek NSRF, Greece; BSF-NSF and MINERVA, Israel; NCN and NAWA, Poland; La Caixa Banking Foundation, CERCA Programme Generalitat de Catalunya and PROMETEO and GenT Programmes Generalitat Valenciana, Spain; Göran Gustafssons Stiftelse, Sweden; The Royal Society and Leverhulme Trust, United Kingdom. In addition, individual members wish to acknowledge support from Armenia: Yerevan Physics Institute (FAPERJ); CERN: European Organization for Nuclear Research (CERN PJAS); Chile: Agencia Nacional de Investigación y Desarrollo (FONDECYT 1230812, FONDECYT 1230987, FONDECYT 1240864); China: Chinese Ministry of Science and Technology (MOST-2023YFA1605700), National Natural Science Foundation of China (NSFC-12175119, NSFC 12275265, NSFC-12075060); Czech Republic: Czech Science Foundation (GACR-24-11373S), Ministry of Education Youth and Sports (FORTE CZ.02.01.01/00/22_008/0004632), PRIMUS Research Programme (PRIMUS/21/SCI/017); EU: H2020 European Research Council (ERC - 101002463); European Union: European Research Council (ERC-948254, ERC 101089007), Horizon 2020 Framework Programme (MUCCA - CHIST-ERA-19-XAI-00), European Union, Future Artificial Intelligence Research (FAIR-NextGenerationEU PE00000013), Italian Center for High Performance Computing, Big Data and Quantum Computing (ICSC, NextGenerationEU); France: Agence Nationale de la Recherche (ANR-20-CE31-0013, ANR-21-CE31-0013, ANR-21-CE31-0022, ANR-22-EDIR-00 02), Investissements d'Avenir Labex (ANR-11-LABX-0012); Germany: Baden-Württemberg Stiftung (BW Stiftung-Postdoc Eliteprogramme), Deutsche Forschungsgemeinschaft (DFG-469666862, DFG-CR 312/5-2); Italy: Istituto Nazionale di Fisica Nucleare (ICSC, NextGenerationEU), Ministero dell'Università e della Ricerca (PRIN-20223N7F8K-PNRR M4.C2.1.1); Japan: Japan Society for the Promotion of Science (JSPS KAKENHI JP22H01227, JSPS KAKENHI JP22H04944, JSPS KAKENHI JP22KK0227, JSPS KAKENHI JP23KK0245); Netherlands: Netherlands Organisation for Scientific Research (NWO Veni 2020-VI.Veni.202.179); Norway: Research Council of Norway (RCN-314472); Poland: Ministry of Science and Higher Education (IDUB AGH, POB8, D4 no 9722), Polish National Agency for Academic Exchange (PPN/PPO/2020/1/00002/U/00001), Polish National Science Centre (NCN 2021/42/E/ST2/00350, NCN OPUS nr 2022/47/B/ST2/03059, NCN UMO-2019/34/E/ST2/00393, NCN and H2020 MSCA 945339, UMO-2020/37/B/ST2/01043, UMO-2021/40/C/ST2/00187, UMO-2022/47/O/ST2/00148, UMO-2023/49/B/ST2/04085, UMO-2023/51/B/ST2/00920); Slovenia: Slovenian Research Agency (ARIS grant J1-3010); Spain: Generalitat Valenciana (Artemisa, FEDER, IDIFEDER/2018/048), Ministry of Science and Innovation (MCIN and NextGenEU PCI2022-135018-2, MICIN and FEDER PID2021-125273NB, RYC2019-028510-I, RYC2020-030254-I, RYC2021-031273-I, RYC2022-038164-I), PROMETEO and GenT Programmes Generalitat Valenciana (CIDEGENT/2019/027); Sweden: Swedish Research Council (Swedish Research Council 2023-04654, VR 2018-00482, VR 2022-03845, VR 2022-04683, VR 2023-03403, VR grant 2021-03651), Knut and Alice Wallenberg Foundation (KAW 2018.0157, KAW 2018.0458, KAW 2019.0447, KAW 2022.0358); Switzerland: Swiss National Science Foundation (SNSF-PCEFP2_194658); United Kingdom: Leverhulme Trust (Leverhulme Trust RPG-2020-004), Royal Society (NIF-R1-231091); United States of America: U.S. Department of Energy (ECA DE-AC02-76SF00515), Neubauer Family Foundation.

Data Availability Statement My manuscript has associated data in a data repository. [Author's comment: HepData Link: https://www.hepdata.net/record/154176].

Code Availability Statement My manuscript has associated code/software in a data repository. [Author's comment: ATLAS collaboration software is open source, and all code necessary to recreate an analysis is publicly available. The Athena (http://gitlab.cern.ch/atlas/athena) software repository provides all code needed for calibration and uncertainty application, with configuration files that are also publicly available via Docker containers and cvmfs. The specific code and configurations written in support of this analysis are not public; however, these are internally preserved.]

Funded by SCOAP[3].

References

1. ATLAS Collaboration, Observation of a new particle in the search for the Standard Model Higgs boson with the ATLAS detector at the LHC. Phys. Lett. B **716**, 1 (2012). https://doi.org/10.1016/j.physletb.2012.08.020. arXiv:1207.7214 [hep-ex]
2. CMS Collaboration, Observation of a new boson at a mass of 125 GeV with the CMS experiment at the LHC. Phys. Lett. B **716**, 30 (2012). https://doi.org/10.1016/j.physletb.2012.08.021. arXiv:1207.7235 [hep-ex]
3. ATLAS Collaboration, A detailed map of Higgs boson interactions by the ATLAS experiment ten years after the discovery. Nature **607**, 52 (2022). https://doi.org/10.1038/s41586-022-04893-w. arXiv:2207.00092 [hep-ex]. [Erratum: https://doi.org/10.1038/s41586-022-05581-5Nature 612 (2022) E24]
4. CMS Collaboration, A portrait of the Higgs boson by the CMS experiment ten years after the discovery. Nature **607**, 60 (2022). https://doi.org/10.1038/s41586-022-04892-x. arXiv:2207.00043 [hep-ex]. [Erratum: 10.1038/s41586-023-06164-8 Nature 623 (2023) E4]
5. A. Riotto, M. Trodden, Recent progress in baryogenesis. Annu. Rev. Nucl. Part. Sci. **49**, 35 (1999). https://doi.org/10.1146/annurev.nucl.49.1.35. arXiv:hep-ph/9901362
6. A.G. Akeroyd et al., Prospects for charged Higgs searches at the LHC. Eur. Phys. J. C **77**, 276 (2017). https://doi.org/10.1140/epjc/s10052-017-4829-2. arXiv:1607.01320 [hep-ph]
7. G. Arcadi, A. Djouadi, M. Raidal, Dark matter through the Higgs portal. Phys. Rep. **842**, 1 (2020). https://doi.org/10.1016/j.physrep.2019.11.003. arXiv:1903.03616 [hep-ph]

8. R.D. Peccei, H.R. Quinn, CP conservation in the presence of pseudoparticles. Phys. Rev. Lett. **38**, 1440 (1977). https://doi.org/10.1103/PhysRevLett.38.1440
9. S.P. Martin, A supersymmetry primer. Adv. Ser. Direct. High Energy Phys. **18**, 1 (1998). https://doi.org/10.1142/9789812839657_0001. arXiv:hep-ph/9709356
10. T.P. Cheng, L.-F. Li, Neutrino masses, mixings, and oscillations in SU(2)×U(1) models of electroweak interactions. Phys. Rev. D **22**, 2860 (1980). https://doi.org/10.1103/PhysRevD.22.2860
11. J. Schechter, J.W.F. Valle, Neutrino masses in SU(2) ⊗ U(1) theories. Phys. Rev. D **22**, 2227 (1980). https://doi.org/10.1103/PhysRevD.22.2227
12. G. Lazarides, Q. Shafi, C. Wetterich, Proton lifetime and fermion masses in an SO(10) model. Nucl. Phys. B **181**, 287 (1981). https://doi.org/10.1016/0550-3213(81)90354-0
13. M.S. Chanowitz, M. Golden, Higgs boson triplets with $M_W = M_Z \cos\theta_W$. Phys. Lett. B **165**, 105 (1985). https://doi.org/10.1016/0370-2693(85)90700-2
14. J.F. Gunion, R. Vega, J. Wudka, Higgs triplets in the standard model. Phys. Rev. D **42**, 1673 (1990). https://doi.org/10.1103/PhysRevD.42.1673
15. G.C. Branco et al., Theory and phenomenology of two-Higgs-doublet models. Phys. Rep. **516**, 1 (2012). https://doi.org/10.1016/j.physrep.2012.02.002. arXiv:1106.0034 [hep-ph]
16. J.F. Gunion, H.E. Haber, CP-conserving two-Higgs-doublet model: the approach to the decoupling limit. Phys. Rev. D **67**, 075019 (2003). https://doi.org/10.1103/PhysRevD.67.075019. arXiv:hep-ph/0207010
17. W. Altmannshofer et al., Collider signatures of flavorful Higgs bosons. Phys. Rev. D **94**, 115032 (2016). https://doi.org/10.1103/PhysRevD.94.115032. arXiv:1610.02398 [hep-ph]
18. ATLAS Collaboration, Search for a light charged Higgs boson in the decay channel $H^+ \to c\bar{s}$ in $t\bar{t}$ events using pp collisions at $\sqrt{s} = 7$ TeV with the ATLAS detector. Eur. Phys. J. C **73**, 2465 (2013). https://doi.org/10.1140/epjc/s10052-013-2465-z. arXiv:1302.3694 [hep-ex]
19. C.M.S. Collaboration, Search for a light charged Higgs boson in the $H^\pm \to cs$ channel in proton–proton collisions at $\sqrt{s} = 13$ TeV. Phys. Rev. D **102**, 072001 (2020). https://doi.org/10.1103/PhysRevD.102.072001. arXiv:2005.08900 [hep-ex]
20. ATLAS Collaboration, Search for a light charged Higgs boson in $t \to H^\pm b$ decays, with $H^\pm \to cb$, in the lepton+jets final state in proton–proton collisions at $\sqrt{s} = 13$ TeV with the ATLAS detector. JHEP **09**, 004 (2023). https://doi.org/10.1007/JHEP09(2023)004. arXiv:2302.11739 [hep-ex]
21. C.M.S. Collaboration, Search for a charged Higgs boson decaying to charm and bottom quarks in proton–proton collisions at $\sqrt{s} = 8$ TeV. JHEP **11**, 115 (2018). https://doi.org/10.1007/JHEP11(2018)115. arXiv:1808.06575 [hep-ex]
22. ATLAS Collaboration, Search for charged Higgs bosons decaying via $H^\pm \to \tau^\pm \nu_\tau$ in the τ+jets and τ+lepton final states with 36 fb^{-1} of pp collision data recorded at $\sqrt{s} = 13$ TeV with the ATLAS experiment. JHEP **09**, 139 (2018). https://doi.org/10.1007/JHEP09(2018)139. arXiv:1807.07915 [hep-ex]
23. C.M.S. Collaboration, Search for charged Higgs bosons in the $H^\pm \to \tau^\pm \nu_\tau$ decay channel in proton–proton collisions at $\sqrt{s} = 13$ TeV. JHEP **07**, 142 (2019). https://doi.org/10.1007/JHEP07(2019)142. arXiv:1903.04560 [hep-ex]
24. M. Misiak, M. Steinhauser, Weak radiative decays of the B meson and bounds on $M_{H^\pm}$ in the two-Higgs-doublet model. Eur. Phys. J. C **77**, 201 (2017). https://doi.org/10.1140/epjc/s10052-017-4776-y. arXiv:1702.04571 [hep-ph]
25. ATLAS Collaboration, The ATLAS Experiment at the CERN Large Hadron Collider. JINST **3**, S08003 (2008). https://doi.org/10.1088/1748-0221/3/08/S08003
26. ATLAS Collaboration, ATLAS Insertable B-layer: technical design report, ATLAS-TDR-19; CERN-LHCC-2010-013, 2010, Addendum: ATLAS-TDR-19-ADD-1; CERN-LHCC-2012-009 (2012). https://cds.cern.ch/record/1291633. https://cds.cern.ch/record/1451888
27. B. Abbott et al., Production and integration of the ATLAS Insertable B-Layer. JINST **13**, T05008 (2018). https://doi.org/10.1088/1748-0221/13/05/T05008. arXiv:1803.00844 [physics.ins-det]
28. G. Avoni et al., The new LUCID-2 detector for luminosity measurement and monitoring in ATLAS. JINST **13**, P07017 (2018). https://doi.org/10.1088/1748-0221/13/07/P07017
29. ATLAS Collaboration, Performance of the ATLAS trigger system in 2015. Eur. Phys. J. C **77,** 317 (2017). https://doi.org/10.1140/epjc/s10052-017-4852-3. arXiv:1611.09661 [hep-ex]
30. ATLAS Collaboration, Software and computing for Run 3 of the ATLAS experiment at the LHC. (2024). arXiv:2404.06335 [hep-ex]
31. ATLAS Collaboration, Luminosity determination in pp collisions at $\sqrt{s} = 13$ TeV using the ATLAS detector at the LHC. Eur. Phys. J. C **83**, 982, (2023). https://doi.org/10.1140/epjc/s10052-023-11747-w. arXiv:2212.09379 [hep-ex]
32. S. Frixione, G. Ridolfi, P. Nason, A positive-weight next-to-leading-order Monte Carlo for heavy flavour hadroproduction. JHEP **09**, 126 (2007). https://doi.org/10.1088/1126-6708/2007/09/126. arXiv:0707.3088 [hep-ph]
33. P. Nason, A new method for combining NLO QCD with shower Monte Carlo algorithms. JHEP **11**, 040 (2004). https://doi.org/10.1088/1126-6708/2004/11/040. arXiv:hep-ph/0409146
34. S. Frixione, P. Nason, C. Oleari, Matching NLO QCD computations with parton shower simulations: the POWHEG method. JHEP **11**, 070 (2007). https://doi.org/10.1088/1126-6708/2007/11/070. arXiv:0709.2092 [hep-ph]
35. S. Alioli, P. Nason, C. Oleari, E. Re, A general framework for implementing NLO calculations in shower Monte Carlo programs: the POWHEG BOX. JHEP **06**, 043 (2010). https://doi.org/10.1007/JHEP06(2010)043. arXiv:1002.2581 [hep-ph]
36. NNPDF Collaboration, R.D. Ball et al., Parton distributions for the LHC run II. JHEP **04**, 040 (2015). https://doi.org/10.1007/JHEP04(2015)040. arXiv:1410.8849 [hep-ph]
37. ATLAS Collaboration, Studies on top-quark Monte Carlo modelling for Top2016, ATL-PHYS-PUB-2016-020 (2016). https://cds.cern.ch/record/2216168
38. T. Sjöstrand et al., An introduction to PYTHIA 8.2. Comput. Phys. Commun. **191**, 159 (2015). https://doi.org/10.1016/j.cpc.2015.01.024. arXiv:1410.3012 [hep-ph]
39. NNPDF Collaboration, R.D. Ball et al., Parton distributions with LHC data. Nucl. Phys. B **867**, 244 (2013). https://doi.org/10.1016/j.nuclphysb.2012.10.003. arXiv:1207.1303 [hep-ph]
40. ATLAS Collaboration, ATLAS Pythia 8 tunes to 7 TeV data, ATL-PHYS-PUB-2014-021 (2014). https://cds.cern.ch/record/1966419
41. D.J. Lange, The EvtGen particle decay simulation package. Nucl. Instrum. Methods A **462**, 152 (2001). https://doi.org/10.1016/S0168-9002(01)00089-4
42. J. Alwall et al., The automated computation of tree-level and next-to-leading order differential cross sections, and their matching to parton shower simulations. JHEP **07**, 079 (2014). https://doi.org/10.1007/JHEP07(2014)079. arXiv:1405.0301 [hep-ph]
43. M. Bähr et al., Herwig++ physics and manual. Eur. Phys. J. C **58**, 639 (2008). https://doi.org/10.1140/epjc/s10052-008-0798-9. arXiv:0803.0883 [hep-ph]
44. J. Bellm et al., Herwig 7.0/Herwig++ 3.0 release note. Eur. Phys. J. C **76**, 196 (2016). https://doi.org/10.1140/epjc/s10052-016-4018-8. arXiv:1512.01178 [hep-ph]

45. J. Bellm et al., Herwig 7.1 Release Note. (2017). arXiv:1705.06919 [hep-ph]
46. L.A. Harland-Lang, A.D. Martin, P. Motylinski, R.S. Thorne, Parton distributions in the LHC era: MMHT 2014 PDFs. Eur. Phys. J. C **75**, 204 (2015). https://doi.org/10.1140/epjc/s10052-015-3397-6. arXiv:1412.3989 [hep-ph]
47. S. Frixione, E. Laenen, P. Motylinski, C. White, B.R. Webber, Single-top hadroproduction in association with a W boson. JHEP **07**, 029 (2008). https://doi.org/10.1088/1126-6708/2008/07/029. arXiv:0805.3067 [hep-ph]
48. M. Czakon, A. Mitov, Top++: a program for the calculation of the top-pair cross-section at hadron colliders. Comput. Phys. Commun. **185**, 2930 (2014). https://doi.org/10.1016/j.cpc.2014.06.021. arXiv:1112.5675 [hep-ph]
49. N. Kidonakis, Next-to-next-to-leading-order collinear and soft gluon corrections for t-channel single top quark production. Phys. Rev. D **83**, 091503 (2011). https://doi.org/10.1103/PhysRevD.83.091503. arXiv:1103.2792 [hep-ph]
50. N. Kidonakis, Next-to-next-to-leading logarithm resummation for s-channel single top quark production. Phys. Rev. D **81**, 054028 (2010). https://doi.org/10.1103/PhysRevD.81.054028. arXiv:1001.5034 [hep-ph]
51. N. Kidonakis, Two-loop soft anomalous dimensions for single top quark associated production with a W^- or H^-. Phys. Rev. D **82**, 054018 (2010). https://doi.org/10.1103/PhysRevD.82.054018. arXiv:1005.4451 [hep-ph]
52. ATLAS Collaboration, Search for the Standard Model Higgs boson produced in association with top quarks and decaying into $b\bar{b}$ in pp collisions at $\sqrt{s} = 8$ TeV with the ATLAS detector. Eur. Phys. J. C **75**, 349 (2015). https://doi.org/10.1140/epjc/s10052-015-3543-1. arXiv:1503.05066 [hep-ex]
53. D. de Florian et al., Handbook of LHC Higgs cross sections: 4. Deciphering the nature of the Higgs sector. (2017). https://doi.org/10.23731/CYRM-2017-002. arXiv:1610.07922 [hep-ph]
54. E. Bothmann et al., Event generation with Sherpa 2.2. SciPost Phys. **7**, 034 (2019). https://doi.org/10.21468/SciPostPhys.7.3.034. arXiv:1905.09127 [hep-ph]
55. T. Gleisberg, S. Höche, Comix, a new matrix element generator. JHEP **12**, 039 (2008). https://doi.org/10.1088/1126-6708/2008/12/039. arXiv:0808.3674 [hep-ph]
56. F. Buccioni et al., OpenLoops 2. Eur. Phys. J. C **79**, 866 (2019). https://doi.org/10.1140/epjc/s10052-019-7306-2. arXiv:1907.13071 [hep-ph]
57. F. Cascioli, P. Maierhöfer, S. Pozzorini, Scattering amplitudes with open loops. Phys. Rev. Lett. **108**, 111601 (2012). https://doi.org/10.1103/PhysRevLett.108.111601. arXiv:1111.5206 [hep-ph]
58. A. Denner, S. Dittmaier, L. Hofer, Collier: a Fortran-based complex one-loop library in extended regularizations. Comput. Phys. Commun. **212**, 220 (2017). https://doi.org/10.1016/j.cpc.2016.10.013. arXiv:1604.06792 [hep-ph]
59. S. Schumann, F. Krauss, A parton shower algorithm based on Catani–Seymour dipole factorisation. JHEP **03**, 038 (2008). https://doi.org/10.1088/1126-6708/2008/03/038. arXiv:0709.1027 [hep-ph]
60. S. Höche, F. Krauss, M. Schönherr, F. Siegert, A critical appraisal of NLO + PS matching methods. JHEP **09**, 049 (2012). https://doi.org/10.1007/JHEP09(2012)049. arXiv:1111.1220 [hep-ph]
61. S. Höche, F. Krauss, M. Schönherr, F. Siegert, QCD matrix elements + parton showers, the NLO case. JHEP **04**, 027 (2013). https://doi.org/10.1007/JHEP04(2013)027. arXiv:1207.5030 [hep-ph]
62. S. Catani, F. Krauss, B.R. Webber, R. Kuhn, QCD matrix elements + parton showers. JHEP **11**, 063 (2001). https://doi.org/10.1088/1126-6708/2001/11/063. arXiv:hep-ph/0109231
63. S. Höche, F. Krauss, S. Schumann, F. Siegert, QCD matrix elements and truncated showers. JHEP **05**, 053 (2009). https://doi.org/10.1088/1126-6708/2009/05/053. arXiv:0903.1219 [hep-ph]
64. P. Artoisenet, R. Frederix, O. Mattelaer, R. Rietkerk, Automatic spin-entangled decays of heavy resonances in Monte Carlo simulations. JHEP **03**, 015 (2013). https://doi.org/10.1007/JHEP03(2013)015. arXiv:1212.3460 [hep-ph]
65. A. Alloul, N.D. Christensen, C. Degrande, C. Duhr, B. Fuks, FeynRules 2.0—a complete toolbox for tree-level phenomenology. Comput. Phys. Commun. **185**, 2250 (2014). https://doi.org/10.1016/j.cpc.2014.04.012. arXiv:1310.1921 [hep-ph]
66. S.M. Moosavi Nejad, S. Abbaspour, R. Farashahian, Interference effects for the top quark decays $t \to b + W^+/H^+(\to \tau^+\nu_\tau)$. Phys. Rev. D **99**, 095012 (2019). https://doi.org/10.1103/PhysRevD.99.095012. arXiv:1904.09680 [hep-ph]
67. T. Sjöstrand, S. Mrenna, P. Skands, A brief introduction to PYTHIA 8.1. Comput. Phys. Commun. **178**, 852 (2008). https://doi.org/10.1016/j.cpc.2008.01.036. arXiv:0710.3820 [hep-ph]
68. ATLAS Collaboration, The Pythia 8 A3 tune description of ATLAS minimum bias and inelastic measurements incorporating the Donnachie–Landshoff diffractive model, ATL-PHYS-PUB-2016-017. (2016). https://cds.cern.ch/record/2206965
69. ATLAS Collaboration, The ATLAS Simulation Infrastructure. Eur. Phys. J. C **70**, 823 (2010). https://doi.org/10.1140/epjc/s10052-010-1429-9. arXiv:1005.4568 [physics.ins-det]
70. S. Agostinelli et al., Geant4-a simulation toolkit. Nucl. Instrum. Methods A **506**, 250 (2003). https://doi.org/10.1016/S0168-9002(03)01368-8
71. ATLAS Collaboration, The simulation principle and performance of the ATLAS fast calorimeter simulation FastCaloSim, ATL-PHYS-PUB-2010-013. (2010). https://cds.cern.ch/record/1300517
72. ATLAS Collaboration, Performance of the ATLAS track reconstruction algorithms in dense environments in LHC Run 2. Eur. Phys. J. C **77**, 673 (2017). https://doi.org/10.1140/epjc/s10052-017-5225-7. arXiv:1704.07983 [hep-ex]
73. ATLAS Collaboration, Vertex reconstruction performance of the ATLAS detector at $\sqrt{s} = 13$ TeV, ATL-PHYS-PUB-2015-026. (2015). https://cds.cern.ch/record/2037717
74. ATLAS Collaboration, Electron and photon performance measurements with the ATLAS detector using the 2015–2017 LHC proton–proton collision data. JINST **14**, P12006 (2019). https://doi.org/10.1088/1748-0221/14/12/P12006. arXiv:1908.00005 [hep-ex]
75. ATLAS Collaboration, Evidence for the associated production of the Higgs boson and a top quark pair with the ATLAS detector. Phys. Rev. D **97**, 072003 (2018). https://doi.org/10.1103/PhysRevD.97.072003. arXiv:1712.08891 [hep-ex]
76. ATLAS Collaboration, Tools for estimating fake/non-prompt lepton backgrounds with the ATLAS detector at the LHC. JINST **18**, T11004 (2023). https://doi.org/10.1088/1748-0221/18/11/T11004. arXiv:2211.16178 [hep-ex]
77. ATLAS Collaboration, Muon reconstruction and identification efficiency in ATLAS using the full Run 2 pp collision data set at $\sqrt{s} = 13$ TeV. Eur. Phys. J. C **81**, 578 (2021). https://doi.org/10.1140/epjc/s10052-021-09233-2. arXiv:2012.00578 [hep-ex]
78. M. Cacciari, G.P. Salam, G. Soyez, The anti-k_t jet clustering algorithm. JHEP **04**, 063 (2008). https://doi.org/10.1088/1126-6708/2008/04/063. arXiv:0802.1189 [hep-ph]
79. M. Cacciari, G.P. Salam, G. Soyez, FastJet user manual. Eur. Phys. J. C **72**, 1896 (2012). https://doi.org/10.1140/epjc/s10052-012-1896-2. arXiv:1111.6097 [hep-ph]
80. ATLAS Collaboration, Topological cell clustering in the ATLAS calorimeters and its performance in LHC Run 1. Eur. Phys. J. C **77**, 490 (2017). https://doi.org/10.1140/epjc/s10052-017-5004-5. arXiv:1603.02934 [hep-ex]

81. ATLAS Collaboration, Properties of jets and inputs to jet reconstruction and calibration with the ATLAS detector using proton–proton collisions at $\sqrt{s} = 13$TeV, ATL-PHYS-PUB-2015-036. (2015). https://cds.cern.ch/record/2044564
82. ATLAS Collaboration, Jet reconstruction and performance using particle flow with the ATLAS Detector, Eur. Phys. J. C **77** 466, (2017). https://doi.org/10.1140/epjc/s10052-017-5031-2. arXiv:1703.10485 [hep-ex]
83. ATLAS Collaboration, Jet energy scale and resolution measured in proton–proton collisions at $\sqrt{s} = 13$ TeV with the ATLAS detector. Eur. Phys. J. C **81**, 689 (2021). https://doi.org/10.1140/epjc/s10052-021-09402-3. arXiv:2007.02645 [hep-ex]
84. ATLAS Collaboration, Performance of pile-up mitigation techniques for jets in pp collisions at $\sqrt{s} = 8$ TeV using the ATLAS detector. Eur. Phys. J. C **76**, 581 (2016). https://doi.org/10.1140/epjc/s10052-016-4395-z. arXiv:1510.03823 [hep-ex]
85. ATLAS Collaboration, ATLAS flavour-tagging algorithms for the LHC Run 2 pp collision dataset. Eur. Phys. J. C **83**, 681 (2023). https://doi.org/10.1140/epjc/s10052-023-11699-1. arXiv:2211.16345 [physics.data-an]
86. ATLAS Collaboration, ATLAS b-jet identification performance and efficiency measurement with $t\bar{t}$ events in pp collisions at $\sqrt{s} = 13$ TeV. Eur. Phys. J. C **79**, 970 (2019). https://doi.org/10.1140/epjc/s10052-019-7450-8. arXiv:1907.05120 [hep-ex]
87. ATLAS Collaboration, Measurement of the c-jet mistagging efficiency in $t\bar{t}$ events using pp collision data at $\sqrt{s} = 13$ TeV collected with the ATLAS detector. Eur. Phys. J. C **82**, 95 (2022). https://doi.org/10.1140/epjc/s10052-021-09843-w. arXiv:2109.10627 [hep-ex]
88. ATLAS Collaboration, Calibration of the light-flavour jet mistagging efficiency of the b-tagging algorithms with Z+jets events using 139 fb^{-1} of ATLAS proton–proton collision data at $\sqrt{s} = 13$ TeV. Eur. Phys. J. C **83**, 728 (2023). https://doi.org/10.1140/epjc/s10052-023-11736-z. arXiv:2301.06319 [hep-ex]
89. ATLAS Collaboration, Measurements of WH and ZH production with Higgs boson decays into bottom quarks and direct constraints on the charm Yukawa coupling in 13 TeV pp collisions with the ATLAS detector. (2024). arXiv:2410.19611 [hep-ex]
90. ATLAS Collaboration, The performance of missing transverse momentum reconstruction and its significance with the ATLAS detector using 140 fb^{-1} of $\sqrt{s} = 13$ TeV pp collisions. (2024). arXiv:2402.05858 [hep-ex]
91. M. Cacciari, G.P. Salam, G. Soyez, The catchment area of jets. JHEP **04**, 005 (2008). https://doi.org/10.1088/1126-6708/2008/04/005. arXiv:0802.1188 [hep-ph]
92. ATLAS Collaboration, Performance of the ATLAS muon triggers in Run 2. JINST **15**, P09015 (2020). https://doi.org/10.1088/1748-0221/15/09/p09015. arXiv:2004.13447 [physics.ins-det]
93. ATLAS Collaboration, Performance of electron and photon triggers in ATLAS during LHC Run 2. Eur. Phys. J. C **80**, 47 (2020). https://doi.org/10.1140/epjc/s10052-019-7500-2. arXiv:1909.00761 [hep-ex]
94. ATLAS Collaboration, Operation of the ATLAS trigger system in Run 2. JINST **15**, P10004 (2020). https://doi.org/10.1088/1748-0221/15/10/P10004. arXiv:2007.12539 [hep-ex]
95. ATLAS Collaboration, Measurement of the $t\bar{t}$ production cross-section in the lepton+jets channel at $\sqrt{s} = 13$ TeV with the ATLAS experiment. Phys. Lett. B **810**, 135797 (2020). https://doi.org/10.1016/j.physletb.2020.135797. arXiv:2006.13076 [hep-ex]
96. M. Czakon et al., Top-pair production at the LHC through NNLO QCD and NLO EW. JHEP **10**, 186 (2017). https://doi.org/10.1007/JHEP10(2017)186. arXiv:1705.04105 [hep-ph]
97. C.D.F. Collaboration, A Measurement of $\sigma B(W \to e\nu)$ and $\sigma B(Z^0 \to e^+e^-)$ in $\overline{p}p$ collisions at $\sqrt{s} = 1800$ GeV. Phys. Rev. D **44**, 29 (1991). https://doi.org/10.1103/PhysRevD.44.29
98. Particle Data Group, P. Zyla et al., Review of particle physics. Prog. Theor. Exp. Phys. **2020**, 083C01 (2020). https://doi.org/10.1093/ptep/ptaa104
99. J. E. Gaiser, Charmonium spectroscopy from radiative decays of the J/ψ and ψ', Appendix F, Ph.D. thesis (1982)
100. M. Oreglia, A Study of the Reactions $\psi' \to \gamma\gamma\psi$, Appendix D, Ph.D. thesis (1980)
101. T. Skwarnicki, A study of the radiative CASCADE transitions between the Upsilon-Prime and Upsilon resonances, Appendix E, Ph.D. thesis: Cracow, INP (1986)
102. T. Hastie, R. Tibshirani, J. Friedman, *The Elements of Statistical Learning: Data Mining, Inference and Prediction*, 2nd edn. (Springer, Berlin, 2009)
103. T. Chen, C. Guestrin, XGBoost: a scalable tree boosting system. (2016), https://doi.org/10.1145/2939672.2939785. arXiv:1603.02754 [cs.LG]
104. J. Bergstra, B. Komer, C. Eliasmith, D. Yamins, D.D. Cox, Hyperopt: a Python library for model selection and hyperparameter optimization. Comput. Sci. Discov. **8**, 014008 (2015). https://doi.org/10.1088/1749-4699/8/1/014008
105. ATLAS Collaboration, Measurement of the inelastic proton–proton cross section at $\sqrt{s} = 13$ TeV with the ATLAS detector at the LHC. Phys. Rev. Lett. **117**, 182002 (2016). https://doi.org/10.1103/PhysRevLett.117.182002. arXiv:1606.02625 [hep-ex]
106. ATLAS Collaboration, Studies of the muon momentum calibration and performance of the ATLAS detector with pp collisions at $\sqrt{s} = 13$ TeV. Eur. Phys. J. C **83**, 686 (2023). https://doi.org/10.1140/epjc/s10052-023-11584-x. arXiv:2212.07338 [hep-ex]
107. ATLAS Collaboration, Jet energy scale measurements and their systematic uncertainties in proton–proton collisions at $\sqrt{s} = 13$ TeV with the ATLAS detector. Phys. Rev. D **96**, 072002 (2017). https://doi.org/10.1103/PhysRevD.96.072002. arXiv:1703.09665 [hep-ex]
108. ATLAS Collaboration, Jet energy resolution in proton–proton collisions at $\sqrt{s} = 7$ TeV recorded in 2010 with the ATLAS detector. Eur. Phys. J. C **73**, 2306 (2013). https://doi.org/10.1140/epjc/s10052-013-2306-0. arXiv:1210.6210 [hep-ex]
109. A.D. Martin, W.J. Stirling, R.S. Thorne, G. Watt, Parton distributions for the LHC. Eur. Phys. J. C **63**, 189 (2009). https://doi.org/10.1140/epjc/s10052-009-1072-5. arXiv:0901.0002 [hep-ph]
110. A.D. Martin, W.J. Stirling, R.S. Thorne, G. Watt, Uncertainties on α_S in global PDF analyses and implications for predicted hadronic cross sections. Eur. Phys. J. C **64**, 653 (2009). https://doi.org/10.1140/epjc/s10052-009-1164-2. arXiv:0905.3531 [hep-ph]
111. M. Aliev et al., HATHOR-HAdronic Top and Heavy quarks crOss section calculatoR. Comput. Phys. Commun. **182**, 1034 (2011). https://doi.org/10.1016/j.cpc.2010.12.040. arXiv:1007.1327 [hep-ph]
112. P. Kant et al., HatHor for single top-quark production: updated predictions and uncertainty estimates for single top-quark production in hadronic collisions. Comput. Phys. Commun. **191**, 74 (2015). https://doi.org/10.1016/j.cpc.2015.02.001. arXiv:1406.4403 [hep-ph]
113. S. Kallweit, J.M. Lindert, P. Maierhöfer, S. Pozzorini, M. Schönherr, NLO electroweak automation and precise predictions for W + multijet production at the LHC. JHEP **04**, 012 (2015). https://doi.org/10.1007/JHEP04(2015)012. arXiv:1412.5157 [hep-ph]
114. ATLAS Collaboration, Modelling and computational improvements to the simulation of single vector-boson plus jet processes for the ATLAS experiment. JHEP **08**, 089 (2022). https://doi.org/10.1007/JHEP08(2022)089. arXiv:2112.09588 [hep-ex]
115. R. Barlow, C. Beeston, Fitting using finite Monte Carlo samples. Comput. Phys. Commun. **77**, 219 (1993). https://doi.org/10.1016/0010-4655(93)90005-W

116. K. Cranmer, G. Lewis, L. Moneta, A. Shibata, W. Verkerke, HistFactory: a tool for creating statistical models for use with RooFit and RooStats. Technical report, New York U. (2012). https://cds.cern.ch/record/1456844
117. L. Heinrich, M. Feickert, G. Stark, K. Cranmer, pyhf: pure-Python implementation of HistFactory statistical models. J. Open Source Softw. **6**, 2823 (2021). https://doi.org/10.21105/joss.02823
118. D0 Collaboration, Determination of the width of the top quark. Phys. Rev. Lett. **106**, 022001 (2011). https://doi.org/10.1103/PhysRevLett.106.022001. arXiv:1009.5686 [hep-ex]
119. R.D. Cousins, J.T. Linnemann, J. Tucker, Evaluation of three methods for calculating statistical significance when incorporating a systematic uncertainty into a test of the background-only hypothesis for a Poisson process. Nucl. Instrum. Methods A **595**, 480 (2008). https://doi.org/10.1016/j.nima.2008.07.086. arXiv:physics/0702156 [physics.data-an]
120. G. Cowan, K. Cranmer, E. Gross, O. Vitells, Asymptotic formulae for likelihood-based tests of new physics. Eur. Phys. J. C **71**, 1554 (2011). https://doi.org/10.1140/epjc/s10052-011-1554-0. arXiv:1007.1727 [physics.data-an]. [Erratum: Eur. Phys. J. C 73 (2013) 2501. 10.1140/epjc/s10052-013-2501-z]
121. A.L. Read, Presentation of search results: the CL_S technique. J. Phys. G **28**, 2693 (2002). https://doi.org/10.1088/0954-3899/28/10/313
122. ATLAS Collaboration, Measurements of fiducial cross-sections for $t\bar{t}$ production with one or two additional b-jets in pp collisions at $\sqrt{s} = 8$ TeV using the ATLAS detector. Eur. Phys. J. C **76**, 11 (2016). https://doi.org/10.1140/epjc/s10052-015-3852-4. arXiv:1508.06868 [hep-ex]
123. ATLAS Collaboration, Measurements of inclusive and differential fiducial cross-sections of $t\bar{t}$ production with additional heavy-flavour jets in proton–proton collisions at $\sqrt{s} = 13$ TeV with the ATLAS detector. JHEP **04**, 046 (2019). https://doi.org/10.1007/JHEP04(2019)046. arXiv:1811.12113 [hep-ex]
124. CMS Collaboration, Measurement of the cross section for $t\bar{t}$ production with additional jets and b jets in pp collisions at $\sqrt{s} = 13$ TeV. JHEP **07**, 125 (2020). https://doi.org/10.1007/JHEP07(2020)125. arXiv:2003.06467 [hep-ex]
125. ATLAS Collaboration, Search for charged Higgs bosons decaying into a top quark and a bottom quark at $\sqrt{s} = 13$ TeV with the ATLAS detector. JHEP **06**, 145 (2021). https://doi.org/10.1007/JHEP06(2021)145. arXiv:2102.10076 [hep-ex]
126. ATLAS Collaboration, Measurement of the $t\bar{t}t\bar{t}$ production cross section in pp collisions at $\sqrt{s} = 13$ TeV with the ATLAS detector. JHEP **11**, 118 (2021). https://doi.org/10.1007/JHEP11(2021)118. arXiv:2106.11683 [hep-ex]
127. ATLAS Collaboration, ATLAS Computing Acknowledgements, ATL-SOFT-PUB-2023-001. (2023). https://cds.cern.ch/record/2869272

ATLAS Collaboration[★]

G. Aad[104], E. Aakvaag[17], B. Abbott[123], S. Abdelhameed[119a], K. Abeling[56], N.J. Abicht[50], S.H. Abidi[30], M. Aboelela[45], A. Aboulhorma[36e], H. Abramowicz[155], H. Abreu[154], Y. Abulaiti[120], B.S. Acharya[70a,70b,k], A. Ackermann[64a], C. Adam Bourdarios[4], L. Adamczyk[87a], S.V. Addepalli[27], M.J. Addison[103], J. Adelman[118], A. Adiguzel[22c], T. Adye[137], A.A. Affolder[139], Y. Afik[40], M.N. Agaras[13], J. Agarwala[74a,74b], A. Aggarwal[102], C. Agheorghiesei[28c], F. Ahmadov[39,y], W.S. Ahmed[106], S. Ahuja[97], X. Ai[63e], G. Aielli[77a,77b], A. Aikot[166], M. Ait Tamlihat[36e], B. Aitbenchikh[36a], M. Akbiyik[102], T.P.A. Åkesson[100], A.V. Akimov[38], D. Akiyama[171], N.N. Akolkar[25], S. Aktas[22a], K. Al Khoury[42], G.L. Alberghi[24b], J. Albert[168], P. Albicocco[54], G.L. Albouy[61], S. Alderweireldt[53], Z.L. Alegria[124], M. Aleksa[37], I.N. Aleksandrov[39], C. Alexa[28b], T. Alexopoulos[10], F. Alfonsi[24b], M. Algren[57], M. Alhroob[170], B. Ali[135], H.M.J. Ali[93,s], S. Ali[32], S.W. Alibocus[94], M. Aliev[34c], G. Alimonti[72a], W. Alkakhi[56], C. Allaire[67], B.M.M. Allbrooke[150], J.S. Allen[103], J.F. Allen[53], C.A. Allendes Flores[140f], P.P. Allport[21], A. Aloisio[73a,73b], F. Alonso[92], C. Alpigiani[142], Z.M.K. Alsolami[93], M. Alvarez Estevez[101], A. Alvarez Fernandez[102], M. Alves Cardoso[57], M.G. Alviggi[73a,73b], M. Aly[103], Y. Amaral Coutinho[84b], A. Ambler[106], C. Amelung[37], M. Amerl[103], C.G. Ames[111], D. Amidei[108], B. Amini[55], K.J. Amirie[158], S.P. Amor Dos Santos[133a], K.R. Amos[166], D. Amperiadou[156], S. An[85], V. Ananiev[128], C. Anastopoulos[143], T. Andeen[11], J.K. Anders[37], A.C. Anderson[60], S.Y. Andrean[48a,48b], A. Andreazza[72a,72b], S. Angelidakis[9], A. Angerami[42], A.V. Anisenkov[38], A. Annovi[75a], C. Antel[57], E. Antipov[149], M. Antonelli[54], F. Anulli[76a], M. Aoki[85], T. Aoki[157], M.A. Aparo[150], L. Aperio Bella[49], C. Appelt[19], A. Apyan[27], S.J. Arbiol Val[88], C. Arcangeletti[54], A.T.H. Arce[52], J-F. Arguin[110], S. Argyropoulos[55], J.-H. Arling[49], O. Arnaez[4], H. Arnold[149], G. Artoni[76a,76b], H. Asada[113], K. Asai[121], S. Asai[157], N.A. Asbah[37], R.A. Ashby Pickering[170], K. Assamagan[30], R. Astalos[29a], K.S.V. Astrand[100], S. Atashi[162], R.J. Atkin[34a], M. Atkinson[165], H. Atmani[36f], P.A. Atmasiddha[131], K. Augsten[135], S. Auricchio[73a,73b], A.D. Auriol[21], V.A. Austrup[103], G. Avolio[37], K. Axiotis[57], G. Azuelos[110,ad], D. Babal[29b], H. Bachacou[138], K. Bachas[156,o], A. Bachiu[35], F. Backman[48a,48b], A. Badea[40], T.M. Baer[108], P. Bagnaia[76a,76b], M. Bahmani[19], D. Bahner[55], K. Bai[126], J.T. Baines[137], L. Baines[96], O.K. Baker[175], E. Bakos[16], D. Bakshi Gupta[8], L.E. Balabram Filho[84b], V. Balakrishnan[123], R. Balasubramanian[4], E.M. Baldin[38], P. Balek[87a], E. Ballabene[24b,24a], F. Balli[138], L.M. Baltes[64a], W.K. Balunas[33], J. Balz[102], I. Bamwidhi[119b], E. Banas[88], M. Bandieramonte[132], A. Bandyopadhyay[25], S. Bansal[25], L. Barak[155], M. Barakat[49], E.L. Barberio[107], D. Barberis[58a,58b], M. Barbero[104], M.Z. Barel[117], T. Barillari[112], M-S. Barisits[37], T. Barklow[147], P. Baron[125], D.A. Baron Moreno[103], A. Baroncelli[63a], A.J. Barr[129], J.D. Barr[98], F. Barreiro[101], J. Barreiro Guimarães da Costa[14], U. Barron[155], M.G. Barros Teixeira[133a], S. Barsov[38], F. Bartels[64a], R. Bartoldus[147], A.E. Barton[93], P. Bartos[29a], A. Basan[102], M. Baselga[50], A. Bassalat[67,b], M.J. Basso[159a], S. Bataju[45], R. Bate[167], R.L. Bates[60], S. Batlamous[101], B. Batool[145], M. Battaglia[139], D. Battulga[19], M. Bauce[76a,76b], M. Bauer[80], P. Bauer[25], L.T. Bazzano Hurrell[31], J.B. Beacham[52], T. Beau[130], J.Y. Beaucamp[92], P.H. Beauchemin[161], P. Bechtle[25], H.P. Beck[20,n], K. Becker[170], A.J. Beddall[83], V.A. Bednyakov[39], C.P. Bee[149], L.J. Beemster[16], T.A. Beermann[37], M. Begalli[84d], M. Begel[30], A. Behera[149], J.K. Behr[49], J.F. Beirer[37], F. Beisiegel[25], M. Belfkir[119b], G. Bella[155], L. Bellagamba[24b], A. Bellerive[35], P. Bellos[21], K. Beloborodov[38], D. Benchekroun[36a], F. Bendebba[36a], Y. Benhammou[155], K.C. Benkendorfer[62], L. Beresford[49], M. Beretta[54], E. Bergeaas Kuutmann[164], N. Berger[4], B. Bergmann[135], J. Beringer[18a], G. Bernardi[5], C. Bernius[147], F.U. Bernlochner[25], F. Bernon[37], A. Berrocal Guardia[13], T. Berry[97], P. Berta[136], A. Berthold[51], S. Bethke[112], A. Betti[76a,76b], A.J. Bevan[96], N.K. Bhalla[55], S. Bhatta[149], D.S. Bhattacharya[169], P. Bhattarai[147], K.D. Bhide[55], V.S. Bhopatkar[124], R.M. Bianchi[132], G. Bianco[24b,24a], O. Biebel[111], R. Bielski[126], M. Biglietti[78a], C. S. Billingsley[45], Y. Bimgdi[36f], M. Bindi[56], A. Bingul[22b], C. Bini[76a,76b], G.A. Bird[33], M. Birman[172], M. Biros[136], S. Biryukov[150], T. Bisanz[50], E. Bisceglie[44a,44b], J.P. Biswal[137], D. Biswas[145], I. Bloch[49], A. Blue[60], U. Blumenschein[96], J. Blumenthal[102], V.S. Bobrovnikov[38], M. Boehler[55], B. Boehm[169], D. Bogavac[37], A.G. Bogdanchikov[38], L.S. Boggia[130], C. Bohm[48a], V. Boisvert[97], P. Bokan[37], T. Bold[87a], M. Bomben[5], M. Bona[96], M. Boonekamp[138], C. D. Booth[97], A. G. Borbély[60], I.S. Bordulev[38], G. Borissov[93], D. Bortoletto[129], D. Boscherini[24b], M. Bosman[13], J.D. Bossio Sola[37], K. Bouaouda[36a], N. Bouchhar[166], L. Boudet[4], J. Boudreau[132], E.V. Bouhova-Thacker[93], D. Boumediene[41], R. Bouquet[58a,58b], A. Boveia[122], J. Boyd[37], D. Boye[30], I.R. Boyko[39], L. Bozianu[57], J. Bracinik[21], N. Brahimi[4], G. Brandt[174], O. Brandt[33], F. Braren[49], B. Brau[105], J.E. Brau[126],

R. Brener[172], L. Brenner[117], R. Brenner[164], S. Bressler[172], G. Brianti[79a,79b], D. Britton[60], D. Britzger[112], I. Brock[25], R. Brock[109], G. Brooijmans[42], E.M. Brooks[159b], E. Brost[30], L.M. Brown[168], L.E. Bruce[62], T.L. Bruckler[129], P.A. Bruckman de Renstrom[88], B. Brüers[49], A. Bruni[24b], G. Bruni[24b], M. Bruschi[24b], N. Bruscino[76a,76b], T. Buanes[17], Q. Buat[142], D. Buchin[112], A.G. Buckley[60], O. Bulekov[38], B. A. Bullard[147], S. Burdin[94], C. D. Burgard[50], A. M. Burger[37], B. Burghgrave[8], O. Burlayenko[55], J. Burleson[165], J. T. P. Burr[33], J. C. Burzynski[146], E. L. Busch[42], V. Büscher[102], P. J. Bussey[60], J. M. Butler[26], C. M. Buttar[60], J. M. Butterworth[98], W. Buttinger[137], C. J. Buxo Vazquez[109], A. R. Buzykaev[38], S. Cabrera Urbán[166], L. Cadamuro[67], D. Caforio[59], H. Cai[132], Y. Cai[14,114c], Y. Cai[114a], V. M. M. Cairo[37], O. Cakir[3a], N. Calace[37], P. Calafiura[18a], G. Calderini[130], P. Calfayan[69], G. Callea[60], L. P. Caloba[84b], D. Calvet[41], S. Calvet[41], M. Calvetti[75a,75b], R. Camacho Toro[130], S. Camarda[37], D. Camarero Munoz[27], P. Camarri[77a,77b], M.T. Camerlingo[73a,73b], D. Cameron[37], C. Camincher[168], M. Campanelli[98], A. Camplani[43], V. Canale[73a,73b], A.C. Canbay[3a], E. Canonero[97], J. Cantero[166], Y. Cao[165], F. Capocasa[27], M. Capua[44b,44a], A. Carbone[72a,72b], R. Cardarelli[77a], J.C.J. Cardenas[8], G. Carducci[44a,44b], T. Carli[37], G. Carlino[73a], J.I. Carlotto[13], B.T. Carlson[132,p], E.M. Carlson[168,159a], J. Carmignani[94], L. Carminati[72a,72b], A. Carnelli[138], M. Carnesale[37], S. Caron[116], E. Carquin[140f], I.B. Carr[107], S. Carrá[72a], G. Carratta[24a,24b], A.M. Carroll[126], M.P. Casado[13,h], M. Caspar[49], F.L. Castillo[4], L. Castillo Garcia[13], V. Castillo Gimenez[166], N.F. Castro[133a,133e], A. Catinaccio[37], J.R. Catmore[128], T. Cavaliere[4], V. Cavaliere[30], N. Cavalli[24a,24b], L.J. Caviedes Betancourt[23b], Y.C. Cekmecelioglu[49], E. Celebi[83], S. Cella[37], M.S. Centonze[71a,71b], V. Cepaitis[57], K. Cerny[125], A.S. Cerqueira[84a], A. Cerri[150], L. Cerrito[77a,77b], F. Cerutti[18a], B. Cervato[145], A. Cervelli[24b], G. Cesarini[54], S.A. Cetin[83], D. Chakraborty[118], J. Chan[18a], W.Y. Chan[157], J.D. Chapman[33], E. Chapon[138], B. Chargeishvili[153b], D.G. Charlton[21], M. Chatterjee[20], C. Chauhan[136], Y. Che[114a], S. Chekanov[6], S.V. Chekulaev[159a], G.A. Chelkov[39,a], A. Chen[108], B. Chen[155], B. Chen[168], H. Chen[114a], H. Chen[30], J. Chen[63c], J. Chen[146], M. Chen[129], S. Chen[89], S.J. Chen[114a], X. Chen[63c], X. Chen[15,ac], Y. Chen[63a], C.L. Cheng[173], H.C. Cheng[65a], S. Cheong[147], A. Cheplakov[39], E. Cheremushkina[49], E. Cherepanova[117], R. Cherkaoui El Moursli[36e], E. Cheu[7], K. Cheung[66], L. Chevalier[138], V. Chiarella[54], G. Chiarelli[75a], N. Chiedde[104], G. Chiodini[71a], A.S. Chisholm[21], A. Chitan[28b], M. Chitishvili[166], M.V. Chizhov[39,q], K. Choi[11], Y. Chou[142], E.Y.S. Chow[116], K.L. Chu[172], M.C. Chu[65a], X. Chu[14,114c], Z. Chubinidze[54], J. Chudoba[134], J.J. Chwastowski[88], D. Cieri[112], K.M. Ciesla[87a], V. Cindro[95], A. Ciocio[18a], F. Cirotto[73a,73b], Z.H. Citron[172], M. Citterio[72a], D. A. Ciubotaru[28b], A. Clark[57], P.J. Clark[53], N. Clarke Hall[98], C. Clarry[158], J.M. Clavijo Columbie[49], S.E. Clawson[49], C. Clement[48a,48b], Y. Coadou[104], M. Cobal[70a,70c], A. Coccaro[58b], R.F. Coelho Barrue[133a], R. Coelho Lopes De Sa[105], S. Coelli[72a], B. Cole[42], J. Collot[61], P. Conde Muiño[133a,133g], M.P. Connell[34c], S.H. Connell[34c], E.I. Conroy[129], F. Conventi[73a,ae], H.G. Cooke[21], A.M. Cooper-Sarkar[129], F.A. Corchia[24a,24b], A. Cordeiro Oudot Choi[130], L.D. Corpe[41], M. Corradi[76a,76b], F. Corriveau[106,x], A. Cortes-Gonzalez[19], M.J. Costa[166], F. Costanza[4], D. Costanzo[143], B.M. Cote[122], J. Couthures[4], G. Cowan[97], K. Cranmer[173], L. Cremer[50], D. Cremonini[24a,24b], S. Crépé-Renaudin[61], F. Crescioli[130], M. Cristinziani[145], M. Cristoforetti[79a,79b], V. Croft[117], J.E. Crosby[124], G. Crosetti[44a,44b], A. Cueto[101], H. Cui[98], Z. Cui[7], W.R. Cunningham[60], F. Curcio[166], J.R. Curran[53], P. Czodrowski[37], M.J. Da Cunha Sargedas De Sousa[58a,58b], J.V. Da Fonseca Pinto[84b], C. Da Via[103], W. Dabrowski[87a], T. Dado[37], S. Dahbi[152], T. Dai[108], D. Dal Santo[20], C. Dallapiccola[105], M. Dam[43], G. D'amen[30], V. D'Amico[111], J. Damp[102], J.R. Dandoy[35], D. Dannheim[37], M. Danninger[146], V. Dao[149], G. Darbo[58b], S.J. Das[30], F. Dattola[49], S. D'Auria[72a,72b], A. D'Avanzo[73a,73b], C. David[34a], T. Davidek[136], I. Dawson[96], H.A. Day-hall[135], K. De[8], R. De Asmundis[73a], N. De Biase[49], S. De Castro[24a,24b], N. De Groot[116], P. de Jong[117], H. De la Torre[118], A. De Maria[114a], A. De Salvo[76a], U. De Sanctis[77a,77b], F. De Santis[71a,71b], A. De Santo[150], J.B. De Vivie De Regie[61], J. Debevc[95], D. V. Dedovich[39], J. Degens[94], A.M. Deiana[45], F. Del Corso[24a,24b], J. Del Peso[101], L. Delagrange[130], F. Deliot[138], C.M. Delitzsch[50], M. Della Pietra[73a,73b], D. Della Volpe[57], A. Dell'Acqua[37], L. Dell'Asta[72a,72b], M. Delmastro[4], P.A. Delsart[61], S. Demers[175], M. Demichev[39], S.P. Denisov[38], L. D'Eramo[41], D. Derendarz[88], F. Derue[130], P. Dervan[94], K. Desch[25], C. Deutsch[25], F.A. Di Bello[58a,58b], A. Di Ciaccio[77a,77b], L. Di Ciaccio[4], A. Di Domenico[76a,76b], C. Di Donato[73a,73b], A. Di Girolamo[37], G. Di Gregorio[37], A. Di Luca[79a,79b], B. Di Micco[78a,78b], R. Di Nardo[78a,78b], K.F. Di Petrillo[40], M. Diamantopoulou[35], F.A. Dias[117], T. Dias Do Vale[146], M.A. Diaz[140a,140b], F.G. Diaz Capriles[25], A.R. Didenko[39], M. Didenko[166], E.B. Diehl[108], S. Díez Cornell[49], C. Diez Pardos[145], C. Dimitriadi[164], A. Dimitrievska[21], J. Dingfelder[25], T. Dingley[129], I-M. Dinu[28b], S.J. Dittmeier[64b], F. Dittus[37], M. Divisek[136], B. Dixit[94], F. Djama[104], T. Djobava[153b], C. Doglioni[100,103],

A. Dohnalova[29a], J. Dolejsi[136], Z. Dolezal[136], K. Domijan[87a], K.M. Dona[40], M. Donadelli[84d], B. Dong[109], J. Donini[41], A. D'Onofrio[73a,73b], M. D'Onofrio[94], J. Dopke[137], A. Doria[73a], N. Dos Santos Fernandes[133a], P. Dougan[103], M.T. Dova[92], A.T. Doyle[60], M.A. Draguet[129], M.P. Drescher[56], E. Dreyer[172], I. Drivas-koulouris[10], M. Drnevich[120], M. Drozdova[57], D. Du[63a], T.A. du Pree[117], F. Dubinin[38], M. Dubovsky[29a], E. Duchovni[172], G. Duckeck[111], O.A. Ducu[28b], D. Duda[53], A. Dudarev[37], E.R. Duden[27], M. D'uffizi[103], L. Duflot[67], M. Dührssen[37], I. Duminica[28g], A.E. Dumitriu[28b], M. Dunford[64a], S. Dungs[50], K. Dunne[48a,48b], A. Duperrin[104], H. Duran Yildiz[3a], M. Düren[59], A. Durglishvili[153b], B.L. Dwyer[118], G.I. Dyckes[18a], M. Dyndal[87a], B.S. Dziedzic[37], Z.O. Earnshaw[150], G.H. Eberwein[129], B. Eckerova[29a], S. Eggebrecht[56], E. Egidio Purcino De Souza[84e], L.F. Ehrke[57], G. Eigen[17], K. Einsweiler[18a], T. Ekelof[164], P.A. Ekman[100], S. El Farkh[36b], Y. El Ghazali[63a], H. El Jarrari[37], A. El Moussaouy[36a], V. Ellajosyula[164], M. Ellert[164], F. Ellinghaus[174], N. Ellis[37], J. Elmsheuser[30], M. Elsawy[119a], M. Elsing[37], D. Emeliyanov[137], Y. Enari[85], I. Ene[18a], S. Epari[13], P.A. Erland[88], D. Ernani Martins Neto[88], M. Errenst[174], M. Escalier[67], C. Escobar[166], E. Etzion[155], G. Evans[133a], H. Evans[69], L.S. Evans[97], A. Ezhilov[38], S. Ezzarqtouni[36a], F. Fabbri[24a,24b], L. Fabbri[24a,24b], G. Facini[98], V. Fadeyev[139], R.M. Fakhrutdinov[38], D. Fakoudis[102], S. Falciano[76a], L.F. Falda Ulhoa Coelho[37], F. Fallavollita[112], G. Falsetti[44a,44b], J. Faltova[136], C. Fan[165], K.Y. Fan[65b], Y. Fan[14], Y. Fang[14,114c], M. Fanti[72a,72b], M. Faraj[70a,70b], Z. Farazpay[99], A. Farbin[8], A. Farilla[78a], T. Farooque[109], S.M. Farrington[53], F. Fassi[36e], D. Fassouliotis[9], M. Faucci Giannelli[77a,77b], W.J. Fawcett[33], L. Fayard[67], P. Federic[136], P. Federicova[134], O.L. Fedin[38,a], M. Feickert[173], L. Feligioni[104], D.E. Fellers[126], C. Feng[63b], Z. Feng[117], M.J. Fenton[162], L. Ferencz[49], R.A.M. Ferguson[93], S.I. Fernandez Luengo[140f], P. Fernandez Martinez[68], M.J.V. Fernoux[104], J. Ferrando[93], A. Ferrari[164], P. Ferrari[116,117], R. Ferrari[74a], D. Ferrere[57], C. Ferretti[108], D. Fiacco[76a,76b], F. Fiedler[102], P. Fiedler[135], S. Filimonov[38], A. Filipčič[95], E.K. Filmer[1], F. Filthaut[116], M.C.N. Fiolhais[133a,133c,c], L. Fiorini[166], W.C. Fisher[109], T. Fitschen[103], P. M. Fitzhugh[138], I. Fleck[145], P. Fleischmann[108], T. Flick[174], M. Flores[34d,aa], L.R. Flores Castillo[65a], L. Flores Sanz De Acedo[37], F.M. Follega[79a,79b], N. Fomin[33], J.H. Foo[158], A. Formica[138], A.C. Forti[103], E. Fortin[37], A.W. Fortman[18a], M.G. Foti[18a], L. Fountas[9,i], D. Fournier[67], H. Fox[93], P. Francavilla[75a,75b], S. Francescato[62], S. Franchellucci[57], M. Franchini[24b,24a], S. Franchino[64a], D. Francis[37], L. Franco[116], V. Franco Lima[37], L. Franconi[49], M. Franklin[62], G. Frattari[27], Y.Y. Frid[155], J. Friend[60], N. Fritzsche[37], A. Froch[55], D. Froidevaux[37], J.A. Frost[129], Y. Fu[63a], S. Fuenzalida Garrido[140f], M. Fujimoto[104], K.Y. Fung[65a], E. Furtado De Simas Filho[84e], M. Furukawa[157], J. Fuster[166], A. Gaa[56], A. Gabrielli[24a,24b], A. Gabrielli[158], P. Gadow[37], G. Gagliardi[58a,58b], L.G. Gagnon[18a], S. Gaid[163], S. Galantzan[155], J. Gallagher[1], E.J. Gallas[129], B.J. Gallop[137], K.K. Gan[122], S. Ganguly[157], Y. Gao[53], F.M. Garay Walls[140a,140b], B. Garcia[30], C. García[166], A. Garcia Alonso[117], A.G. Garcia Caffaro[175], J.E. García Navarro[166], M. Garcia-Sciveres[18a], G.L. Gardner[131], R.W. Gardner[40], N. Garelli[161], D. Garg[81], R.B. Garg[147], J.M. Gargan[53], C. A. Garner[158], C.M. Garvey[34a], V. K. Gassmann[161], G. Gaudio[74a], V. Gautam[13], P. Gauzzi[76a,76b], J. Gavranovic[95], I.L. Gavrilenko[38], A. Gavrilyuk[38], C. Gay[167], G. Gaycken[126], E.N. Gazis[10], A.A. Geanta[28b], C.M. Gee[139], A. Gekow[122], C. Gemme[58b], M.H. Genest[61], A.D. Gentry[115], S. George[97], W.F. George[21], T. Geralis[47], P. Gessinger-Befurt[37], M.E. Geyik[174], M. Ghani[170], K. Ghorbanian[96], A. Ghosal[145], A. Ghosh[162], A. Ghosh[7], B. Giacobbe[24b], S. Giagu[76a,76b], T. Giani[117], A. Giannini[63a], S.M. Gibson[97], M. Gignac[139], D.T. Gil[87b], A.K. Gilbert[87a], B.J. Gilbert[42], D. Gillberg[35], G. Gilles[117], L. Ginabat[130], D.M. Gingrich[2,ad], M.P. Giordani[70a,70c], P.F. Giraud[138], G. Giugliarelli[70a,70c], D. Giugni[72a], F. Giuli[77a,77b], I. Gkialas[9,i], L.K. Gladilin[38], C. Glasman[101], G.R. Gledhill[126], G. Glemža[49], M. Glisic[126], I. Gnesi[44b], Y. Go[30], M. Goblirsch-Kolb[37], B. Gocke[50], D. Godin[110], B. Gokturk[22a], S. Goldfarb[107], T. Golling[57], M.G.D. Gololo[34g], D. Golubkov[38], J.P. Gombas[109], A. Gomes[133a,133b], G. Gomes Da Silva[145], A.J. Gomez Delegido[166], R. Gonçalo[133a], L. Gonella[21], A. Gongadze[153c], F. Gonnella[21], J.L. Gonski[147], R.Y. González Andana[53], S. González de la Hoz[166], R. Gonzalez Lopez[94], C. Gonzalez Renteria[18a], M.V. Gonzalez Rodrigues[49], R. Gonzalez Suarez[164], S. Gonzalez-Sevilla[57], L. Goossens[37], B. Gorini[37], E. Gorini[71a,71b], A. Gorišek[95], T.C. Gosart[131], A.T. Goshaw[52], M.I. Gostkin[39], S. Goswami[124], C.A. Gottardo[37], S.A. Gotz[111], M. Gouighri[36b], V. Goumarre[49], A.G. Goussiou[142], N. Govender[34c], R.P. Grabarczyk[129], I. Grabowska-Bold[87a], K. Graham[35], E. Gramstad[128], S. Grancagnolo[71a,71b], C. M. Grant[1,138], P.M. Gravila[28f], F.G. Gravili[71a,71b], H.M. Gray[18a], M. Greco[71a,71b], M.J. Green[1], C. Grefe[25], A.S. Grefsrud[17], I.M. Gregor[49], K.T. Greif[162], P. Grenier[147], S. G. Grewe[112], A.A. Grillo[139], K. Grimm[32], S. Grinstein[13,t], J.-F. Grivaz[67], E. Gross[172], J. Grosse-Knetter[56], L. Guan[108], J.G.R. Guerrero Rojas[166], G. Guerrieri[37], R. Gugel[102], J.A.M. Guhit[108], A. Guida[19],

E. Guilloton[170], S. Guindon[37], F. Guo[14,114c], J. Guo[63c], L. Guo[49], Y. Guo[108], A. Gupta[50], R. Gupta[132], S. Gurbuz[25], S.S. Gurdasani[55], G. Gustavino[76a,76b], P. Gutierrez[123], L.F. Gutierrez Zagazeta[131], M. Gutsche[51], C. Gutschow[98], C. Gwenlan[129], C.B. Gwilliam[94], E.S. Haaland[128], A. Haas[120], M. Habedank[60], C. Haber[18a], H.K. Hadavand[8], A. Hadef[51], S. Hadzic[112], A.I. Hagan[93], J.J. Hahn[145], E.H. Haines[98], M. Haleem[169], J. Haley[124], G.D. Hallewell[104], L. Halser[20], K. Hamano[168], M. Hamer[25], E.J. Hampshire[97], J. Han[63b], L. Han[114a], L. Han[63a], S. Han[18a], Y.F. Han[158], K. Hanagaki[85], M. Hance[139], D.A. Hangal[42], H. Hanif[146], M.D. Hank[131], J.B. Hansen[43], P.H. Hansen[43], D. Harada[57], T. Harenberg[174], S. Harkusha[38], M.L. Harris[105], Y.T. Harris[25], J. Harrison[13], N.M. Harrison[122], P. F. Harrison[170], N.M. Hartman[112], N.M. Hartmann[111], R.Z. Hasan[97,137], Y. Hasegawa[144], F. Haslbeck[129], S. Hassan[17], R. Hauser[109], C.M. Hawkes[21], R.J. Hawkings[37], Y. Hayashi[157], D. Hayden[109], C. Hayes[108], R.L. Hayes[117], C.P. Hays[129], J.M. Hays[96], H.S. Hayward[94], F. He[63a], M. He[14,114c], Y. He[49], Y. He[98], N.B. Heatley[96], V. Hedberg[100], A.L. Heggelund[128], N.D. Hehir[96,*], C. Heidegger[55], K.K. Heidegger[55], J. Heilman[35], S. Heim[49], T. Heim[18a], J.G. Heinlein[131], J.J. Heinrich[126], L. Heinrich[112,ab], J. Hejbal[134], A. Held[173], S. Hellesund[17], C.M. Helling[167], S. Hellman[48a,48b], R. C. W. Henderson[93], L. Henkelmann[33], A. M. Henriques Correia[37], H. Herde[100], Y. Hernández Jiménez[149], L.M. Herrmann[25], T. Herrmann[51], G. Herten[55], R. Hertenberger[111], L. Hervas[37], M.E. Hesping[102], N.P. Hessey[159a], J. Hessler[112], M. Hidaoui[36b], N. Hidic[136], E. Hill[158], S.J. Hillier[21], J.R. Hinds[109], F. Hinterkeuser[25], M. Hirose[127], S. Hirose[160], D. Hirschbuehl[174], T.G. Hitchings[103], B. Hiti[95], J. Hobbs[149], R. Hobincu[28e], N. Hod[172], M.C. Hodgkinson[143], B.H. Hodkinson[129], A. Hoecker[37], D.D. Hofer[108], J. Hofer[166], T. Holm[25], M. Holzbock[37], L.B.A.H. Hommels[33], B.P. Honan[103], J.J. Hong[69], J. Hong[63c], T.M. Hong[132], B.H. Hooberman[165], W.H. Hopkins[6], M.C. Hoppesch[165], Y. Horii[113], M.E. Horstmann[112], S. Hou[152], A.S. Howard[95], J. Howarth[60], J. Hoya[6], M. Hrabovsky[125], A. Hrynevich[49], T. Hryn'ova[4], P.J. Hsu[66], S.-C. Hsu[142], T. Hsu[67], M. Hu[18a], Q. Hu[63a], S. Huang[65b], X. Huang[14,114c], Y. Huang[143], Y. Huang[102], Y. Huang[14], Z. Huang[103], Z. Hubacek[135], M. Huebner[25], F. Huegging[25], T.B. Huffman[129], M. Hufnagel Maranha De Faria[84a], C.A. Hugli[49], M. Huhtinen[37], S.K. Huiberts[17], R. Hulsken[106], N. Huseynov[12,f], J. Huston[109], J. Huth[62], R. Hyneman[147], G. Iacobucci[57], G. Iakovidis[30], L. Iconomidou-Fayard[67], J.P. Iddon[37], P. Iengo[73a,73b], R. Iguchi[157], Y. Iiyama[157], T. Iizawa[129], Y. Ikegami[85], N. Ilic[158], H. Imam[84c], G. Inacio Goncalves[84d], T. Ingebretsen Carlson[48a,48b], J.M. Inglis[96], G. Introzzi[74a,74b], M. Iodice[78a], V. Ippolito[76a,76b], R.K. Irwin[94], M. Ishino[157], W. Islam[173], C. Issever[19], S. Istin[22a,ah], H. Ito[171], R. Iuppa[79a,79b], A. Ivina[172], J.M. Izen[46], V. Izzo[73a], P. Jacka[134], P. Jackson[1], C.S. Jagfeld[111], G. Jain[159a], P. Jain[49], K. Jakobs[55], T. Jakoubek[172], J. Jamieson[60], W. Jang[157], M. Javurkova[105], P. Jawahar[103], L. Jeanty[126], J. Jejelava[153a,z], P. Jenni[55,e], C.E. Jessiman[35], C. Jia[63b], H. Jia[167], J. Jia[149], X. Jia[14,114c], Z. Jia[114a], C. Jiang[53], S. Jiggins[49], J. Jimenez Pena[13], S. Jin[114a], A. Jinaru[28b], O. Jinnouchi[141], P. Johansson[143], K.A. Johns[7], J.W. Johnson[139], F.A. Jolly[49], D.M. Jones[150], E. Jones[49], K. S. Jones[8], P. Jones[33], R.W.L. Jones[93], T.J. Jones[94], H.L. Joos[56,37], R. Joshi[122], J. Jovicevic[16], X. Ju[18a], J.J. Junggeburth[105], T. Junkermann[64a], A. Juste Rozas[13,t], M.K. Juzek[88], S. Kabana[140e], A. Kaczmarska[88], M. Kado[112], H. Kagan[122], M. Kagan[147], A. Kahn[131], C. Kahra[102], T. Kaji[157], E. Kajomovitz[154], N. Kakati[172], I. Kalaitzidou[55], C.W. Kalderon[30], N.J. Kang[139], D. Kar[34g], K. Karava[129], M.J. Kareem[159b], E. Karentzos[55], O. Karkout[117], S.N. Karpov[39], Z.M. Karpova[39], V. Kartvelishvili[93], A.N. Karyukhin[38], E. Kasimi[156], J. Katzy[49], S. Kaur[35], K. Kawade[144], M.P. Kawale[123], C. Kawamoto[89], T. Kawamoto[63a], E.F. Kay[37], F.I. Kaya[161], S. Kazakos[109], V.F. Kazanin[38], Y. Ke[149], J.M. Keaveney[34a], R. Keeler[168], G.V. Kehris[62], J.S. Keller[35], J.J. Kempster[150], O. Kepka[134], B.P. Kerridge[137], S. Kersten[174], B.P. Kerševan[95], L. Keszeghova[29a], S. Ketabchi Haghighat[158], R.A. Khan[132], A. Khanov[124], A.G. Kharlamov[38], T. Kharlamova[38], E.E. Khoda[142], M. Kholodenko[133a], T.J. Khoo[19], G. Khoriauli[169], J. Khubua[153b,*], Y.A.R. Khwaira[130], B. Kibirige[34g], D. Kim[6], D.W. Kim[48a,48b], Y.K. Kim[40], N. Kimura[98], M.K. Kingston[56], A. Kirchhoff[56], C. Kirfel[25], F. Kirfel[25], J. Kirk[137], A.E. Kiryunin[112], S. Kita[160], C. Kitsaki[10], O. Kivernyk[25], M. Klassen[161], C. Klein[35], L. Klein[169], M.H. Klein[45], S.B. Klein[57], U. Klein[94], A. Klimentov[30], T. Klioutchnikova[37], P. Kluit[117], S. Kluth[112], E. Kneringer[80], T.M. Knight[158], A. Knue[50], D. Kobylianskii[172], S.F. Koch[129], M. Kocian[147], P. Kodyš[136], D.M. Koeck[126], P.T. Koenig[25], T. Koffas[35], O. Kolay[51], I. Koletsou[4], T. Komarek[88], K. Köneke[55], A.X.Y. Kong[1], T. Kono[121], N. Konstantinidis[98], P. Kontaxakis[57], B. Konya[100], R. Kopeliansky[42], S. Koperny[87a], K. Korcyl[88], K. Kordas[156,d], A. Korn[98], S. Korn[56], I. Korolkov[13], N. Korotkova[38], B. Kortman[117], O. Kortner[112], S. Kortner[112], W.H. Kostecka[118], V.V. Kostyukhin[145], A. Kotsokechagia[37], A. Kotwal[52], A. Koulouris[37], A. Kourkoumeli-Charalampidi[74a,74b], C. Kourkoumelis[9], E. Kourlitis[112,ab], O. Kovanda[126],

R. Kowalewski[168], W. Kozanecki[126], A.S. Kozhin[38], V.A. Kramarenko[38], G. Kramberger[95], P. Kramer[102], M.W. Krasny[130], A. Krasznahorkay[37], A.C. Kraus[118], J.W. Kraus[174], J.A. Kremer[49], T. Kresse[51], L. Kretschmann[174], J. Kretzschmar[94], K. Kreul[19], P. Krieger[158], M. Krivos[136], K. Krizka[21], K. Kroeninger[50], H. Kroha[112], J. Kroll[134], J. Kroll[131], K.S. Krowpman[109], U. Kruchonak[39], H. Krüger[25], N. Krumnack[82], M.C. Kruse[52], O. Kuchinskaia[38], S. Kuday[3a], S. Kuehn[37], R. Kuesters[55], T. Kuhl[49], V. Kukhtin[39], Y. Kulchitsky[38,a], S. Kuleshov[140b,140d], M. Kumar[34g], N. Kumari[49], P. Kumari[159b], A. Kupco[134], T. Kupfer[50], A. Kupich[38], O. Kuprash[55], H. Kurashige[86], L.L. Kurchaninov[159a], O. Kurdysh[67], Y.A. Kurochkin[38], A. Kurova[38], M. Kuze[141], A.K. Kvam[105], J. Kvita[125], T. Kwan[106], N.G. Kyriacou[108], L.A.O. Laatu[104], C. Lacasta[166], F. Lacava[76a,76b], H. Lacker[19], D. Lacour[130], N.N. Lad[98], E. Ladygin[39], A. Lafarge[41], B. Laforge[130], T. Lagouri[175], F.Z. Lahbabi[36a], S. Lai[56], J.E. Lambert[168], S. Lammers[69], W. Lampl[7], C. Lampoudis[156,d], G. Lamprinoudis[102], A.N. Lancaster[118], E. Lançon[30], U. Landgraf[55], M.P.J. Landon[96], V.S. Lang[55], O.K.B. Langrekken[128], A.J. Lankford[162], F. Lanni[37], K. Lantzsch[25], A. Lanza[74a], M. Lanzac Berrocal[166], J.F. Laporte[138], T. Lari[72a], F. Lasagni Manghi[24b], M. Lassnig[37], V. Latonova[134], A. Laurier[154], S.D. Lawlor[143], Z. Lawrence[103], R. Lazaridou[170], M. Lazzaroni[72a,72b], B. Le[103], H.D.M. Le[109], E.M. Le Boulicaut[175], L.T. Le Pottier[18a], B. Leban[24a,24b], A. Lebedev[82], M. LeBlanc[103], F. Ledroit-Guillon[61], S.C. Lee[152], S. Lee[48a,48b], T.F. Lee[94], L.L. Leeuw[34c], H.P. Lefebvre[97], M. Lefebvre[168], C. Leggett[18a], G. Lehmann Miotto[37], M. Leigh[57], W.A. Leight[105], W. Leinonen[116], A. Leisos[156,r], M.A.L. Leite[84c], C.E. Leitgeb[19], R. Leitner[136], K.J.C. Leney[45], T. Lenz[25], S. Leone[75a], C. Leonidopoulos[53], A. Leopold[148], R. Les[109], C.G. Lester[33], M. Levchenko[38], J. Levêque[4], L.J. Levinson[172], G. Levrini[24a,24b], M.P. Lewicki[88], C. Lewis[142], D.J. Lewis[4], L. Lewitt[143], A. Li[30], B. Li[63b], C. Li[63a], C-Q. Li[112], H. Li[63a], H. Li[63b], H. Li[114a], H. Li[15], H. Li[63b], J. Li[63c], K. Li[14], L. Li[63c], M. Li[14,114c], S. Li[14,114c], S. Li[63c,63d], T. Li[5], X. Li[106], Z. Li[157], Z. Li[14,114c], Z. Li[63a], S. Liang[14,114c], Z. Liang[14], M. Liberatore[138], B. Liberti[77a], K. Lie[65c], J. Lieber Marin[84e], H. Lien[69], H. Lin[108], K. Lin[109], R.E. Lindley[7], J.H. Lindon[2], J. Ling[62], E. Lipeles[131], A. Lipniacka[17], A. Lister[167], J.D. Little[69], B. Liu[14], B.X. Liu[114b], D. Liu[63c,63d], E.H.L. Liu[21], J.B. Liu[63a], J.K.K. Liu[33], K. Liu[63d], K. Liu[63c,63d], M. Liu[63a], M.Y. Liu[63a], P. Liu[14], Q. Liu[63c,63d,142], X. Liu[63a], X. Liu[63b], Y. Liu[114b,114c], Y.L. Liu[63b], Y.W. Liu[63a], S.L. Lloyd[96], E.M. Lobodzinska[49], P. Loch[7], E. Lodhi[158], T. Lohse[19], K. Lohwasser[143], E. Loiacono[49], M. Lokajicek[134,*], J.D. Lomas[21], J.D. Long[42], I. Longarini[162], R. Longo[165], I. Lopez Paz[68], A. Lopez Solis[49], N.A. Lopez-canelas[7], N. Lorenzo Martinez[4], A.M. Lory[111], M. Losada[119a], G. Löschcke Centeno[150], O. Loseva[38], X. Lou[48a,48b], X. Lou[14,114c], A. Lounis[67], P.A. Love[93], G. Lu[14,114c], M. Lu[67], S. Lu[131], Y.J. Lu[66], H.J. Lubatti[142], C. Luci[76a,76b], F.L. Lucio Alves[114a], F. Luehring[69], O. Lukianchuk[67], B.S. Lunday[131], O. Lundberg[148], B. Lund-Jensen[148,*], N.A. Luongo[6], M.S. Lutz[37], A.B. Lux[26], D. Lynn[30], R. Lysak[134], E. Lytken[100], V. Lyubushkin[39], T. Lyubushkina[39], M.M. Lyukova[149], M.Firdaus M. Soberi[53], H. Ma[30], K. Ma[63a], L.L. Ma[63b], W. Ma[63a], Y. Ma[124], J.C. MacDonald[102], P.C. Machado De Abreu Farias[84e], R. Madar[41], T. Madula[98], J. Maeda[86], T. Maeno[30], H. Maguire[143], V. Maiboroda[138], A. Maio[133a,133b,133d], K. Maj[87a], O. Majersky[49], S. Majewski[126], N. Makovec[67], V. Maksimovic[16], B. Malaescu[130], Pa. Malecki[88], V.P. Maleev[38], F. Malek[61,m], M. Mali[95], D. Malito[97], U. Mallik[81,*], S. Maltezos[10], S. Malyukov[39], J. Mamuzic[13], G. Mancini[54], M.N. Mancini[27], G. Manco[74a,74b], J.P. Mandalia[96], S.S. Mandarry[150], I. Mandić[95], L. Manhaes de Andrade Filho[84a], I.M. Maniatis[172], J. Manjarres Ramos[91], D.C. Mankad[172], A. Mann[111], S. Manzoni[37], L. Mao[63c], X. Mapekula[34c], A. Marantis[156,r], G. Marchiori[5], M. Marcisovsky[134], C. Marcon[72a], M. Marinescu[21], S. Marium[49], M. Marjanovic[123], A. Markhoos[55], M. Markovitch[67], E.J. Marshall[93], Z. Marshall[18a], S. Marti-Garcia[166], J. Martin[98], T.A. Martin[137], V.J. Martin[53], B. Martin dit Latour[17], L. Martinelli[76a,76b], M. Martinez[13,t], P. Martinez Agullo[166], V.I. Martinez Outschoorn[105], P. Martinez Suarez[13], S. Martin-Haugh[137], G. Martinovicova[136], V.S. Martoiu[28b], A.C. Martyniuk[98], A. Marzin[37], D. Mascione[79a,79b], L. Masetti[102], J. Masik[103], A.L. Maslennikov[38], S.L. Mason[42], P. Massarotti[73a,73b], P. Mastrandrea[75a,75b], A. Mastroberardino[44a,44b], T. Masubuchi[127], T.T. Mathew[126], T. Mathisen[164], J. Matousek[136], D.M. Mattern[50], J. Maurer[28b], T. Maurin[60], A.J. Maury[67], B. Maček[95], D.A. Maximov[38], A.E. May[103], R. Mazini[152], I. Maznas[118], M. Mazza[109], S.M. Mazza[139], E. Mazzeo[72a,72b], C. Mc Ginn[30], J.P. Mc Gowan[168], S.P. Mc Kee[108], C.A. Mc Lean[6], C.C. McCracken[167], E.F. McDonald[107], A.E. McDougall[117], J.A. Mcfayden[150], R.P. McGovern[131], R.P. Mckenzie[34g], T.C. Mclachlan[49], D.J. Mclaughlin[98], S.J. McMahon[137], C.M. Mcpartland[94], R.A. McPherson[168,x], S. Mehlhase[111], A. Mehta[94], D. Melini[166], B.R. Mellado Garcia[34g], A.H. Melo[56], F. Meloni[49], A.M. Mendes Jacques Da Costa[103], H.Y. Meng[158], L. Meng[93], S. Menke[112], M. Mentink[37],

E. Meoni[44a,44b], G. Mercado[118], S. Merianos[156], C. Merlassino[70a,70c], L. Merola[73a,73b], C. Meroni[72a,72b], J. Metcalfe[6], A.S. Mete[6], E. Meuser[102], C. Meyer[69], J-P. Meyer[138], R.P. Middleton[137], L. Mijović[53], G. Mikenberg[172], M. Mikestikova[134], M. Mikuž[95], H. Mildner[102], A. Milic[37], D.W. Miller[40], E.H. Miller[147], L.S. Miller[35], A. Milov[172], D. A. Milstead[48a,48b], T. Min[114a], A.A. Minaenko[38], I.A. Minashvili[153b], L. Mince[60], A.I. Mincer[120], B. Mindur[87a], M. Mineev[39], Y. Mino[89], L.M. Mir[13], M. Miralles Lopez[60], M. Mironova[18a], M.C. Missio[116], A. Mitra[170], V.A. Mitsou[166], Y. Mitsumori[113], O. Miu[158], P.S. Miyagawa[96], T. Mkrtchyan[64a], M. Mlinarevic[98], T. Mlinarevic[98], M. Mlynarikova[37], S. Mobius[20], P. Mogg[111], M.H. Mohamed Farook[115], A.F. Mohammed[14,114c], S. Mohapatra[42], G. Mokgatitswane[34g], L. Moleri[172], B. Mondal[145], S. Mondal[135], K. Mönig[49], E. Monnier[104], L. Monsonis Romero[166], J. Montejo Berlingen[13], A. Montella[48a,48b], M. Montella[122], F. Montereali[78a,78b], F. Monticelli[92], S. Monzani[70a,70c], A. Morancho Tarda[43], N. Morange[67], A.L. Moreira De Carvalho[49], M. Moreno Llácer[166], C. Moreno Martinez[57], J. M. Moreno Perez[23b], P. Morettini[58b], S. Morgenstern[37], M. Morii[62], M. Morinaga[157], M. Moritsu[90], F. Morodei[76a,76b], P. Moschovakos[37], B. Moser[129], M. Mosidze[153b], T. Moskalets[45], P. Moskvitina[116], J. Moss[32,j], P. Moszkowicz[87a], A. Moussa[36d], E.J.W. Moyse[105], O. Mtintsilana[34g], S. Muanza[104], J. Mueller[132], D. Muenstermann[93], R. Müller[37], G.A. Mullier[164], A. J. Mullin[33], J. J. Mullin[131], A.E. Mulski[62], D.P. Mungo[158], D. Munoz Perez[166], F.J. Munoz Sanchez[103], M. Murin[103], W.J. Murray[170,137], M. Muškinja[95], C. Mwewa[30], A.G. Myagkov[38,a], A.J. Myers[8], G. Myers[108], M. Myska[135], B.P. Nachman[18a], O. Nackenhorst[50], K. Nagai[129], K. Nagano[85], R. Nagasaka[157], J.L. Nagle[30,af], E. Nagy[104], A.M. Nairz[37], Y. Nakahama[85], K. Nakamura[85], K. Nakkalil[5], H. Nanjo[127], E.A. Narayanan[45], I. Naryshkin[38], L. Nasella[72a,72b], M. Naseri[35], S. Nasri[119b], C. Nass[25], G. Navarro[23a], J. Navarro-Gonzalez[166], R. Nayak[155], A. Nayaz[19], P.Y. Nechaeva[38], S. Nechaeva[24b,24a], F. Nechansky[134], L. Nedic[129], T.J. Neep[21], A. Negri[74a,74b], M. Negrini[24b], C. Nellist[117], C. Nelson[106], K. Nelson[108], S. Nemecek[134], M. Nessi[37,g], M.S. Neubauer[165], F. Neuhaus[102], J. Neundorf[49], J. Newell[94], P.R. Newman[21], C.W. Ng[132], Y.W.Y. Ng[49], B. Ngair[119a], H.D.N. Nguyen[110], R.B. Nickerson[129], R. Nicolaidou[138], J. Nielsen[139], M. Niemeyer[56], J. Niermann[56], N. Nikiforou[37], V. Nikolaenko[38,a], I. Nikolic-Audit[130], K. Nikolopoulos[21], P. Nilsson[30], I. Ninca[49], G. Ninio[155], A. Nisati[76a], N. Nishu[2], R. Nisius[112], J-E. Nitschke[51], E.K. Nkadimeng[34g], T. Nobe[157], T. Nommensen[151], M.B. Norfolk[143], B.J. Norman[35], M. Noury[36a], J. Novak[95], T. Novak[95], L. Novotny[135], R. Novotny[115], L. Nozka[125], K. Ntekas[162], N.M.J. Nunes De Moura Junior[84b], J. Ocariz[130], A. Ochi[86], I. Ochoa[133a], S. Oerdek[49,u], J.T. Offermann[40], A. Ogrodnik[136], A. Oh[103], C.C. Ohm[148], H. Oide[85], R. Oishi[157], M.L. Ojeda[37], Y. Okumura[157], L.F. Oleiro Seabra[133a], I. Oleksiyuk[57], S.A. Olivares Pino[140d], G. Oliveira Correa[13], D. Oliveira Damazio[30], J.L. Oliver[162], Ö.O. Öncel[55], A.P. O'Neill[20], A. Onofre[133a,133e], P.U.E. Onyisi[11], M.J. Oreglia[40], G.E. Orellana[92], D. Orestano[78a,78b], N. Orlando[13], R.S. Orr[158], L.M. Osojnak[131], R. Ospanov[63a], Y. Osumi[113], G. Otero y Garzon[31], H. Otono[90], P.S. Ott[64a], G.J. Ottino[18a], M. Ouchrif[36d], F. Ould-Saada[128], T. Ovsiannikova[142], M. Owen[60], R.E. Owen[137], V.E. Ozcan[22a], F. Ozturk[88], N. Ozturk[8], S. Ozturk[83], H.A. Pacey[129], A. Pacheco Pages[13], C. Padilla Aranda[13], G. Padovano[76a,76b], S. Pagan Griso[18a], G. Palacino[69], A. Palazzo[71a,71b], J. Pampel[25], J. Pan[175], T. Pan[65a], D.K. Panchal[11], C.E. Pandini[117], J.G. Panduro Vazquez[137], H.D. Pandya[1], H. Pang[15], P. Pani[49], G. Panizzo[70a,70c], L. Panwar[130], L. Paolozzi[57], S. Parajuli[165], A. Paramonov[6], C. Paraskevopoulos[54], D. Paredes Hernandez[65b], A. Pareti[74a,74b], K.R. Park[42], T.H. Park[158], M.A. Parker[33], F. Parodi[58a,58b], E.W. Parrish[118], V.A. Parrish[53], J.A. Parsons[42], U. Parzefall[55], B. Pascual Dias[110], L. Pascual Dominguez[101], E. Pasqualucci[76a], S. Passaggio[58b], F. Pastore[97], P. Patel[88], U.M. Patel[52], J.R. Pater[103], T. Pauly[37], F. Pauwels[136], C.I. Pazos[161], M. Pedersen[128], R. Pedro[133a], S.V. Peleganchuk[38], O. Penc[37], E.A. Pender[53], S. Peng[15], G.D. Penn[175], K.E. Penski[111], M. Penzin[38], B.S. Peralva[84d], A.P. Pereira Peixoto[142], L. Pereira Sanchez[147], D.V. Perepelitsa[30,af], G. Perera[105], E. Perez Codina[159a], M. Perganti[10], H. Pernegger[37], S. Perrella[76a,76b], O. Perrin[41], K. Peters[49], R.F.Y. Peters[103], B.A. Petersen[37], T.C. Petersen[43], E. Petit[104], V. Petousis[135], C. Petridou[156,d], T. Petru[136], A. Petrukhin[145], M. Pettee[18a], A. Petukhov[38], K. Petukhova[37], R. Pezoa[140f], L. Pezzotti[37], G. Pezzullo[175], A.J. Pfleger[37], T.M. Pham[173], T. Pham[107], P.W. Phillips[137], G. Piacquadio[149], E. Pianori[18a], F. Piazza[126], R. Piegaia[31], D. Pietreanu[28b], A.D. Pilkington[103], M. Pinamonti[70a,70c], J.L. Pinfold[2], B.C. Pinheiro Pereira[133a], J. Pinol Bel[13], A.E. Pinto Pinoargote[138], L. Pintucci[70a,70c], K.M. Piper[150], A. Pirttikoski[57], D.A. Pizzi[35], L. Pizzimento[65b], A. Pizzini[117], M.-A. Pleier[30], V. Pleskot[136], E. Plotnikova[39], G. Poddar[96], R. Poettgen[100], L. Poggioli[130], I. Pokharel[56], S. Polacek[136], G. Polesello[74a], A. Poley[146,159a], A. Polini[24b], C.S. Pollard[170], Z.B. Pollock[122], E. Pompa Pacchi[76a,76b], N.I. Pond[98], D. Ponomarenko[69],

L. Pontecorvo[37], S. Popa[28a], G.A. Popeneciu[28d], A. Poreba[37], D.M. Portillo Quintero[159a], S. Pospisil[135], M.A. Postill[143], P. Postolache[28c], K. Potamianos[170], P.A. Potepa[87a], I.N. Potrap[39], C.J. Potter[33], H. Potti[151], J. Poveda[166], M.E. Pozo Astigarraga[37], A. Prades Ibanez[77a,77b], J. Pretel[168], D. Price[103], M. Primavera[71a], L. Primomo[70a,70c], M.A. Principe Martin[101], R. Privara[125], T. Procter[60], M.L. Proffitt[142], N. Proklova[131], K. Prokofiev[65c], G. Proto[112], J. Proudfoot[6], M. Przybycien[87a], W.W. Przygoda[87b], A. Psallidas[47], J.E. Puddefoot[143], D. Pudzha[55], D. Pyatiizbyantseva[38], J. Qian[108], D. Qichen[103], Y. Qin[13], T. Qiu[53], A. Quadt[56], M. Queitsch-Maitland[103], G. Quetant[57], R.P. Quinn[167], G. Rabanal Bolanos[62], D. Rafanoharana[55], F. Raffaeli[77a,77b], F. Ragusa[72a,72b], J.L. Rainbolt[40], J.A. Raine[57], S. Rajagopalan[30], E. Ramakoti[38], L. Rambelli[58b,58a], I.A. Ramirez-Berend[35], K. Ran[49,114c], D.S. Rankin[131], N.P. Rapheeha[34g], H. Rasheed[28b], V. Raskina[130], D.F. Rassloff[64a], A. Rastogi[18a], S. Rave[102], S. Ravera[58b,58a], B. Ravina[56], I. Ravinovich[172], M. Raymond[37], A.L. Read[128], N.P. Readioff[143], D.M. Rebuzzi[74a,74b], G. Redlinger[30], A.S. Reed[112], K. Reeves[27], J.A. Reidelsturz[174], D. Reikher[126], A. Rej[50], C. Rembser[37], M. Renda[28b], F. Renner[49], A.G. Rennie[162], A.L. Rescia[49], S. Resconi[72a], M. Ressegotti[58b,58a], S. Rettie[37], J.G. Reyes Rivera[109], E. Reynolds[18a], O.L. Rezanova[38], P. Reznicek[136], H. Riani[36d], N. Ribaric[52], E. Ricci[79a,79b], R. Richter[112], S. Richter[48a,48b], E. Richter-Was[87b], M. Ridel[130], S. Ridouani[36d], P. Rieck[120], P. Riedler[37], E.M. Riefel[48a,48b], J.O. Rieger[117], M. Rijssenbeek[149], M. Rimoldi[37], L. Rinaldi[24b,24a], P. Rincke[56,164], T.T. Rinn[30], M.P. Rinnagel[111], G. Ripellino[164], I. Riu[13], J.C. Rivera Vergara[168], F. Rizatdinova[124], E. Rizvi[96], B.R. Roberts[18a], S.S. Roberts[139], S.H. Robertson[106,x], D. Robinson[33], M. Robles Manzano[102], A. Robson[60], A. Rocchi[77a,77b], C. Roda[75a,75b], S. Rodriguez Bosca[37], Y. Rodriguez Garcia[23a], A. Rodriguez Rodriguez[55], A.M. Rodríguez Vera[118], S. Roe[37], J.T. Roemer[37], A.R. Roepe-Gier[139], O. Røhne[128], R.A. Rojas[105], C.P.A. Roland[130], J. Roloff[30], A. Romaniouk[80], E. Romano[74a,74b], M. Romano[24b], A.C. Romero Hernandez[165], N. Rompotis[94], L. Roos[130], S. Rosati[76a], B.J. Rosser[40], E. Rossi[129], E. Rossi[73a,73b], L.P. Rossi[62], L. Rossini[55], R. Rosten[122], M. Rotaru[28b], B. Rottler[55], C. Rougier[91], D. Rousseau[67], D. Rousso[49], A. Roy[165], S. Roy-Garand[158], A. Rozanov[104], Z.M.A. Rozario[60], Y. Rozen[154], A. Rubio Jimenez[166], A.J. Ruby[94], V.H. Ruelas Rivera[19], T.A. Ruggeri[1], A. Ruggiero[129], A. Ruiz-Martinez[166], A. Rummler[37], Z. Rurikova[55], N.A. Rusakovich[39], H.L. Russell[168], G. Russo[76a,76b], J.P. Rutherfoord[7], S. Rutherford Colmenares[33], M. Rybar[136], E.B. Rye[128], A. Ryzhov[45], J.A. Sabater Iglesias[57], H.F-W. Sadrozinski[139], F. Safai Tehrani[76a], B. Safarzadeh Samani[137], S. Saha[1], M. Sahinsoy[83], A. Saibel[166], M. Saimpert[138], M. Saito[157], T. Saito[157], A. Sala[72a,72b], D. Salamani[37], A. Salnikov[147], J. Salt[166], A. Salvador Salas[155], D. Salvatore[44a,44b], F. Salvatore[150], A. Salzburger[37], D. Sammel[55], E. Sampson[93], D. Sampsonidis[156,d], D. Sampsonidou[126], J. Sánchez[166], V. Sanchez Sebastian[166], H. Sandaker[128], C.O. Sander[49], J.A. Sandesara[105], M. Sandhoff[174], C. Sandoval[23b], L. Sanfilippo[64a], D.P.C. Sankey[137], T. Sano[89], A. Sansoni[54], L. Santi[37,76b], C. Santoni[41], H. Santos[133a,133b], A. Santra[172], E. Sanzani[24a,24b], K.A. Saoucha[163], J.G. Saraiva[133a,133d], J. Sardain[7], O. Sasaki[85], K. Sato[160], C. Sauer[64b], E. Sauvan[4], P. Savard[158,ad], R. Sawada[157], C. Sawyer[137], L. Sawyer[99], C. Sbarra[24b], A. Sbrizzi[24a,24b], T. Scanlon[98], J. Schaarschmidt[142], U. Schäfer[102], A.C. Schaffer[45,67], D. Schaile[111], R.D. Schamberger[149], C. Scharf[19], M.M. Schefer[20], V.A. Schegelsky[38], D. Scheirich[136], M. Schernau[162], C. Scheulen[56], C. Schiavi[58a,58b], M. Schioppa[44a,44b], B. Schlag[147], S. Schlenker[37], J. Schmeing[174], M.A. Schmidt[174], K. Schmieden[102], C. Schmitt[102], N. Schmitt[102], S. Schmitt[49], L. Schoeffel[138], A. Schoening[64b], P.G. Scholer[35], E. Schopf[129], M. Schott[25], J. Schovancova[37], S. Schramm[57], T. Schroer[57], H-C. Schultz-Coulon[64a], M. Schumacher[55], B.A. Schumm[139], Ph. Schune[138], A.J. Schuy[142], H.R. Schwartz[139], A. Schwartzman[147], T.A. Schwarz[108], Ph. Schwemling[138], R. Schwienhorst[109], F.G. Sciacca[20], A. Sciandra[30], G. Sciolla[27], F. Scuri[75a], C.D. Sebastiani[94], K. Sedlaczek[118], S.C. Seidel[115], A. Seiden[139], B.D. Seidlitz[42], C. Seitz[49], J.M. Seixas[84b], G. Sekhniaidze[73a], L. Selem[61], N. Semprini-Cesari[24a,24b], D. Sengupta[57], V. Senthilkumar[166], L. Serin[67], M. Sessa[77a,77b], H. Severini[123], F. Sforza[58a,58b], A. Sfyrla[57], Q. Sha[14], E. Shabalina[56], A.H. Shah[33], R. Shaheen[148], J.D. Shahinian[131], D. Shaked Renous[172], L.Y. Shan[14], M. Shapiro[18a], A. Sharma[37], A.S. Sharma[167], P. Sharma[81], P.B. Shatalov[38], K. Shaw[150], S.M. Shaw[103], Q. Shen[63c], D.J. Sheppard[146], P. Sherwood[98], L. Shi[98], X. Shi[14], S. Shimizu[85], C.O. Shimmin[175], J.D. Shinner[97], I.P.J. Shipsey[129,*], S. Shirabe[90], M. Shiyakova[39,v], M.J. Shochet[40], D.R. Shope[128], B. Shrestha[123], S. Shrestha[122,ag], I. Shreyber[38], M.J. Shroff[168], P. Sicho[134], A.M. Sickles[165], E. Sideras Haddad[34g], A.C. Sidley[117], A. Sidoti[24b], F. Siegert[51], Dj. Sijacki[16], F. Sili[92], J.M. Silva[53], I. Silva Ferreira[84b], M.V. Silva Oliveira[30], S.B. Silverstein[48a], S. Simion[67], R. Simoniello[37], E.L. Simpson[103], H. Simpson[150], L.R. Simpson[108], S. Simsek[83], S. Sindhu[56], P. Sinervo[158], S. Singh[158], S. Sinha[49], S. Sinha[103], M. Sioli[24a,24b], I. Siral[37],

E. Sitnikova[49], J. Sjölin[48a,48b], A. Skaf[56], E. Skorda[21], P. Skubic[123], M. Slawinska[88], V. Smakhtin[172], B.H. Smart[137], S.Yu. Smirnov[38], Y. Smirnov[38], L.N. Smirnova[38,a], O. Smirnova[100], A.C. Smith[42], D. R. Smith[162], E.A. Smith[40], J.L. Smith[103], R. Smith[147], M. Smizanska[93], K. Smolek[135], A.A. Snesarev[38], H.L. Snoek[117], S. Snyder[30], R. Sobie[168,x], A. Soffer[155], C.A. Solans Sanchez[37], E.Yu. Soldatov[38], U. Soldevila[166], A.A. Solodkov[38], S. Solomon[27], A. Soloshenko[39], K. Solovieva[55], O.V. Solovyanov[41], P. Sommer[51], A. Sonay[13], W.Y. Song[159b], A. Sopczak[135], A.L. Sopio[53], F. Sopkova[29b], J.D. Sorenson[115], I.R. Sotarriva Alvarez[141], V. Sothilingam[64a], O.J. Soto Sandoval[140c,140b], S. Sottocornola[69], R. Soualah[163], Z. Soumaimi[36e], D. South[49], N. Soybelman[172], S. Spagnolo[71a,71b], M. Spalla[112], D. Sperlich[55], G. Spigo[37], B. Spisso[73a,73b], D.P. Spiteri[60], M. Spousta[136], E.J. Staats[35], R. Stamen[64a], A. Stampekis[21], E. Stanecka[88], W. Stanek-Maslouska[49], M.V. Stange[51], B. Stanislaus[18a], M.M. Stanitzki[49], B. Stapf[49], E.A. Starchenko[38], G.H. Stark[139], J. Stark[91], P. Staroba[134], P. Starovoitov[64a], S. Stärz[106], R. Staszewski[88], G. Stavropoulos[47], A. Stefl[37], P. Steinberg[30], B. Stelzer[146,159a], H.J. Stelzer[132], O. Stelzer-Chilton[159a], H. Stenzel[59], T.J. Stevenson[150], G.A. Stewart[37], J.R. Stewart[124], M.C. Stockton[37], G. Stoicea[28b], M. Stolarski[133a], S. Stonjek[112], A. Straessner[51], J. Strandberg[148], S. Strandberg[48a,48b], M. Stratmann[174], M. Strauss[123], T. Strebler[104], P. Strizenec[29b], R. Ströhmer[169], D.M. Strom[126], R. Stroynowski[45], A. Strubig[48a,48b], S.A. Stucci[30], B. Stugu[17], J. Stupak[123], N.A. Styles[49], D. Su[147], S. Su[63a], W. Su[63d], X. Su[63a], D. Suchy[29a], K. Sugizaki[157], V.V. Sulin[38], M.J. Sullivan[94], D.M.S. Sultan[129], L. Sultanaliyeva[38], S. Sultansoy[3b], T. Sumida[89], S. Sun[173], O. Sunneborn Gudnadottir[164], N. Sur[104], M.R. Sutton[150], H. Suzuki[160], M. Svatos[134], M. Swiatlowski[159a], T. Swirski[169], I. Sykora[29a], M. Sykora[136], T. Sykora[136], D. Ta[102], K. Tackmann[49,u], A. Taffard[162], R. Tafirout[159a], J.S. Tafoya Vargas[67], Y. Takubo[85], M. Talby[104], A.A. Talyshev[38], K.C. Tam[65b], N. M. Tamir[155], A. Tanaka[157], J. Tanaka[157], R. Tanaka[67], M. Tanasini[149], Z. Tao[167], S. Tapia Araya[140f], S. Tapprogge[102], A. Tarek Abouelfadl Mohamed[109], S. Tarem[154], K. Tariq[14], G. Tarna[28b], G.F. Tartarelli[72a], M.J. Tartarin[91], P. Tas[136], M. Tasevsky[134], E. Tassi[44a,44b], A.C. Tate[165], G. Tateno[157], Y. Tayalati[36e,w], G.N. Taylor[107], W. Taylor[159b], R. Teixeira De Lima[147], P. Teixeira-Dias[97], J.J. Teoh[158], K. Terashi[157], J. Terron[101], S. Terzo[13], M. Testa[54], R.J. Teuscher[158,x], A. Thaler[80], O. Theiner[57], T. Theveneaux-Pelzer[104], O. Thielmann[174], D. W. Thomas[97], J.P. Thomas[21], E.A. Thompson[18a], P.D. Thompson[21], E. Thomson[131], R.E. Thornberry[45], C. Tian[63a], Y. Tian[57], V. Tikhomirov[38,a], Yu.A. Tikhonov[38], S. Timoshenko[38], D. Timoshyn[136], E.X.L. Ting[1], P. Tipton[175], A. Tishelman-Charny[30], S.H. Tlou[34g], K. Todome[141], S. Todorova-Nova[136], S. Todt[51], L. Toffolin[70a,70c], M. Togawa[85], J. Tojo[90], S. Tokár[29a], K. Tokushuku[85], O. Toldaiev[69], M. Tomoto[85,113], L. Tompkins[147,l], K.W. Topolnicki[87b], E. Torrence[126], H. Torres[91], E. Torró Pastor[166], M. Toscani[31], C. Tosciri[40], M. Tost[11], D.R. Tovey[143], I.S. Trandafir[28b], T. Trefzger[169], A. Tricoli[30], I.M. Trigger[159a], S. Trincaz-Duvoid[130], D.A. Trischuk[27], B. Trocmé[61], A. Tropina[39], L. Truong[34c], M. Trzebinski[88], A. Trzupek[88], F. Tsai[149], M. Tsai[108], A. Tsiamis[156], P. V. Tsiareshka[38], S. Tsigaridas[159a], A. Tsirigotis[156,r], V. Tsiskaridze[158], E.G. Tskhadadze[153a], M. Tsopoulou[156], Y. Tsujikawa[89], I.I. Tsukerman[38], V. Tsulaia[18a], S. Tsuno[85], K. Tsuri[121], D. Tsybychev[149], Y. Tu[65b], A. Tudorache[28b], V. Tudorache[28b], A.N. Tuna[62], S. Turchikhin[58a,58b], I. Turk Cakir[3a], R. Turra[72a], T. Turtuvshin[39], P.M. Tuts[42], S. Tzamarias[156,d], E. Tzovara[102], F. Ukegawa[160], P.A. Ulloa Poblete[140c,140b], E.N. Umaka[30], G. Unal[37], A. Undrus[30], G. Unel[162], J. Urban[29b], P. Urrejola[140a], G. Usai[8], R. Ushioda[141], M. Usman[110], F. Ustuner[53], Z. Uysal[83], V. Vacek[135], B. Vachon[106], T. Vafeiadis[37], A. Vaitkus[98], C. Valderanis[111], E. Valdes Santurio[48a,48b], M. Valente[159a], S. Valentinetti[24a,24b], A. Valero[166], E. Valiente Moreno[166], A. Vallier[91], J.A. Valls Ferrer[166], D.R. Van Arneman[117], T.R. Van Daalen[142], A. Van Der Graaf[50], P. Van Gemmeren[6], M. Van Rijnbach[37], S. Van Stroud[98], I. Van Vulpen[117], P. Vana[136], M. Vanadia[77a,77b], U.M. Vande Voorde[148], W. Vandelli[37], E.R. Vandewall[124], D. Vannicola[155], L. Vannoli[54], R. Vari[76a], E.W. Varnes[7], C. Varni[18b], T. Varol[152], D. Varouchas[67], L. Varriale[166], K.E. Varvell[151], M.E. Vasile[28b], L. Vaslin[85], G.A. Vasquez[168], A. Vasyukov[39], L.M. Vaughan[124], R. Vavricka[102], T. Vazquez Schroeder[37], J. Veatch[32], V. Vecchio[103], M.J. Veen[105], I. Veliscek[30], L.M. Veloce[158], F. Veloso[133a,133c], S. Veneziano[76a], A. Ventura[71a,71b], S. Ventura Gonzalez[138], A. Verbytskyi[112], M. Verducci[75a,75b], C. Vergis[96], M. Verissimo De Araujo[84b], W. Verkerke[117], J.C. Vermeulen[117], C. Vernieri[147], M. Vessella[105], M.C. Vetterli[146,ad], A. Vgenopoulos[102], N. Viaux Maira[140f], T. Vickey[143], O.E. Vickey Boeriu[143], G.H.A. Viehhauser[129], L. Vigani[64b], M. Vigl[112], M. Villa[24b,24a], M. Villaplana Perez[166], E. M. Villhauer[53], E. Vilucchi[54], M.G. Vincter[35], A. Visibile[117], C. Vittori[37], I. Vivarelli[24a,24b], E. Voevodina[112], F. Vogel[111], J.C. Voigt[51], P. Vokac[135], Yu. Volkotrub[87b], E. Von Toerne[25], B. Vormwald[37], V. Vorobel[136], K. Vorobev[38], M. Vos[166], K. Voss[145], M. Vozak[117], L. Vozdecky[123],

N. Vranjes[16], M. Vranjes Milosavljevic[16], M. Vreeswijk[117], N.K. Vu[63c,63d], R. Vuillermet[37], O. Vujinovic[102], I. Vukotic[40], I.K. Vyas[35], S. Wada[160], C. Wagner[147], J.M. Wagner[18a], W. Wagner[174], S. Wahdan[174], H. Wahlberg[92], J. Walder[137], R. Walker[111], W. Walkowiak[145], A. Wall[131], E.J. Wallin[100], T. Wamorkar[6], A.Z. Wang[139], C. Wang[102], C. Wang[11], H. Wang[18a], J. Wang[65c], P. Wang[98], R. Wang[62], R. Wang[6], S.M. Wang[152], S. Wang[63b], S. Wang[14], T. Wang[63a], W.T. Wang[81], W. Wang[14], X. Wang[114a], X. Wang[165], X. Wang[63c], Y. Wang[63d], Y. Wang[114a], Y. Wang[63a], Z. Wang[108], Z. Wang[52,63c,63d], Z. Wang[108], A. Warburton[106], R.J. Ward[21], N. Warrack[60], S. Waterhouse[97], A.T. Watson[21], H. Watson[53], M.F. Watson[21], E. Watton[60,137], G. Watts[142], B.M. Waugh[98], J.M. Webb[55], C. Weber[30], H.A. Weber[19], M.S. Weber[20], S.M. Weber[64a], C. Wei[63a], Y. Wei[55], A.R. Weidberg[129], E.J. Weik[120], J. Weingarten[50], C. Weiser[55], C.J. Wells[49], T. Wenaus[30], B. Wendland[50], T. Wengler[37], N. S. Wenke[112], N. Wermes[25], M. Wessels[64a], A.M. Wharton[93], A.S. White[62], A. White[8], M.J. White[1], D. Whiteson[162], L. Wickremasinghe[127], W. Wiedenmann[173], M. Wielers[137], C. Wiglesworth[43], D. J. Wilbern[123], H.G. Wilkens[37], J.J.H. Wilkinson[33], D.M. Williams[42], H. H. Williams[131], S. Williams[33], S. Willocq[105], B.J. Wilson[103], P.J. Windischhofer[40], F.I. Winkel[31], F. Winklmeier[126], B.T. Winter[55], J.K. Winter[103], M. Wittgen[147], M. Wobisch[99], T. Wojtkowski[61], Z. Wolffs[117], J. Wollrath[162], M.W. Wolter[88], H. Wolters[133a,133c], M. C. Wong[139], E.L. Woodward[42], S.D. Worm[49], B.K. Wosiek[88], K.W. Woźniak[88], S. Wozniewski[56], K. Wraight[60], C. Wu[21], M. Wu[114b], M. Wu[116], S.L. Wu[173], X. Wu[57], Y. Wu[63a], Z. Wu[4], J. Wuerzinger[112,ab], T.R. Wyatt[103], B.M. Wynne[53], S. Xella[43], L. Xia[114a], M. Xia[15], M. Xie[63a], S. Xin[14,114c], A. Xiong[126], J. Xiong[18a], D. Xu[14], H. Xu[63a], L. Xu[63a], R. Xu[131], T. Xu[108], Y. Xu[15], Z. Xu[53], Z. Xu[114a], B. Yabsley[151], S. Yacoob[34a], Y. Yamaguchi[85], E. Yamashita[157], H. Yamauchi[160], T. Yamazaki[18a], Y. Yamazaki[86], S. Yan[60], Z. Yan[105], H.J. Yang[63c,63d], H.T. Yang[63a], S. Yang[63a], T. Yang[65c], X. Yang[37], X. Yang[14], Y. Yang[45], Y. Yang[63a], Z. Yang[63a], W-M. Yao[18a], H. Ye[114a], H. Ye[56], J. Ye[14], S. Ye[30], X. Ye[63a], Y. Yeh[98], I. Yeletskikh[39], B. Yeo[18b], M.R. Yexley[98], T.P. Yildirim[129], P. Yin[42], K. Yorita[171], S. Younas[28b], C.J.S. Young[37], C. Young[147], C. Yu[14,114c], Y. Yu[63a], J. Yuan[14,114c], M. Yuan[108], R. Yuan[63d,63c], L. Yue[98], M. Zaazoua[63a], B. Zabinski[88], E. Zaid[53], Z.K. Zak[88], T. Zakareishvili[166], S. Zambito[57], J.A. Zamora Saa[140d,140b], J. Zang[157], D. Zanzi[55], O. Zaplatilek[135], C. Zeitnitz[174], H. Zeng[14], J.C. Zeng[165], D.T. Zenger Jr[27], O. Zenin[38], T. Ženiš[29a], S. Zenz[96], S. Zerradi[36a], D. Zerwas[67], M. Zhai[14,114c], D.F. Zhang[143], J. Zhang[63b], J. Zhang[6], K. Zhang[14,114c], L. Zhang[63a], L. Zhang[114a], P. Zhang[14,114c], R. Zhang[173], S. Zhang[108], S. Zhang[91], T. Zhang[157], X. Zhang[63c], X. Zhang[63b], Y. Zhang[63c], Y. Zhang[98], Y. Zhang[114a], Z. Zhang[18a], Z. Zhang[63b], Z. Zhang[67], H. Zhao[142], T. Zhao[63b], Y. Zhao[139], Z. Zhao[63a], Z. Zhao[63a], A. Zhemchugov[39], J. Zheng[114a], K. Zheng[165], X. Zheng[63a], Z. Zheng[147], D. Zhong[165], B. Zhou[108], H. Zhou[7], N. Zhou[63c], Y. Zhou[15], Y. Zhou[114a], Y. Zhou[7], C.G. Zhu[63b], J. Zhu[108], X. Zhu[63d], Y. Zhu[63c], Y. Zhu[63a], X. Zhuang[14], K. Zhukov[69], N.I. Zimine[39], J. Zinsser[64b], M. Ziolkowski[145], L. Živković[16], A. Zoccoli[24b,24a], K. Zoch[62], T.G. Zorbas[143], O. Zormpa[47], W. Zou[42], L. Zwalinski[37]

[1] Department of Physics, University of Adelaide, Adelaide, Australia
[2] Department of Physics, University of Alberta, Edmonton, AB, Canada
[3] [(a)]Department of Physics, Ankara University, Ankara, Turkey; [(b)]Division of Physics, TOBB University of Economics and Technology, Ankara, Turkey
[4] LAPP, Université Savoie Mont Blanc, CNRS/IN2P3, Annecy, France
[5] APC, Université Paris Cité, CNRS/IN2P3, Paris, France
[6] High Energy Physics Division, Argonne National Laboratory, Argonne, IL, USA
[7] Department of Physics, University of Arizona, Tucson, AZ, USA
[8] Department of Physics, University of Texas at Arlington, Arlington, TX, USA
[9] Physics Department, National and Kapodistrian University of Athens, Athens, Greece
[10] Physics Department, National Technical University of Athens, Zografou, Greece
[11] Department of Physics, University of Texas at Austin, Austin, TX, USA
[12] Institute of Physics, Azerbaijan Academy of Sciences, Baku, Azerbaijan
[13] Institut de Física d'Altes Energies (IFAE), Barcelona Institute of Science and Technology, Barcelona, Spain
[14] Institute of High Energy Physics, Chinese Academy of Sciences, Beijing, China
[15] Physics Department, Tsinghua University, Beijing, China
[16] Institute of Physics, University of Belgrade, Belgrade, Serbia
[17] Department for Physics and Technology, University of Bergen, Bergen, Norway

[18] [(a)]Physics Division, Lawrence Berkeley National Laboratory, Berkeley, CA, USA; [(b)]University of California, Berkeley, CA, USA
[19] Institut für Physik, Humboldt Universität zu Berlin, Berlin, Germany
[20] Albert Einstein Center for Fundamental Physics and Laboratory for High Energy Physics, University of Bern, Bern, Switzerland
[21] School of Physics and Astronomy, University of Birmingham, Birmingham, UK
[22] [(a)]Department of Physics, Bogazici University, Istanbul, Turkey; [(b)]Department of Physics Engineering, Gaziantep University, Gaziantep, Turkey; [(c)]Department of Physics, Istanbul University, Istanbul, Turkey
[23] [(a)]Facultad de Ciencias y Centro de Investigaciónes, Universidad Antonio Nariño, Bogotá, Colombia; [(b)]Departamento de Física, Universidad Nacional de Colombia, Bogotá, Colombia
[24] [(a)]Dipartimento di Fisica e Astronomia A. Righi, Universitá di Bologna, Bologna, Italy; [(b)]INFN Sezione di Bologna, Bologna, Italy
[25] Physikalisches Institut, Universität Bonn, Bonn, Germany
[26] Department of Physics, Boston University, Boston, MA, USA
[27] Department of Physics, Brandeis University, Waltham, MA, USA
[28] [(a)]Transilvania University of Brasov, Brasov, Romania; [(b)]Horia Hulubei National Institute of Physics and Nuclear Engineering, Bucharest, Romania; [(c)]Department of Physics, Alexandru Ioan Cuza University of Iasi, Iasi, Romania; [(d)]National Institute for Research and Development of Isotopic and Molecular Technologies, Physics Department, Cluj-Napoca, Romania; [(e)]National University of Science and Technology Politechnica, Bucharest, Romania; [(f)]West University in Timisoara, Timisoara, Romania; [(g)]Faculty of Physics, University of Bucharest, Bucharest, Romania
[29] [(a)]Faculty of Mathematics, Physics and Informatics, Comenius University, Bratislava, Slovakia; [(b)]Department of Subnuclear Physics, Institute of Experimental Physics of the Slovak Academy of Sciences, Kosice, Slovak Republic
[30] Physics Department, Brookhaven National Laboratory, Upton, NY, USA
[31] Universidad de Buenos Aires, Facultad de Ciencias Exactas y Naturales, Departamento de Física, y CONICET, Instituto de Físca de Buenos Aires (IFIBA), Buenos Aires, Argentina
[32] California State University, Los Angeles, CA, USA
[33] Cavendish Laboratory, University of Cambridge, Cambridge, UK
[34] [(a)]Department of Physics, University of Cape Town, Cape Town, South Africa; [(b)]iThemba Labs, Western Cape, South Africa; [(c)]Department of Mechanical Engineering Science, University of Johannesburg, Johannesburg, South Africa; [(d)]National Institute of Physics, University of the Philippines Diliman (Philippines), Quezon City, Philippines; [(e)]University of South Africa, Department of Physics, Pretoria, South Africa; [(f)]University of Zululand, KwaDlangezwa, South Africa; [(g)]School of Physics, University of the Witwatersrand, Johannesburg, South Africa
[35] Department of Physics, Carleton University, Ottawa, ON, Canada
[36] [(a)]Faculté des Sciences Ain Chock, Université Hassan II de Casablanca, Casablanca, Morocco; [(b)]Faculté des Sciences, Université Ibn-Tofail, Kénitra, Morocco; [(c)]Faculté des Sciences Semlalia, Université Cadi Ayyad, LPHEA-Marrakech, Marrakech, Morocco; [(d)]LPMR, Faculté des Sciences, Université Mohamed Premier, Oujda, Morocco; [(e)]Faculté des sciences, Université Mohammed V, Rabat, Morocco; [(f)]Institute of Applied Physics, Mohammed VI Polytechnic University, Ben Guerir, Morocco
[37] CERN, Geneva, Switzerland
[38] Affiliated with an institute covered by a cooperation agreement with CERN, Geneva, Switzerland
[39] Affiliated with an international laboratory covered by a cooperation agreement with CERN, Geneva, Switzerland
[40] Enrico Fermi Institute, University of Chicago, Chicago, IL, USA
[41] LPC, Université Clermont Auvergne, CNRS/IN2P3, Clermont-Ferrand, France
[42] Nevis Laboratory, Columbia University, Irvington, NY, USA
[43] Niels Bohr Institute, University of Copenhagen, Copenhagen, Denmark
[44] [(a)]Dipartimento di Fisica, Università della Calabria, Rende, Italy; [(b)]INFN Gruppo Collegato di Cosenza, Laboratori Nazionali di Frascati, Italy
[45] Physics Department, Southern Methodist University, Dallas, TX, USA
[46] Physics Department, University of Texas at Dallas, Richardson, TX, USA
[47] National Centre for Scientific Research "Demokritos", Agia Paraskevi, Greece
[48] [(a)]Department of Physics, Stockholm University, Stockholm, Sweden; [(b)]Oskar Klein Centre, Stockholm, Sweden
[49] Deutsches Elektronen-Synchrotron DESY, Hamburg and Zeuthen, Germany

[50] Fakultät Physik , Technische Universität Dortmund, Dortmund, Germany
[51] Institut für Kern- und Teilchenphysik, Technische Universität Dresden, Dresden, Germany
[52] Department of Physics, Duke University, Durham, NC, USA
[53] SUPA-School of Physics and Astronomy, University of Edinburgh, Edinburgh, UK
[54] INFN e Laboratori Nazionali di Frascati, Frascati, Italy
[55] Physikalisches Institut, Albert-Ludwigs-Universität Freiburg, Freiburg, Germany
[56] II. Physikalisches Institut, Georg-August-Universität Göttingen, Göttingen, Germany
[57] Département de Physique Nucléaire et Corpusculaire, Université de Genève, Geneva, Switzerland
[58] [(a)]Dipartimento di Fisica, Università di Genova, Genoa, Italy; [(b)]INFN Sezione di Genova, Genoa, Italy
[59] II. Physikalisches Institut, Justus-Liebig-Universität Giessen, Giessen, Germany
[60] SUPA-School of Physics and Astronomy, University of Glasgow, Glasgow, UK
[61] LPSC, Université Grenoble Alpes, CNRS/IN2P3, Grenoble INP, Grenoble, France
[62] Laboratory for Particle Physics and Cosmology, Harvard University, Cambridge, MA, USA
[63] [(a)]Department of Modern Physics and State Key Laboratory of Particle Detection and Electronics, University of Science and Technology of China, Hefei, China; [(b)]Institute of Frontier and Interdisciplinary Science and Key Laboratory of Particle Physics and Particle Irradiation (MOE), Shandong University, Qingdao, China; [(c)]School of Physics and Astronomy, Shanghai Jiao Tong University, Key Laboratory for Particle Astrophysics and Cosmology (MOE), SKLPPC, Shanghai, China; [(d)]Tsung-Dao Lee Institute, Shanghai, China; [(e)]School of Physics, Zhengzhou University, China
[64] [(a)]Kirchhoff-Institut für Physik, Ruprecht-Karls-Universität Heidelberg, Heidelberg, Germany; [(b)]Physikalisches Institut, Ruprecht-Karls-Universität Heidelberg, Heidelberg, Germany
[65] [(a)]Department of Physics, Chinese University of Hong Kong, Shatin, N.T., Hong Kong; [(b)]Department of Physics, University of Hong Kong, Hong Kong, China; [(c)]Department of Physics and Institute for Advanced Study, Hong Kong University of Science and Technology, Clear Water Bay, Kowloon, Hong Kong, China
[66] Department of Physics, National Tsing Hua University, Hsinchu, Taiwan
[67] IJCLab, Université Paris-Saclay, CNRS/IN2P3, 91405 Orsay, France
[68] Centro Nacional de Microelectrónica (IMB-CNM-CSIC), Barcelona, Spain
[69] Department of Physics, Indiana University, Bloomington, IN, USA
[70] [(a)]INFN Gruppo Collegato di Udine, Sezione di Trieste, Udine, Italy; [(b)]ICTP, Trieste, Italy; [(c)]Dipartimento Politecnico di Ingegneria e Architettura, Università di Udine, Udine, Italy
[71] [(a)]INFN Sezione di Lecce, Lecce, Italy; [(b)]Dipartimento di Matematica e Fisica, Università del Salento, Lecce, Italy
[72] [(a)]INFN Sezione di Milano, Milan, Italy; [(b)]Dipartimento di Fisica, Università di Milano, Milan, Italy
[73] [(a)]INFN Sezione di Napoli, Naples, Italy; [(b)]Dipartimento di Fisica, Università di Napoli, Naples, Italy
[74] [(a)]INFN Sezione di Pavia, Pavia, Italy; [(b)]Dipartimento di Fisica, Università di Pavia, Pavia, Italy
[75] [(a)]INFN Sezione di Pisa, Pisa, Italy; [(b)]Dipartimento di Fisica E. Fermi, Università di Pisa, Pisa, Italy
[76] [(a)]INFN Sezione di Roma, Rome, Italy; [(b)]Dipartimento di Fisica, Sapienza Università di Roma, Rome, Italy
[77] [(a)]INFN Sezione di Roma Tor Vergata, Rome, Italy; [(b)]Dipartimento di Fisica, Università di Roma Tor Vergata, Rome, Italy
[78] [(a)]INFN Sezione di Roma Tre, Rome, Italy; [(b)]Dipartimento di Matematica e Fisica, Università Roma Tre, Rome, Italy
[79] [(a)]INFN-TIFPA, Rome, Italy; [(b)]Università degli Studi di Trento, Trento, Italy
[80] Universität Innsbruck, Department of Astro and Particle Physics, Innsbruck, Austria
[81] University of Iowa, Iowa City, IA, USA
[82] Department of Physics and Astronomy, Iowa State University, Ames, IA, USA
[83] Istinye University, Sariyer, Istanbul, Turkey
[84] [(a)]Departamento de Engenharia Elétrica, Universidade Federal de Juiz de Fora (UFJF), Juiz de Fora, Brazil; [(b)]Universidade Federal do Rio De Janeiro COPPE/EE/IF, Rio de Janeiro, Brazil; [(c)]Instituto de Física, Universidade de São Paulo, São Paulo, Brazil; [(d)]Rio de Janeiro State University, Rio de Janeiro, Brazil ; [(e)]Federal University of Bahia, Bahia, Brazil
[85] KEK, High Energy Accelerator Research Organization, Tsukuba, Japan
[86] Graduate School of Science, Kobe University, Kobe, Japan
[87] [(a)]AGH University of Krakow, Faculty of Physics and Applied Computer Science, Krakow, Poland; [(b)]Marian Smoluchowski Institute of Physics, Jagiellonian University, Krakow, Poland
[88] Institute of Nuclear Physics Polish Academy of Sciences, Krakow, Poland
[89] Faculty of Science, Kyoto University, Kyoto, Japan

[90] Research Center for Advanced Particle Physics and Department of Physics, Kyushu University, Fukuoka , Japan
[91] L2IT, Université de Toulouse, CNRS/IN2P3, UPS, Toulouse, France
[92] Instituto de Física La Plata, Universidad Nacional de La Plata and CONICET, La Plata, Argentina
[93] Physics Department, Lancaster University, Lancaster, UK
[94] Oliver Lodge Laboratory, University of Liverpool, Liverpool, UK
[95] Department of Experimental Particle Physics, Jožef Stefan Institute and Department of Physics, University of Ljubljana, Ljubljana, Slovenia
[96] School of Physics and Astronomy, Queen Mary University of London, London, UK
[97] Department of Physics, Royal Holloway University of London, Egham, UK
[98] Department of Physics and Astronomy, University College London, London, UK
[99] Louisiana Tech University, Ruston, LA, USA
[100] Fysiska institutionen, Lunds universitet, Lund, Sweden
[101] Departamento de Física Teorica C-15 and CIAFF, Universidad Autónoma de Madrid, Madrid, Spain
[102] Institut für Physik, Universität Mainz, Mainz, Germany
[103] School of Physics and Astronomy, University of Manchester, Manchester, UK
[104] CPPM, Aix-Marseille Université, CNRS/IN2P3, Marseille, France
[105] Department of Physics, University of Massachusetts, Amherst, MA, USA
[106] Department of Physics, McGill University, Montreal, QC, Canada
[107] School of Physics, University of Melbourne, Victoria, Australia
[108] Department of Physics, University of Michigan, Ann Arbor, MI, USA
[109] Department of Physics and Astronomy, Michigan State University, East Lansing, MI, USA
[110] Group of Particle Physics, University of Montreal, Montreal, QC, Canada
[111] Fakultät für Physik, Ludwig-Maximilians-Universität München, München, Germany
[112] Max-Planck-Institut für Physik (Werner-Heisenberg-Institut), München, Germany
[113] Graduate School of Science and Kobayashi-Maskawa Institute, Nagoya University, Nagoya, Japan
[114] [(a)]Department of Physics, Nanjing University, Nanjing, China; [(b)]School of Science, Shenzhen Campus of Sun Yat-sen University, Shenzhen, China; [(c)]University of Chinese Academy of Science (UCAS), Beijing, China
[115] Department of Physics and Astronomy, University of New Mexico, Albuquerque, NM, USA
[116] Institute for Mathematics, Astrophysics and Particle Physics, Radboud University/Nikhef, Nijmegen, The Netherlands
[117] Nikhef National Institute for Subatomic Physics and University of Amsterdam, Amsterdam, The Netherlands
[118] Department of Physics, Northern Illinois University, DeKalb, IL, USA
[119] [(a)]New York University Abu Dhabi, Abu Dhabi, United Arab Emirates; [(b)]United Arab Emirates University, Al Ain, United Arab Emirates
[120] Department of Physics, New York University, New York, NY, USA
[121] Ochanomizu University, Otsuka, Bunkyo-ku, Tokyo, Japan
[122] Ohio State University, Columbus, OH, USA
[123] Homer L. Dodge Department of Physics and Astronomy, University of Oklahoma, Norman, OK, USA
[124] Department of Physics, Oklahoma State University, Stillwater, OK, USA
[125] Palacký University, Joint Laboratory of Optics, Olomouc, Czech Republic
[126] Institute for Fundamental Science, University of Oregon, Eugene, OR, USA
[127] Graduate School of Science, Osaka University, Osaka, Japan
[128] Department of Physics, University of Oslo, Oslo, Norway
[129] Department of Physics, Oxford University, Oxford, UK
[130] LPNHE, Sorbonne Université, Université Paris Cité, CNRS/IN2P3, Paris, France
[131] Department of Physics, University of Pennsylvania, Philadelphia, PA, USA
[132] Department of Physics and Astronomy, University of Pittsburgh, Pittsburgh, PA, USA
[133] [(a)]Laboratório de Instrumentação e Física Experimental de Partículas - LIP, Lisbon, Portugal; [(b)]Departamento de Física, Faculdade de Ciências, Universidade de Lisboa, Lisbon, Portugal; [(c)]Departamento de Física, Universidade de Coimbra, Coimbra, Portugal; [(d)]Centro de Física Nuclear da Universidade de Lisboa, Lisbon, Portugal; [(e)]Departamento de Física, Universidade do Minho, Braga, Portugal; [(f)]Departamento de Física Teórica y del Cosmos, Universidad de Granada, Granada, Spain; [(g)]Departamento de Física, Instituto Superior Técnico, Universidade de Lisboa, Lisboa, Portugal
[134] Institute of Physics of the Czech Academy of Sciences, Prague, Czech Republic
[135] Czech Technical University in Prague, Prague, Czech Republic

[136] Charles University, Faculty of Mathematics and Physics, Prague, Czech Republic
[137] Particle Physics Department, Rutherford Appleton Laboratory, Didcot, UK
[138] IRFU, CEA, Université Paris-Saclay, Gif-sur-Yvette, France
[139] Santa Cruz Institute for Particle Physics, University of California Santa Cruz, Santa Cruz, CA, USA
[140] [(a)]Departamento de Física, Pontificia Universidad Católica de Chile, Santiago, Chile; [(b)]Millennium Institute for Subatomic physics at high energy frontier (SAPHIR), Santiago, Chile; [(c)]Instituto de Investigación Multidisciplinario en Ciencia y Tecnología y Departamento de Física, Universidad de La Serena, La Serena, Chile; [(d)]Universidad Andres Bello, Department of Physics, Santiago, Chile; [(e)]Instituto de Alta Investigación, Universidad de Tarapacá, Arica, Chile; [(f)]Departamento de Física, Universidad Técnica Federico Santa María, Valparaíso, Chile
[141] Department of Physics, Institute of Science, Tokyo, Japan
[142] Department of Physics, University of Washington, Seattle, WA, USA
[143] Department of Physics and Astronomy, University of Sheffield, Sheffield, UK
[144] Department of Physics, Shinshu University, Nagano, Japan
[145] Department Physik, Universität Siegen, Siegen, Germany
[146] Department of Physics, Simon Fraser University, Burnaby, BC, Canada
[147] SLAC National Accelerator Laboratory, Stanford, CA, USA
[148] Department of Physics, Royal Institute of Technology, Stockholm, Sweden
[149] Departments of Physics and Astronomy, Stony Brook University, Stony Brook, NY, USA
[150] Department of Physics and Astronomy, University of Sussex, Brighton, UK
[151] School of Physics, University of Sydney, Sydney, Australia
[152] Institute of Physics, Academia Sinica, Taipei, Taiwan
[153] [(a)]E. Andronikashvili Institute of Physics, Iv. Javakhishvili Tbilisi State University, Tbilisi, Georgia; [(b)]High Energy Physics Institute, Tbilisi State University, Tbilisi, Georgia; [(c)]University of Georgia, Tbilisi, Georgia
[154] Department of Physics, Technion, Israel Institute of Technology, Haifa, Israel
[155] Raymond and Beverly Sackler School of Physics and Astronomy, Tel Aviv University, Tel Aviv, Israel
[156] Department of Physics, Aristotle University of Thessaloniki, Thessaloniki, Greece
[157] International Center for Elementary Particle Physics and Department of Physics, University of Tokyo, Tokyo, Japan
[158] Department of Physics, University of Toronto, Toronto, ON, Canada
[159] [(a)]TRIUMF, Vancouver, BC, Canada; [(b)]Department of Physics and Astronomy, York University, Toronto, ON, Canada
[160] Division of Physics and Tomonaga Center for the History of the Universe, Faculty of Pure and Applied Sciences, University of Tsukuba, Tsukuba, Japan
[161] Department of Physics and Astronomy, Tufts University, Medford, MA, USA
[162] Department of Physics and Astronomy, University of California Irvine, Irvine, CA, USA
[163] University of Sharjah, Sharjah, United Arab Emirates
[164] Department of Physics and Astronomy, University of Uppsala, Uppsala, Sweden
[165] Department of Physics, University of Illinois, Urbana, IL, USA
[166] Instituto de Física Corpuscular (IFIC), Centro Mixto Universidad de Valencia - CSIC, Valencia, Spain
[167] Department of Physics, University of British Columbia, Vancouver, BC, Canada
[168] Department of Physics and Astronomy, University of Victoria, Victoria, BC, Canada
[169] Fakultät für Physik und Astronomie, Julius-Maximilians-Universität Würzburg, Würzburg, Germany
[170] Department of Physics, University of Warwick, Coventry, UK
[171] Waseda University, Tokyo, Japan
[172] Department of Particle Physics and Astrophysics, Weizmann Institute of Science, Rehovot, Israel
[173] Department of Physics, University of Wisconsin, Madison, WI, USA
[174] Fakultät für Mathematik und Naturwissenschaften, Fachgruppe Physik, Bergische Universität Wuppertal, Wuppertal, Germany
[175] Department of Physics, Yale University, New Haven, CT, USA

[a] Also Affiliated with an Institute Covered by a Cooperation Agreement with CERN, Geneva, Switzerland
[b] Also at An-Najah National University, Nablus, Palestine
[c] Also at Borough of Manhattan Community College, City University of New York, New York, NY, USA
[d] Also at Center for Interdisciplinary Research and Innovation (CIRI-AUTH), Thessaloniki, Greece
[e] Also at CERN, Geneva, Switzerland

[f] Also at CMD-AC UNEC Research Center, Azerbaijan State University of Economics (UNEC), Azerbaijan
[g] Also at Département de Physique Nucléaire et Corpusculaire, Université de Genève, Genève, Switzerland
[h] Also at Departament de Fisica de la Universitat Autonoma de Barcelona, Barcelona, Spain
[i] Also at Department of Financial and Management Engineering, University of the Aegean, Chios, Greece
[j] Also at Department of Physics, California State University, Sacramento, USA
[k] Also at Department of Physics, King's College London, London, UK
[l] Also at Department of Physics, Stanford University, Stanford, CA, USA
[m] Also at Department of Physics, Stellenbosch University, South Africa
[n] Also at Department of Physics, University of Fribourg, Fribourg, Switzerland
[o] Also at Department of Physics, University of Thessaly, Greece
[p] Also at Department of Physics, Westmont College, Santa Barbara, USA
[q] Also at Faculty of Physics, Sofia University, 'St. Kliment Ohridski', Sofia, Bulgaria
[r] Also at Hellenic Open University, Patras, Greece
[s] Also at Imam Mohammad Ibn Saud Islamic University, Riyadh, Saudi Arabia
[t] Also at Institucio Catalana de Recerca i Estudis Avancats, ICREA, Barcelona, Spain
[u] Also at Institut für Experimentalphysik, Universität Hamburg, Hamburg, Germany
[v] Also at Institute for Nuclear Research and Nuclear Energy (INRNE) of the Bulgarian Academy of Sciences, Sofia, Bulgaria
[w] Also at Institute of Applied Physics, Mohammed VI Polytechnic University, Ben Guerir, Morocco
[x] Also at Institute of Particle Physics (IPP), Ottawa, Canada
[y] Also at Institute of Physics, Azerbaijan Academy of Sciences, Baku, Azerbaijan
[z] Also at Institute of Theoretical Physics, Ilia State University, Tbilisi, Georgia
[aa] Also at National Institute of Physics, University of the Philippines Diliman (Philippines), Philippines
[ab] Also at Technical University of Munich, Munich, Germany
[ac] Also at The Collaborative Innovation Center of Quantum Matter (CICQM), Beijing, China
[ad] Also at TRIUMF, Vancouver, BC, Canada
[ae] Also at Università di Napoli Parthenope, Naples, Italy
[af] Also at University of Colorado Boulder, Department of Physics, Colorado, USA
[ag] Also at Washington College, Chestertown, MD, USA
[ah] Also at Yeditepe University, Physics Department, Istanbul, Turkey
*Deceased